

Aus dem Neurowissenschaftlichen Forschungszentrum  
der Medizinischen Fakultät Charité – Universitätsmedizin Berlin

**DISSERTATION**

**Presynaptic Inhibition of Transmitter Release by G-Protein coupled  
Receptors in the Hippocampal Formation**

zur Erlangung des akademischen Grades  
Doctor of Philosophy (PhD)  
im Rahmen des  
International Graduate Program Medical Neurosciences

vorgelegt der Medizinischen Fakultät  
Charité – Universitätsmedizin Berlin

von

Benjamin Rainer Rost

aus Darmstadt



---

Gutachter/in: 1. Prof. Dr. D. Schmitz

2. Prof. Dr. J. Rettig

3. Prof. Dr. V. Leßmann

Datum der Urkundenverleihung: 3.6.2012



---

# Contents

<b>Contents</b> .....	<b>III</b>
<b>Synopsis</b> .....	<b>2</b>
<b>Zusammenfassung</b> .....	<b>4</b>
<b>1 Introduction</b> .....	<b>7</b>
<b>1.1 Principles of neuronal communication</b> .....	<b>7</b>
<b>1.2 Neurotransmitter release at central synapses</b> .....	<b>9</b>
1.2.1 Vesicle pools and the vesicle cycle .....	10
1.2.2 SNARE proteins mediate vesicle fusion.....	12
1.2.3 Calcium triggers fast synaptic transmitter release .....	13
1.2.4 Hyperosmotic solutions as fusogenic stimuli .....	14
<b>1.3 Presynaptic modulation of transmitter release</b> .....	<b>15</b>
1.3.1 Presynaptic signalling pathways of G-protein coupled receptors.....	16
1.3.2 Structure and function of GABA <sub>B</sub> receptors.....	19
1.3.3 Presynaptic metabotropic inhibition independent of calcium channels.....	21
<b>1.4 The hippocampus and its principal neurons</b> .....	<b>22</b>
<b>1.5 Attempts to investigate neural circuitries by silencing specific neuronal populations</b> .....	<b>24</b>
<b>1.6 Aims of this work</b> .....	<b>27</b>
<b>2 Materials and experimental methods</b> .....	<b>29</b>
<b>2.1 Cell culture</b> .....	<b>29</b>
2.1.1 Media and solutions.....	29
2.1.2 Material.....	30

2.1.3	Autaptic cultures .....	30
2.1.3.1	Preparation of coverslips .....	30
2.1.3.2	Astrocyte cultures .....	30
2.1.3.3	Neuronal cultures .....	32
2.1.4	Expression of recombinant proteins in HEK293 cells .....	33
2.1.5	Lentivirus production .....	33
<b>2.2</b>	<b>Electrophysiology .....</b>	<b>34</b>
2.2.1	Material .....	34
2.2.2	Solutions for slice preparations and electrophysiological recordings .....	35
2.2.3	Hippocampal slice preparations .....	37
2.2.4	Field recordings and whole cell patch clamp experiments in hippocampal slices .....	38
2.2.5	Imaging experiments with photodiode and Nipkow spinning disc .....	38
2.2.6	Recordings of autaptic neurons in culture .....	40
<b>2.3</b>	<b>Data analysis and statistics .....</b>	<b>42</b>
<b>2.4</b>	<b>Molecular biology and biochemistry .....</b>	<b>44</b>
2.4.1	Materials .....	44
2.4.2	Buffers and media .....	44
2.4.3	Techniques to work with DNA .....	45
2.4.3.1	DNA purification .....	46
2.4.3.2	Digestion of DNA with restriction enzymes .....	47
2.4.3.3	Agarose gel electrophoresis and fragment isolation .....	47
2.4.3.4	Ligation .....	47
2.4.3.5	Polymerase chain reaction (PCR) .....	48
2.4.4	Protein isolation, SDS polyacrylamide gel electrophoresis and western blots .....	50
2.4.5	Immunofluorescence stainings .....	51
<b>3</b>	<b>Results .....</b>	<b>55</b>
<b>3.1</b>	<b>Presynaptic inhibition by GABA<sub>B</sub>Rs in hippocampus area CA1 .....</b>	<b>55</b>
3.1.1	Presynaptic inhibition by GABA <sub>B</sub> Rs cannot be explained by reduced calcium influx alone .....	55
3.1.2	GABA <sub>B</sub> Rs inhibit spontaneous neurotransmitter release in CA1 in presence and absence of extracellular calcium .....	58
3.1.3	Investigation of GABA <sub>B</sub> R-mediated inhibition in autaptic cultures .....	60

---

3.1.4	Presynaptic inhibition by GABA <sub>B</sub> Rs depends on Gα <sub>i</sub> /Gα <sub>o</sub> -proteins.....	62
3.1.5	GABA <sub>B</sub> Rs inhibit transmitter release evoked by hypertonic stimuli.....	63
3.1.6	Kinetics of sucrose-evoked release are slowed by GABA <sub>B</sub> R activation .....	65
3.1.7	BoNT-A treatment does not abolish direct inhibition of transmitter release by GABA <sub>B</sub> Rs...68	
<b>3.2</b>	<b>GABA<sub>B</sub>R-mediated inhibition at mossy fibre terminals and characterization of autaptic hippocampal granule cells .....</b>	<b>73</b>
3.2.1	Modulation of fEPSPs and presynaptic calcium signals at mossy fibre synapses by GABA <sub>B</sub> Rs.....	75
3.2.2	Baclofen decreases calcium transients in single mossy fibre boutons.....	76
3.2.3	Presynaptic GABAergic inhibition at mossy fibre terminals cannot be explained by a decrease of calcium influx alone .....	78
3.2.4	Establishing autaptic cultures of hippocampal granule cells to study mossy fibre mEPSCs.....	79
3.2.4.1	Morphological and pharmacological characterization of autaptic granule cells .....	80
3.2.4.2	Detailed characterization of granule cell in autaptic cultures.....	84
3.2.5	Baclofen decreases the frequency of mossy fibre mEPSCs in the absence of extracellular calcium .....	89
<b>3.3</b>	<b>Presynaptic inhibition by an artificial receptor as a tool to silence neuronal output.....</b>	<b>91</b>
3.3.1	Development of hm4D, a designer receptor activated by a designer drug.....	91
3.3.2	Cloning of hm4D receptor constructs for functional testing.....	92
3.3.3	Functional tests of hm4D in neuronal cell cultures .....	94
3.3.4	Vector design for a conditional Rosa26 hm4D transgenic mouse .....	97
3.3.5	Testing conditional expression of the FLEX construct in HEK293 cells.....	100
3.3.6	PCR analysis of embryonic stem cells for successful recombination into the Rosa26 locus.....	102
<b>4</b>	<b>Discussion .....</b>	<b>105</b>
<b>4.1</b>	<b>The role of presynaptic inhibition in neuronal networks .....</b>	<b>106</b>
<b>4.2</b>	<b>Functional implications of calcium-independent inhibition .....</b>	<b>108</b>
<b>4.3</b>	<b>Estimated contribution of calcium-independent mechanisms on overall presynaptic inhibition .....</b>	<b>111</b>
<b>4.4</b>	<b>What is the target of presynaptic inhibition acting at the release machinery? .....</b>	<b>113</b>

<b>4.5</b>	<b>Potential experimental use of the Cre-conditional hM4D transgenic mouse .....</b>	<b>115</b>
<b>5</b>	<b>Appendix .....</b>	<b>121</b>
<b>5.1</b>	<b>References.....</b>	<b>121</b>
<b>5.2</b>	<b>List of figures .....</b>	<b>130</b>
<b>5.3</b>	<b>List of tables .....</b>	<b>133</b>
<b>5.4</b>	<b>Frequently used abbreviations .....</b>	<b>134</b>
<b>5.5</b>	<b>Statement of contribution .....</b>	<b>137</b>
<b>5.6</b>	<b>Acknowledgments.....</b>	<b>138</b>
<b>5.7</b>	<b>Curriculum Vitae.....</b>	<b>140</b>
<b>5.8</b>	<b>Publications .....</b>	<b>141</b>
<b>5.9</b>	<b>Symposia and meetings contributions .....</b>	<b>142</b>
<b>5.10</b>	<b>Erklärung an Eides statt .....</b>	<b>143</b>



## Synopsis

Synaptic communication between neurons is tuned by a variety of presynaptic G-protein coupled receptors. Many of these receptors act inhibitory, as they decrease neurotransmitter release, and thereby lower the gain of synaptic transmission. Ligand binding to these presynaptic receptors causes activation of intracellular heterotrimeric G-proteins. The G-protein  $G\beta\gamma$  subunits can interact with presynaptic voltage-dependent calcium channels and lower the channels' opening probability. This results in a decrease of calcium influx after an action potential and ultimately reduces the amount of neurotransmitter release.

Additionally, a second signalling pathway has been suggested that reduces transmitter release independently of voltage-dependent calcium channels, but its molecular mechanisms have not yet been clarified. To gain more insight into this potential second inhibitory signalling pathway, we studied inhibition of glutamate release by presynaptic metabotropic  $\gamma$ -aminobutyric acid receptors ( $GABA_B$ Rs). We found that at Schaffer collateral synapses in CA1 of the hippocampus, the reduction of calcium influx by  $GABA_B$ Rs does not sufficiently account for the observed reduction of transmitter release, and that  $GABA_B$ Rs can also decrease transmitter release rates in calcium-free conditions. In autaptic cell cultures of hippocampal neurons, we used hypertonic solutions to trigger transmitter release in a calcium-independent manner. Here too,  $GABA_B$ R activation inhibits transmitter release. These results argue for a second inhibitory mechanism that acts directly at the vesicular release machinery and increases the energy barrier for vesicle fusion. The carboxy-terminus of SNAP-25, one of the proteins forming the core release apparatus, has been implicated as a target of G-protein-mediated direct inhibition of vesicle fusion. We tested this hypothesis by cleaving off the carboxy-terminus of SNAP-25 with Botulinum neurotoxin A. However, this treatment did not abolish the calcium channel-independent inhibitory effect of presynaptic  $GABA_B$ Rs, indicating that  $G\beta\gamma$  subunits of inhibitory G-proteins interact with another, yet unknown part of the release machinery.

We also found evidence for calcium channel-independent inhibition by  $GABA_B$ Rs at hippocampal mossy fibre synapses in CA3. In order to study these synapses in a cell culture

---

model, we established autaptic cultures of hippocampal granule cells, and describe their morphological and physiological features in detail.

We further investigated presynaptic inhibition by expressing an artificial G-protein coupled receptor in autaptic neurons. An artificial, pharmaco-genetic system to silence transmitter release is potentially useful for studying the role of neuronal populations in networks *in vivo*. Ongoing work aims to generate a transgenic mouse line that would allow restricting presynaptic inhibition to genetically defined neuronal populations.

**Keywords:** presynaptic inhibition, metabotropic receptor, synaptic vesicle fusion, SNARE proteins

## Zusammenfassung

Synaptische Informationsübertragung zwischen Neuronen wird durch präsynaptische, G-Protein gekoppelte Rezeptoren moduliert. Viele dieser Rezeptoren wirken inhibitorisch, da sie die Neurotransmitter Freisetzung verringern, und somit die synaptische Signalweiterleitung dämpfen. Ligandenbindung an diese Rezeptoren aktiviert intrazelluläre, heterotrimere G-Proteine. Deren  $G\beta\gamma$ -Untereinheiten können mit spannungsgesteuerten Calciumkanälen interagieren und dadurch die Öffnungswahrscheinlichkeit der Kanäle verringern. Dies bedingt einen verringerten Calciumeinstrom nach einem Aktionspotential, was wiederum eine Verringerung der Transmitterfreisetzung zur Folge hat.

Zusätzlich wird eine weitere Signalkaskade vermutet, welche die Transmitterfreisetzung unabhängig von spannungsgesteuerten Calciumkanälen hemmen soll, deren molekularer Mechanismus zum gegenwärtigen Zeitpunkt aber noch nicht eindeutig identifiziert ist. Um mehr über diese potentielle Signalkaskade zu lernen, untersuchten wir die Inhibition der Glutamatausschüttung durch präsynaptische, metabotrope Rezeptoren für  $\gamma$ -Aminobuttersäure (engl. "γ-aminobutyric acid",  $GABA_B$ R). Wir fanden an den Synapsen der Schaffer-Kollateralen in CA1 des Hippocampus, dass die Reduktion des Calciumeinstroms nach Aktivierung der  $GABA_B$ R nicht die gesamte beobachtete Verringerung der Glutamatfreisetzung erklären kann, und dass  $GABA_B$ R auch in Calcium-freien Bedingungen die spontane Freisetzungsrates von Glutamat verringern. In autaptischen Zellkulturen hippocampaler Neurone benutzten wir hypertone Lösungen um eine Calcium unabhängige Glutamatausschüttung auszulösen. Auch hier verringerte eine  $GABA_B$ R Aktivierung die Transmitterfreisetzung. Diese Ergebnisse unterstützen die Hypothese eines zweiten inhibitorischen Mechanismus, der direkt an der synaptischen Freisetzungsmaschinerie ansetzt und dadurch die Energiebarriere für die Vesikelfusion erhöht. Als möglicher Angriffspunkt G-Protein vermittelter direkter Inhibition der synaptischer Vesikelfusion wurde der Carboxy-Terminus von SNAP-25 vorgeschlagen, einem Molekül der vesikulären Freisetzungsmaschinerie. Wir testeten diese Hypothese, indem wir das Carboxy-Ende von SNAP-25 mittels Botulinum Toxin A abspalteten. Allerdings hob diese Manipulation nicht

---

die Calciumkanal unabhängige Inhibition durch präsynaptische GABA<sub>B</sub>R auf, was vermuten lässt, dass die G $\beta$  $\gamma$ -Untereinheiten der inhibitorischen G-Proteine mit einer anderen, noch nicht identifizierten Komponente der Freisetzungsmaschinerie interagieren.

Darüber hinaus fanden wir positive Evidenzen für eine Kalzium-Kanal unabhängige Inhibition durch GABA<sub>B</sub>R an hippocampalen Moosfasersynapsen in CA3. Um diese Synapsen im Zellkulturmodell untersuchen zu können, etablierten wir autaptische Zellkulturen von hippocampalen Körnerzellen, deren morphologische und physiologische Charakteristika wir detailliert beschreiben.

Wir haben des Weiteren präsynaptische Inhibition durch einen artifizielle G-Protein gekoppelte Rezeptor in autaptischen Neuronen untersucht. Ein künstliches, pharmakogenetisches System zur Inhibition der Transmitterfreisetzung kann potentiell nützlich sein zur Untersuchung der Rolle einzelner Neuronenpopulationen im Netzwerk *in vivo*. Laufende Arbeiten streben nun die Entwicklung einer transgenen Maus an, um präsynaptische Inhibition auf einzelne, genetisch definierte Neuronengruppen zu beschränken.

**Schlüsselwörter:** Präsynaptische Inhibition, metabotrope Rezeptoren, synaptische Vesikelfusion, SNARE Proteine



---

# 1 Introduction

## 1.1 Principles of neuronal communication

Communication between neurons is crucial for sensory perception, stimulus transduction, information processing, and motor output in every higher-order animal. Neurons receive inputs and forward the encoded information to other neurons by means of two principal mechanisms: They release chemical messengers called neurotransmitters that activate specific receptors on the target cell; or they are directly coupled via intercellular pores called gap-junctions. However, electrical coupling between neurons of the vertebrate central nervous system is very rare, and most of the neuronal output is communicated via the release of small soluble neurotransmitters. Neurotransmitters can be divided into four different classes (Südhof, 2008):

1. “Classical” neurotransmitters comprise several subgroups: amino acid transmitters (glutamate,  $\gamma$ -aminobutyric acid (GABA), and glycine), acetylcholine, and purinergic transmitters (adenosine, adenosine-triphosphate (ATP)), which are packed into small, clear vesicles in highly specialised axonal terminals. These vesicles are rapidly released by calcium ( $\text{Ca}^{2+}$ )-triggered exocytosis, allowing very fast (milliseconds) point to point communication.
2. Monoaminergic neurotransmitters (dopamine, noradrenaline, adrenaline, histamine, and serotonin) are  $\text{Ca}^{2+}$ -dependently released from axonal varicosities by exocytosis of small dense core vesicles. They can diffuse over longer distances and have moderate to fast signalling kinetics.
3. Neuropeptides are signalling peptides consisting of 3 to 36 amino acid residues. They are stored in large dense core vesicles and are  $\text{Ca}^{2+}$ -dependently secreted into the extracellular space. Their secretion is not restricted to certain neuronal structures, but can occur at any given part of the neuron. Neuropeptides can diffuse over very long distances (even outside the brain) and have long-lasting effects.

4. Membrane permeable mediators, such as nitric oxide, endocannabinoids, and other gaseous or lipid signalling molecules, are not stored but released immediately after synthesis. Their signalling duration and range is rather short and also diffuse.

Rapid chemical communication relies on the fast exocytosis of classical neurotransmitters at highly specialised cellular structures termed synapses (a blend term of the Greek *syn*, “together”, and *haptein*, “to attach”, first used by Charles Sherrington in the *Textbook of Physiology*, 1887, prompted by a suggestion by Michael Foster and Pace Verral (Shepherd and Erulkar, 1997). Synapses comprise a presynaptic, transmitter releasing side, and a postsynaptic, receiving side. The two sides are separated by a narrow synaptic cleft located between the transmitting and the receiving cell (see Figure 1-1). To form a synapse, the cellular partners have to assemble highly specialised molecular machineries on both the pre- and postsynaptic sides, which enable reliable transduction and computation of the signal. Synapses have become a major focus of modern neuroscience, and today there is abundant evidence that synaptic development, transmission and plasticity are key elements in higher cortical functions like learning and memory, but are also affected in or even the cause for a number of central nervous system disorders, such as epilepsy, mental retardation, schizophrenia, and Alzheimer’s disease.

Neurotransmitters released by the presynaptic element can bind to and activate membrane spanning receptors on the postsynaptic side. In fast synaptic transmission, the receptors consist of an ion-permeable pore that is gated by ligand binding (ionotropic receptors). These receptors are located in close vicinity to the transmitter release site and immediately re-translate the chemical signal into an electrical signal in the target cell. Depending on the receptor’s ion selectivity and the direction of ion flux, ionotropic receptor opening causes a positive or negative change in the local membrane potential. These voltage deflections are termed excitatory or inhibitory postsynaptic potential (EPSP or IPSP). EPSPs depolarize the membrane and shift it towards the action potential firing threshold, whereas IPSPs stabilize the negative membrane potential and prevent action potential firing. Slow synaptic transmission is mediated by metabotropic, G-protein coupled receptors (GPCRs). With the exception of gaseous neurotransmitters, GPCRs exist for every neurotransmitter. These receptors may also be located distal to the transmitter release site, where they activate biochemical signalling cascades with multiple downstream effectors (see 1.3.1).

---

Although electro-chemical signalling between neurons is often presented as unidirectional (from the axon of the presynaptic side to the dendrite of the postsynaptic partner), it is important to note that receptors of both classes are not only located postsynaptically, but are also found in the presynaptic membrane, where they can modulate transmitter release. Presynaptic receptors function as auto- or heteroreceptors. Autoreceptors are activated by the type of transmitter released from the terminal on which the receptors are situated. Autoreceptors can therefore provide intrasynaptic feedback regulation of transmitter release, and modulate transmission between neighbouring synapses of the same type. Conversely, heteroreceptors are activated by ligands different from the transmitter released by the terminals on which the receptors are located. Heteroreceptors integrate signals from adjacent synapses of different type, and enable intersynaptic regulation of transmitter release. The signalling and functional implications of presynaptic receptors are discussed in chapter 1.3.

In the present work we investigated the regulation of transmitter release by presynaptic GPCRs at glutamatergic synapses in the hippocampus. For a better understanding of the context, I will briefly review the basic mechanisms of “classical” neurotransmitter release before presenting a detailed account of release modulation by GPCRs.

## **1.2 Neurotransmitter release at central synapses**

Synaptic vesicles fuse at the active zone of the nerve terminal when  $\text{Ca}^{2+}$  ions enter the terminal through voltage-dependent  $\text{Ca}^{2+}$  channels (VDCCs) after membrane depolarization by an action potential. A remarkably fast and precisely orchestrated molecular machinery mediates transmitter release, resulting in a pre- to postsynaptic signal delay of only  $\sim 1$  ms. Many of the presynaptic components and their functions have now been elucidated, and a biophysical picture of the basic release mechanisms is slowly emerging (Rizo and Rosenmund, 2008; Sorensen, 2009). One of the most important contributions was made by Bernard Katz in the 1950s, namely, that communication between neurons and their target cells occurs in *quanta*, small packets representing the smallest units of neuronal output (Del Castillo and Katz, 1954). Individual *quanta* resulting from spontaneous fusion of vesicles in the absence of action potentials can be measured in electrophysiological recordings as miniature excitatory or inhibitory postsynaptic potentials (mEPSPs or mIPSPs). The frequency of these events is determined by the number of synaptic contacts onto the cell under

investigation and by the release probability of vesicles in the terminals. If the number of active release sites is assumed to be constant, then the frequency solely depends on the release probability, which is an important presynaptic parameter (see Equation 1). The amplitude of a single miniature event is termed the quantal content and depends on the amount of transmitter molecules in the vesicle and the postsynaptic ionotropic receptors being activated. As the vesicular filling is regarded to be constant, the amplitude of miniature events depends on the number and conductance of the postsynaptic receptors.

Large postsynaptic potentials measured after a presynaptic action potential are the summation of multiple vesicles being released at the same time. Thus, in a quantitative description, the postsynaptic signal ( $A$ ) depends on three parameters: the total number of vesicles ready to be released ( $n$ ), their release probability ( $p$ ), and the quantal content ( $q$ ):

$$(1) A = n \cdot p \cdot q$$

It has long been assumed that each active zone releases only one vesicle at a time (“one site, one vesicle” hypothesis), but the observation of multiquantal release events has challenged this dogma in recent years (Auger and Marty, 2000).

### 1.2.1 Vesicle pools and the vesicle cycle

During exocytosis,  $\text{Ca}^{2+}$  triggers the opening of a fusion pore and transmitter is released into the synaptic cleft. Vesicles that collapse into the presynaptic plasma membrane then have to be recovered, refilled with transmitter and translocated back to the so-called active zone, where they are rendered into a fusion competent state. An alternative mode of transmitter release has been suggested, in which vesicles might not undergo full fusion but instead only open a transient fusion pore that releases the vesicular content (Stevens and Williams, 2000). In this “kiss and run” mechanism the vesicle is preserved and can be reused immediately. However, the molecular machinery for this pathway is unknown, and doubts concerning its existence persist (Rizzoli and Jahn, 2007). The turnover of vesicles in the presynaptic terminal can be best illustrated as a vesicle cycle (Figure 1-1), with at least three different pools of vesicles (Rizzoli and Betz, 2005) and a set of proteins required for each step.

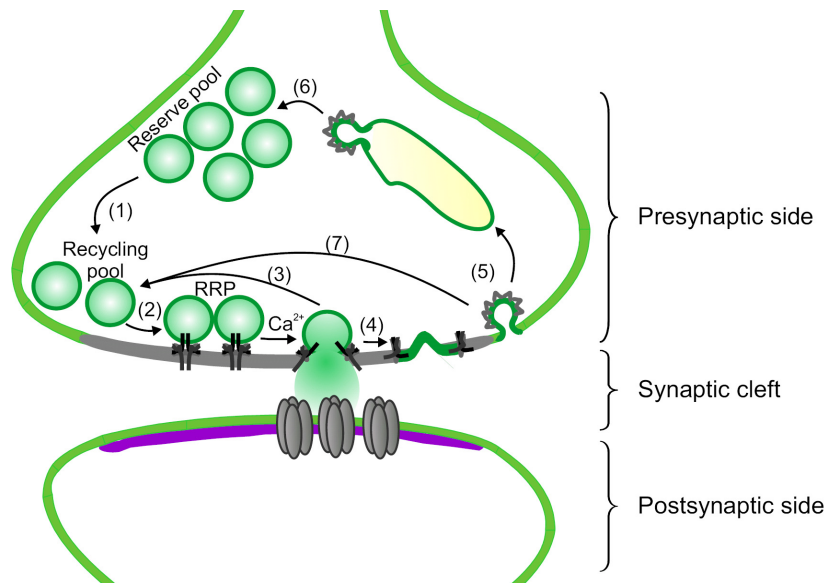


**Figure 1-1: The synaptic vesicle cycle and individual vesicle pools.**

Important steps during the vesicle cycle: (1) Recruitment from the reserve pool to the recycling pool, which occurs at a slow pace. (2) Refilling of empty slots in the active zone (dark grey), which is a fast process. Tethering, docking and priming that render vesicles fusion competent (readily releasable pool, RRP). Vesicles from the RRP can undergo  $\text{Ca}^{2+}$ -triggered exocytosis. (3) Fast recovery after “kiss and run” exocytosis. (4) Alternatively, vesicles undergo full fusion. (5) Clathrin-mediated endocytosis. (6) Budding from the endoplasmic reticulum and entry into the reserve pool. Alternatively, endocytotic vesicles may also be directly recycled (7). The complete turnover process only requires about 30 s to 1 min.

After fusion, the release machinery is disassembled by N-ethylmaleimide-sensitive fusion protein (NSF) and soluble NSF attachment proteins (SNAP) in an ATP consuming process. Vesicles are recovered by endocytosis at the periphery of the active zone, where clathrin coated membrane pits bud off the plasma membrane with the help of the GTPase dynamin. The so formed vesicles may either fuse with early endosomes, from which new vesicles are formed, or are directly uncoated and recycled. In both cases, refilling with transmitter occurs before the vesicles replenish empty slots in the active zone. Filled vesicles that have not yet entered the active zone constitute the recycling pool, which is supplied with vesicles from the reserve pool. In the active zone matrix, a Munc18- Syntaxin complex serves as vesicle tether for the docking of vesicles (Gerber, *et al.*, 2008), which is probably catalysed by Rab3 GTPases (Graham, *et al.*, 2008). The active zone is composed of so-called Rab3-effectors: Munc13s, RIMs (Rab3-interacting molecules), Piccolo and Bassoon, ERC (ELKS/Rab6-interacting protein/CAST) and liprins (for review see Schoch and Gundelfinger, 2006). These proteins help to “proofread” the assembly of the release machinery during the priming step, which renders the vesicles “fusion competent”, a process that further requires SM-proteins

(Sec1/ Munc 18-like proteins, see Rizo and Rosenmund, 2008). The collective of the fusion competent vesicles makes up the readily releasable pool (RRP), as defined in Equation 1 as the total number of vesicles ready to be released ( $n$ ). The core of the vesicular release machinery that mediates vesicle fusion is composed of three SNARE (Soluble (N-ethylmaleimide-sensitive fusion factor) Attachment Receptor) proteins, which I will discuss in more detail in the following section.

### 1.2.2 SNARE proteins mediate vesicle fusion

The three neuronal SNARE proteins comprising the core of the vesicular release machinery are syntaxin 1 and SNAP-25, which are located on the plasma membrane, and synaptobrevin, which is located in the vesicular membrane. During priming, syntaxin 1A and SNAP-25 form a complex with synaptobrevin by a four-helical coiled coil interaction of their SNARE-motives (Jahn and Sudhof, 1999), which tightly binds the vesicle to the plasma membrane (see Figure 1-2 A). Priming occurs in a two step process, namely, the nucleation of the SNARE complex, which is followed by a progressive amino (N)- to carboxy (C)-terminal tight zippering of the SNARE motives. In the fusion competent state, the SNARE complex is held in a metastable, high energy “trans”-conformation (Sorensen, 2009). The  $\text{Ca}^{2+}$ -triggered conformational change of the vesicular  $\text{Ca}^{2+}$ -sensor synaptotagmin (see below) moves the SNARE-complex into a “cis”-conformation and releases energy, which helps to overcome the energy barrier of merging two negatively charged phospholipids bilayers. Several SNARE complexes have to act in concert to coordinate vesicle fusion, but their exact number per vesicle (between 1 and 15) is still under debate (Montecucco, *et al.*, 2005; van den Bogaart, *et al.*, 2010). The central role of the SNARE proteins is reflected by the fatal action of toxins produced by *Clostridium botulinum* and *Clostridium tetani*. The toxins’ light chains are zinc metalloproteases that specifically cleave SNARE proteins and thereby abolish transmitter release (see Figure 1-2 B). SNAP-25 is cleaved by Botulinum toxin A (BoNT-A) at the C-terminus, as well as by BoNT-C and E. Syntaxin 1 is cleaved by BoNT-C, while synaptobrevin is cleaved by Tetanus toxin (TeNT) and BoNT-B, D and F (Schiavo, *et al.*, 2000). Similar to the effect of these toxins, AP-triggered release is entirely abolished in knockout animals (KO) of SNAP-25 and synaptobrevin, while spontaneous fusion of single vesicle is occasionally detected (Schoch, *et al.*, 2001; Washbourne, *et al.*, 2002). Interestingly, several isoforms have been described for all SNARE proteins, which are differentially

expressed in the brain and might have slightly different biophysical properties (Linial, 1997), but few detailed functional analyses of these have been carried out to date.

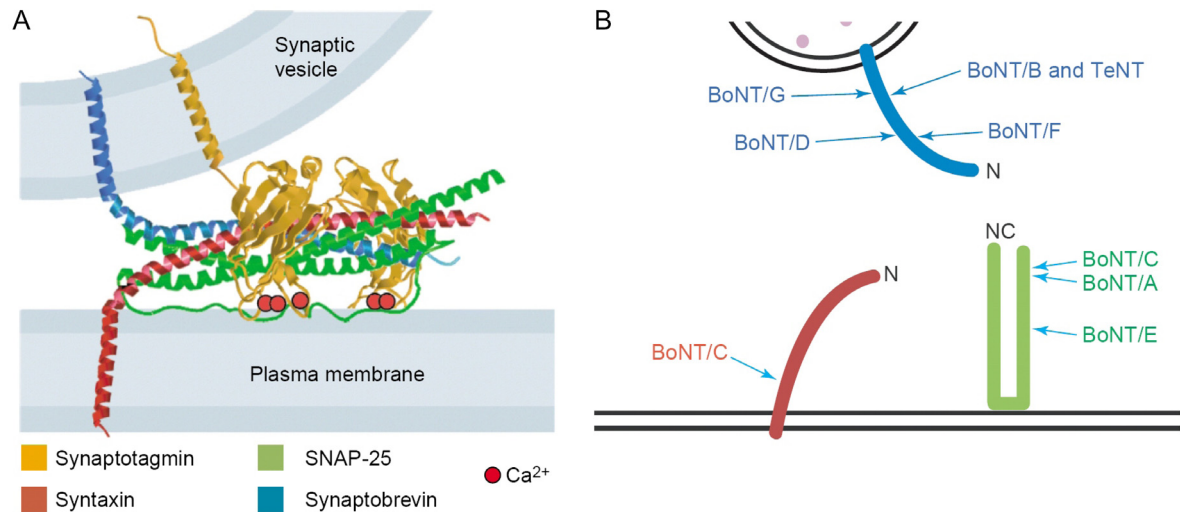


**Figure 1-2: The vesicular release machinery and clostridial toxin activity.**

(A) Structure of the SNARE complex together with synaptotagmin I. SNAP-25 contributes two SNARE motives to the four helical coiled coil.  $\text{Ca}^{2+}$  ions chelated by the C2A and C2B domains of synaptotagmin and the interaction of synaptotagmin with the plasma membrane are also indicated (taken from Koh and Bellen, 2003). (B) Schematic drawing illustrating the proteolytic cleavage sites of clostridial toxins within the SNARE proteins. Colour code as in A (from Breidenbach and Brunger, 2005).

### 1.2.3 Calcium triggers fast synaptic transmitter release

Synaptotagmin I, II and probably IX function as low affinity, fast  $\text{Ca}^{2+}$  sensors for neuronal transmitter release (Geppert, *et al.*, 1994; Pang, *et al.*, 2006; Xu, *et al.*, 2007). They contain two  $\text{Ca}^{2+}$ -binding C2 domains (C2A and C2B) and phospholipid binding domains. Their N-terminus is anchored in the vesicle membrane, while the C-terminus interacts with SNAP-25 and Syntaxin-1 (Sollner, *et al.*, 1993). It is still unclear how exactly  $\text{Ca}^{2+}$  binding to synaptotagmin mechanistically causes membrane fusion. According to a current model, a primed neurotransmitter vesicle faces a certain energy barrier that prevents it from fusing (Sorensen, 2009). Cooperative binding of  $\text{Ca}^{2+}$  to synaptotagmin induces a *cis* to *trans* conformational change of the SNARE complexes while completing the zippering of the SNARE's coiled coil interaction. This movement releases enough energy to cause fusion of the vesicle and plasma membrane and opening of the fusion pore.

At rest, the  $\text{Ca}^{2+}$  concentration in the cytosol is around  $0.1 \mu\text{M}$ , but is  $1.2$  to  $1.4 \text{ mM}$  in the extracellular fluid. This huge gradient causes rapid  $\text{Ca}^{2+}$  fluxes over the membrane once VDCCs are open. The microdomains of  $\text{Ca}^{2+}$  around the open channels are spatially limited by intracellular  $\text{Ca}^{2+}$  buffers and  $\text{Ca}^{2+}$  pumps that remove  $\text{Ca}^{2+}$  from the cytosol. The fast and temporally precise release of neurotransmitters is achieved by a very tight spatial arrangement of  $\text{Ca}^{2+}$  channels and fusion competent vesicles in the active zone. The  $\text{Ca}^{2+}$  sensor synaptotagmin binds  $\text{Ca}^{2+}$  with a half maximal effective concentration ( $\text{EC}_{50}$ ) of  $3\text{-}70 \mu\text{M}$ . Recordings at the Calyx of Held, a giant synapse in the auditory pathway, have shown that a  $\text{Ca}^{2+}$  concentration of only  $10 \mu\text{M}$  suffices to trigger release (Schneppenburger and Neher, 2000). Reported values for the apparent cooperativity of  $\text{Ca}^{2+}$  ions at the sensor are in the range of 3 to 5 (Koh and Bellen, 2003), which is reflected by the power of a non-linear function describing the relation of transmitter release and presynaptic  $\text{Ca}^{2+}$  (see 3.1, Equation 4).

Other  $\text{Ca}^{2+}$  sensors have been implicated in spontaneous release of single vesicles, including synaptotagmin XII and Doc2b (Maximov, *et al.*, 2007; Groffen, *et al.*, 2010). Whether and to which extent different  $\text{Ca}^{2+}$  sensors coexist on a single vesicle or whether they define different pools of release competent vesicles (Sara, *et al.*, 2005; Groemer and Klingauf, 2007) has not yet been resolved.

#### **1.2.4 Hyperosmotic solutions as fusogenic stimuli**

In 1952, Fatt and Katz found that hyperosmotic stimuli like sucrose solutions trigger vesicle release (Fatt and Katz, 1952). This mechanism was later utilized by Rosenmund and Stevens to experimentally probe the total number of vesicles in the RRP (Rosenmund and Stevens, 1996). Short application of  $500 \text{ mM}$  sucrose solutions onto single, self-innervating neurons in cultures (so-called autaptic cultures, see Figure 2-1 and Figure 2-4) causes all docked and primed synaptic vesicles to be rapidly released. Importantly, this form of transmitter release does not require influx of presynaptic  $\text{Ca}^{2+}$ . However, how hypertonic solutions lead to a fusion of primed vesicles is unclear. A possible explanation might be that hypertonicity induces shrinking and local infoldings of the plasma membrane, which drives proximal vesicles to collapse into the synaptic cleft. While sucrose shocks have to be regarded as an unphysiological technique for triggering exocytosis, they have proven invaluable for characterising the function of presynaptic proteins. The energy barrier for vesicle release can

---

be assessed in experiments with application of intermediate concentrations like 250 mM sucrose, as a weaker hypertonic stimulus releases only a fraction of vesicles from the RRP (Basu, *et al.*, 2007; Xue, *et al.*, 2010). The submaximal stimulus is less likely to cause exocytosis of vesicles that face a higher energy barrier for membrane, and consequently the proportion of vesicles released from the RRP by a weak stimulus is indicative for the energy barrier faced by primed vesicle.

Another fusogenic stimulus is  $\alpha$ -latrotoxin from the black widow spider venom, which causes exhaustive transmitter release by raising intracellular  $\text{Ca}^{2+}$  and by a second,  $\text{Ca}^{2+}$ -independent mechanism. The first effect relies on the pore forming action of the toxin, whereas the latter is not yet understood (Sudhof, 2001). This complex action of the toxin has hindered its widespread use in studies of synaptic vesicle release.

### **1.3 Presynaptic modulation of transmitter release**

Release of neurotransmitters is constantly modulated by intrinsic and extrinsic signals. This renders the coupling between action potential firing and transmitter release of a neuron highly variable and is an important level of signal computation, as it regulates to what extent the terminal translates an incoming action potential into transmitter release (Zucker and Regehr, 2002).

At the level of intrinsic modulation, the recent history of the neuron's activity heavily influences the probability of vesicle fusion. Accumulation of  $\text{Ca}^{2+}$  in the terminal during high frequency trains of action potentials can lead to an increase in release probability and a facilitation of transmission (von Gersdorff and Borst, 2002). On the other hand, repetitive action potential firing can deplete the RRP more rapidly than it is refilled, leading to synaptic short-term depression and even failure of transmission. Facilitation improves the signal to noise discrimination, while short-term depression is a synaptic form of adaptation, and both processes may even serve as synaptic working memory on short, milliseconds to seconds timescales (Mongillo, *et al.*, 2008). Intrinsic modulation is usually reversible, however, at some synapses, such as the hippocampal mossy fibre-CA3 synapse, excessive accumulation of  $\text{Ca}^{2+}$  induces a long-lasting increase of transmitter release, which represents a presynaptic form of long-term potentiation (LTP, for review see Nicoll and Schmitz, 2005).

Transmitter release is also constantly regulated by extrinsic modulators: All classes of neurotransmitters (see 1.1) and also growth factors, extracellular matrix proteins and cell-cell adhesion proteins have been demonstrated to affect the output from the presynaptic terminal (Südhof, 2008). The respective receptors and their subcellular signalling cascades are equally diverse: ionotropic receptors like kainate receptors, which are activated by glutamate, or nicotinic acetylcholine receptors; GPCRs that can be activated by members of all classes of neurotransmitters; receptor tyrosine kinases activated by peptide transmitters or cell-cell interacting proteins; and intracellular enzymes like the soluble guanylyl cyclase, which is activated by nitric oxide (NO).

The present thesis deals with presynaptic modulation by metabotropic auto- and heteroreceptors. In the following paragraphs I will therefore focus on GPCRs and their signalling properties, and review their physiological role in synaptic transmission. I will introduce in detail the GABA<sub>B</sub> receptor (GABA<sub>B</sub>R), which represents the major focus of my research.

### **1.3.1 Presynaptic signalling pathways of G-protein coupled receptors**

GPCRs are heptahelical transmembrane receptors with an extracellular N-terminus and an intracellular C-terminus. As their name implies, GPCR signalling is mainly transduced by guanine nucleotide-binding proteins (G-proteins), which are membrane attached, heterotrimeric proteins composed of an  $G\alpha$ ,  $\beta$  and  $\gamma$  subunit (see Figure 1-3). In absence of receptor activation, G-proteins are only loosely associated with GPCRs and have a GDP molecule (guanosine diphosphate) bound by the  $G\alpha$  subunit. Agonist binding to the extracellular part of the receptor causes conformational change of the transmembrane regions, tightly coupling the G-protein to the third intracellular loop and the C-terminus of the GPCR (Ahuja and Smith, 2009). This induces release of GDP and binding of GTP (guanosine triphosphate) by the  $G\alpha$  subunit. In the GTP bound state, the G-protein dissociates from the receptor and separates into the  $G\alpha$  subunit and a  $G\beta\gamma$  dimer, which can each activate downstream effector proteins. Their signalling is terminated by hydrolysis of GTP to GDP and  $P_i$  by the intrinsic GTPase activity of the  $G\alpha$  subunit, which results in re-association of the inactive heterotrimer and the receptor. The G-proteins are referred to as first messengers (of the receptor), while signalling molecules activated further downstream are called second messengers.

---

To date, 16 genes encoding  $G\alpha$  subunits have been identified, as well as 5 genes for  $G\beta$  and 12 for  $G\gamma$  subunits, resulting in a large number of potential combinations (Pierce, *et al.*, 2002). In principle, G-proteins are grouped according to the type of effector proteins the  $G\alpha$  subunit interacts with (see Figure 1-3):

$G\alpha_s$  proteins activate adenylyl cyclases, which generate cyclic adenosine-monophosphate (cAMP) as second messenger. cAMP is the main activator of protein kinase A (PKA), which phosphorylates serine and threonine residues of the target proteins. A number of presynaptic proteins downstream of  $Ca^{2+}$  influx are known PKA substrates, including SNAP-25, synapsin, snapin, rabphilin, and RIM1 $\alpha$  (Südhof, 2008). PKA activity accelerates synaptic vesicle recruitment, vesicle docking and vesicle fusion itself. cAMP also has other downstream targets, such as hyperpolarization-activated cyclic nucleotide gated (HCN) channels.  $G\alpha_s$ -mediated effects can be studied using cholera toxin, which specifically renders this class of G-proteins constantly active by ADP-ribosylation.

$G\alpha_i/G\alpha_o$  proteins have an antagonistic effect on  $G\alpha_s$  proteins by decreasing AC activity and thereby lowering cAMP levels. Consequently, their effect on transmission and the vesicle cycle in presynaptic terminals is inhibitory. Moreover, via  $G\beta\gamma$  subunits, they trigger important signalling pathways, which are not activated by other G-proteins. In neurons, these  $G\beta\gamma$  subunits can inhibit VDCCs and activate G-protein coupled inwardly-rectifying potassium channels (GIRKs).  $G\alpha_i/G\alpha_o$  protein signalling is abolished by pertussis toxin (PTX, produced by the bacterium *Bordetella pertussis*, which causes whooping cough), which ADP-ribosylates the  $G\alpha$  subunit and abolishes reassociation of the G-protein with the GPCR.  $G\alpha_i/G\alpha_o$  proteins are therefore often referred to as PTX-sensitive G-proteins.

$G\alpha_q/G\alpha_{11}$  proteins activate phospholipase C $\beta$  (PLC $\beta$ ), as do  $G\alpha_{11}$ ,  $G\alpha_{14}$ , and  $G\alpha_{15/16}$ . PLC $\beta$  additionally requires  $Ca^{2+}$  for activation, and hydrolyses phosphatidyl-inositol-diphosphate (PIP $_2$ ) into diacylglycerol (DAG) and inositol 1,4,5-trisphosphate (IP3), which function as second messengers. Both IP3 and DAG have a variety of downstream targets, and, among other effects, cause an increase in intracellular  $Ca^{2+}$  levels.

$G\alpha_{12/13}$  proteins are unusual as they directly target multiple downstream effectors, including Rho guanine nucleotide exchange factors, which, in turn, activate Rho family GTPases.

Most GPCRs are specific for one class of G-proteins. The selectivity is achieved by a stretch of five amino-acids at the C-terminus of the  $G\alpha$  subunit that binds to a specific pocket of the GPCR (Conklin, *et al.*, 1993). However, for many neurotransmitters, such as glutamate and acetylcholine, several different GPCRs with different coupling modes exist. For these transmitters, the type of GPCR expressed by the target cell determines whether the ligand has an excitatory or inhibitory effect. Conversely, metabotropic GABA<sub>B</sub>Rs couple only to  $G\alpha_i/G\alpha_o$  proteins, rendering this transmitter purely inhibitory.

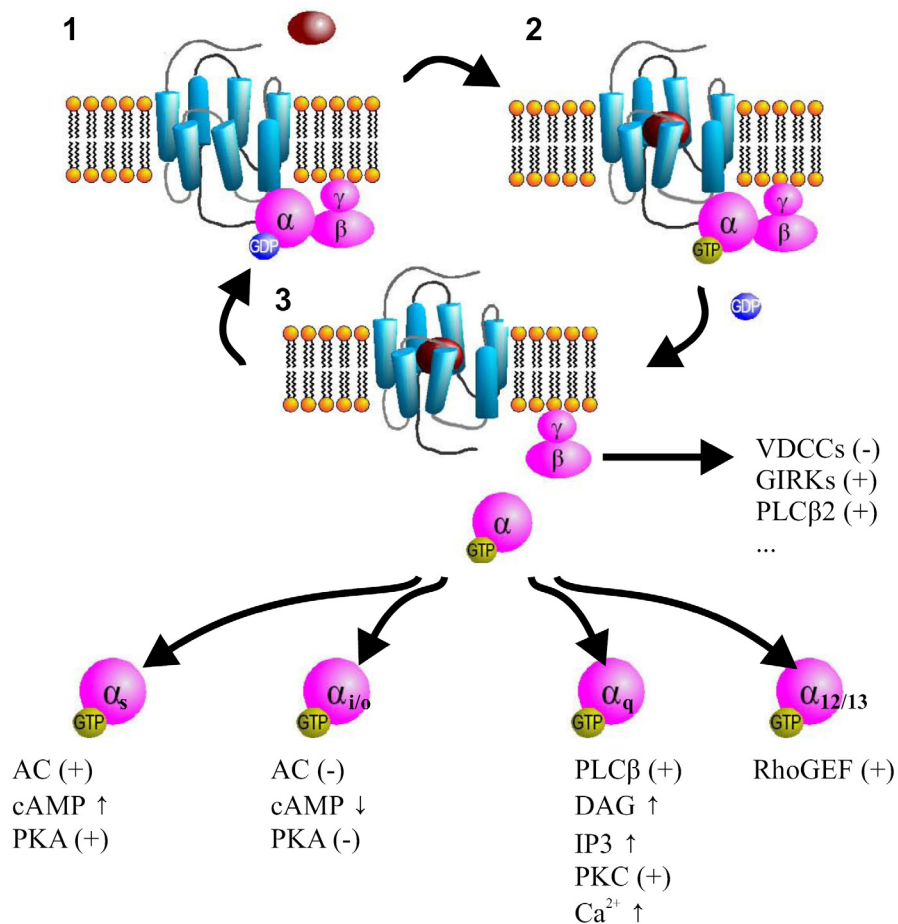


**Figure 1-3: Activation cycle of G-proteins by G-protein coupled receptors.**

Scheme illustrating metabotropic receptor signalling by heterotrimeric G-proteins: (1) Inactive GPCR – G-protein complex. (2) Agonist binding to GPCR, conformational change of the GPCR and GDP - GTP exchange by the G-protein. (3) Dissociation of activate  $G\alpha$  and  $G\beta\gamma$  subunits. GTP hydrolysis to GDP by the  $G\alpha$  subunit leads to re-association of the inactive complex. Adapted from <http://de.wikipedia.org/wiki/Datei:GPCR-Zyklus.png>. Lower panel: Some of the downstream signalling partners of activated G-proteins are indicated. (+) activation of enzyme; (-) inhibition of enzyme;  $\uparrow$  increase of second messenger levels;  $\downarrow$  decrease of second messenger levels.

---

### 1.3.2 Structure and function of GABA<sub>B</sub> receptors

GABA<sub>B</sub>Rs are Gα<sub>i</sub>/Gα<sub>o</sub>-coupled metabotropic receptors. Like all GPCRs, GABA<sub>B</sub>Rs have a heptahelical transmembrane topology, with a long extracellular N-terminus and intracellular C-terminus. Based on their structure and sequence homology, they are grouped together with metabotropic glutamate receptors (mGluRs) and calcium-sensing receptors. As most GPCRs are monomers, it was a surprising finding that GABA<sub>B</sub>Rs can only function as heterodimers (Kaupmann, *et al.*, 1998), comprising two subunits encoded by two different genes (GABA<sub>B</sub>R1 and GABA<sub>B</sub>R2). The two subunits interact by forming a coiled-coil of their intracellular C-termini. The GABA<sub>B</sub>R1 part is essential for ligand binding, whereas GABA<sub>B</sub>R2 relays the signal to the intracellular G-proteins (Huang, 2006). GABA<sub>B</sub>R2 has also been demonstrated as necessary for correct trafficking of the receptor complex from the endoplasmic reticulum to the surface (White, *et al.*, 1998). GABA<sub>B</sub>R1 has two different isoforms (GABA<sub>B</sub>R1a and b), which are generated by alternative start codon usage (Steiger, *et al.*, 2004). Dimers of GABA<sub>B</sub>R1b-GABA<sub>B</sub>R2 are postsynaptic receptors, whereas GABA<sub>B</sub>R1a-GABA<sub>B</sub>R2 dimers are presynaptic heteroreceptors in glutamatergic terminals (see Figure 1-4, and Perez-Garci, *et al.*, 2006; Vigot, *et al.*, 2006; Guetg, *et al.*, 2009). Both GABA<sub>B</sub>R1 isoforms are expressed at GABAergic terminals in the hippocampus, while GABA<sub>B</sub>R1a-containing heteromers function selectively as autoreceptors of cortical interneurons in layer V (Perez-Garci, *et al.*, 2006). A pair of protein interaction motifs called “sushi domains” in the extracellular tail of GABA<sub>B</sub>R1a serves as axonal targeting signal and is the only molecular difference between the two GABA<sub>B</sub>R1 isoforms (Biermann, *et al.*, 2010). While no pharmacological difference could be identified between different GABA<sub>B</sub>R heteromers, independent transcription of the GABA<sub>B</sub>1 subunits, regulated by cAMP-response element-binding protein (CREB), allows differential control of the number of GABA<sub>B</sub>Rs expressed at GABAergic and glutamatergic terminals, and may thereby present a tool for differentially fine-tuning the strength of presynaptic inhibition (Steiger, *et al.*, 2004).

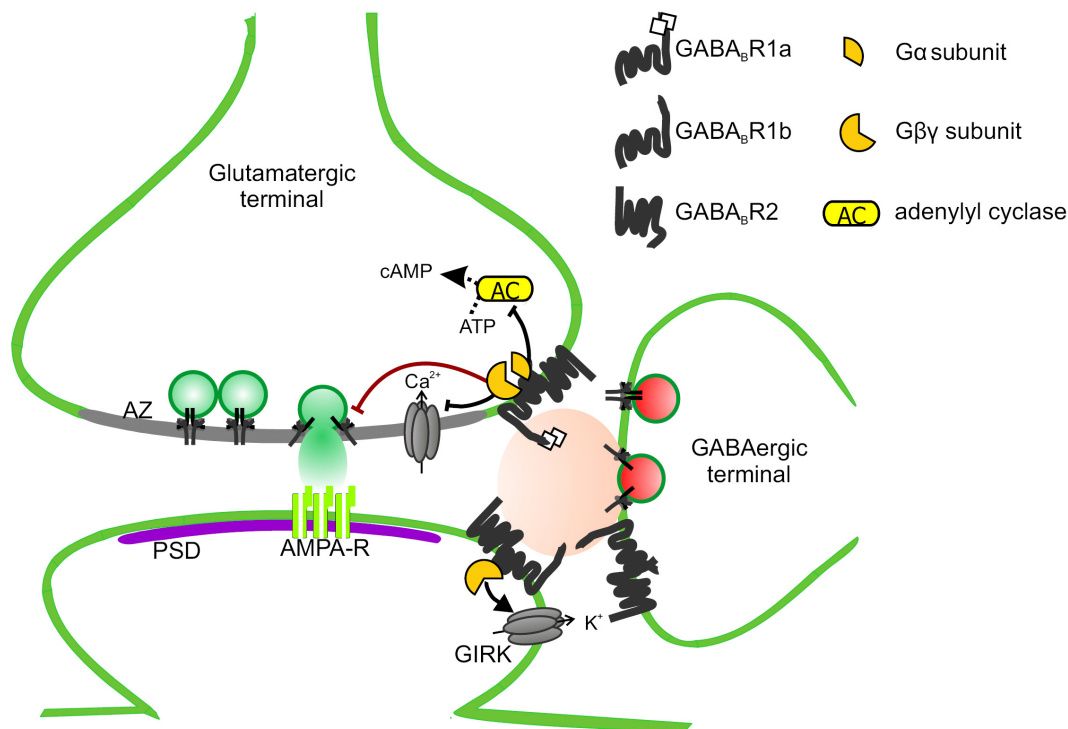


**Figure 1-4: GABA<sub>B</sub>R subunit distribution and GABA<sub>B</sub>R signalling in hippocampal neurons.**

Heterodimers of GABA<sub>B</sub>R1b and 2 localize to presynaptic terminals of interneurons and postsynaptic elements. GABA<sub>B</sub>R1a/2 dimers are selectively found in presynaptic terminals of glutamatergic neurons (diamonds indicate the GABA<sub>B</sub>R1a specific sushi domains). Via the Gβγ dimer, GABA<sub>B</sub>Rs inhibit Ca<sup>2+</sup> channels in the presynapse, but activate GIRK channels in the postsynaptic element. In all compartments, they reduce adenylyl cyclase activity via the Gα subunit. Although not shown in the figure, these signalling cascades also apply for the GABAergic terminal. Indicated in dark red is the direct interference of Gβγ subunits with the presynaptic release machinery. AZ: active zone; PSD: postsynaptic density.

Postsynaptic inhibition consists of a fast GABA<sub>A</sub>R component (<150 ms) followed by a slow component (up to 500 ms) mediated by GABA<sub>B</sub>Rs (Perez-Garci, *et al.*, 2006). Slow hyperpolarization is caused by GABA<sub>B</sub>Rs activating GIRKs (Newberry and Nicoll, 1984; Luscher, *et al.*, 1997). By lowering dendritic cAMP levels, GABA<sub>B</sub>Rs also decrease Ca<sup>2+</sup> flux through postsynaptic NMDA (N-methyl-D-aspartic acid) receptors (Chalifoux and Carter, 2010). Both actions reduce the excitability of the postsynaptic neuron. In presynaptic terminals, GABA<sub>B</sub>Rs and other inhibitory GPCRs reduce transmitter release via G-protein Gβγ subunits that inhibit depolarization-induced opening of N- and P/Q-type Ca<sup>2+</sup> channels (Wu and Saggau, 1995; Isaacson, 1998). Free Gβγ dimers diffuse in a membrane-delimited manner and directly interact with VDCCs, causing a shift of the channel's activation potentials to more positive voltages (Takahashi, *et al.*, 1998; Kajikawa, *et al.*, 2001). This

---

direct modulation is sensitive to Pertussis toxin, and can be reversed by strong depolarization. In terms of the non-linear dependency of transmitter release on presynaptic  $\text{Ca}^{2+}$ , already a mild decrease of  $\text{Ca}^{2+}$  influx through VDCCs is a powerful instrument to effectively modulate neuronal communication (Dodge and Rahamimoff, 1967; Wu and Saggau, 1997; Schneggenburger and Neher, 2005).

### **1.3.3 Presynaptic metabotropic inhibition independent of calcium channels**

In recent years a number of studies have presented evidence that inhibitory GPCRs can trigger a presynaptic signalling cascade that inhibits transmitter release independently of VDCCs. Adenosine receptors were shown to reduce the frequency of mEPSCs in dissociated hippocampal neuronal cell cultures (Scholz and Miller, 1992). The effect was blocked by pre-treatment with Pertussis toxin, but not occluded by blockage of VDCCs with cobalt ions. Activation of  $\text{GABA}_B$ Rs or adenosine receptors also reduced the frequency of mEPSCs in recordings from CA3 pyramidal neurons in hippocampal slice cultures, while the frequency of both mEPSCs and mIPSCs was not altered by blocking VDCCs with cadmium (Scanziani, *et al.*, 1992). Furthermore,  $\text{GABA}_B$ Rs, but not adenosine receptors, were shown to decrease mEPSC frequencies in recordings from rat cerebellar Purkinje cells (Dittman and Regehr, 1996). Metabotropic adenosine and  $\text{GABA}_B$  receptors also inhibit transmitter release evoked artificially by ionomycin and  $\alpha$ -latrotoxin, which occurs independently of VDCCs (Capogna, *et al.*, 1996). Experiments combining  $\text{Ca}^{2+}$  imaging and EPSC measurements at cerebellar granule cell-to-Purkinje cell synapses demonstrated that inhibition of presynaptic  $\text{Ca}^{2+}$  channels alone could not cause the strong inhibition of transmitter release by  $\text{GABA}_B$ Rs. The reduction of the postsynaptic signal after  $\text{GABA}_B$ R activation exceeded the effect of a selective reduction of  $\text{Ca}^{2+}$  influx equivalent to the inhibition of presynaptic  $\text{Ca}^{2+}$  influx by  $\text{GABA}_B$ Rs (Dittman and Regehr, 1996). Experiments at hippocampal mossy fibre terminals showed very similar results (Vogt and Regehr, 2001). Together, these experiments indicate a  $\text{Ca}^{2+}$ -independent component of presynaptic inhibition, not only for spontaneous, but also for evoked transmitter release.

Mechanistically, two scenarios could explain  $\text{Ca}^{2+}$ -independent presynaptic inhibition: firstly, a reduction of cAMP levels caused by the G-protein  $\text{G}\alpha$  subunit, and consequently a reduced level of PKA-mediated phosphorylation; or secondly, a further  $\text{G}\beta\gamma$  subunit-dependent pathway that acts “downstream” of  $\text{Ca}^{2+}$  influx. In a study at the Calyx of Held, Sakaba and

Neher thoroughly investigated the consequences of lowering presynaptic cAMP levels by GABA<sub>B</sub>R activation (Sakaba and Neher, 2003). They found that presynaptic GABA<sub>B</sub>Rs retard vesicle priming during sustained release activity. Specifically, Gα<sub>i</sub>-protein signalling reduced the activity of the cAMP-dependent guanine nucleotide exchange factor, which cooperates with Ca<sup>2+</sup>/calmodulin to recruit vesicles to the active zone. However, they did not describe fast, Ca<sup>2+</sup>-independent inhibition of vesicle fusion. Studies on serotonergic modulation of transmission in the lamprey spinal cord have provided evidence that Gβγ subunits might directly target the SNARE complex member SNAP-25 (Blackmer, *et al.*, 2001). Gβγ subunits were shown to directly interact with SNAP-25 and thereby to compete with synaptotagmin I for binding to the SNARE complex, reducing transmitter release (Blackmer, *et al.*, 2005; Gerachshenko, *et al.*, 2005). Direct binding of SNAP-25 by Gβγ subunits and inhibition of transmitter release was reduced when preparations were incubated with Botulinum neurotoxin A, and the binding site was thus mapped to the C-terminus of SNAP-25. In the mammalian central nervous system, presynaptic inhibition by noradrenaline in the lateral division of the central amygdala were shown not to affect Ca<sup>2+</sup> influx, but to act by a Ca<sup>2+</sup>-independent mechanism (Delaney, *et al.*, 2007). Noradrenergic inhibition was reduced upon incubation of the slice preparation with BoNT-A, which was interpreted as in line with the aforementioned studies. Yet it remains to be clarified whether Ca<sup>2+</sup>-independent presynaptic inhibition is synapse- and receptor-specific, or should be regarded as a general principle. Thus, a question of interest is whether Ca<sup>2+</sup>-independent presynaptic inhibition by adenosine and GABA<sub>B</sub> receptors also depends on SNAP-25 as the target of direct inhibition of synaptic transmitter release. We therefore chose to investigate mechanisms of presynaptic inhibition by GABA<sub>B</sub>Rs at glutamatergic synapses in the hippocampal formation.

#### **1.4 The hippocampus and its principal neurons**

The hippocampus is a three-layered archicortical structure embedded in the medial temporal lobe. It is part of the hippocampal formation that also comprises the adjacent brain areas of entorhinal cortex (EC), subiculum and parasubiculum. Using a silver-staining method invented by and named after Camillo Golgi, early neuroscientists described the principal cytoarchitecture of the hippocampus, and in 1934 Rafael Lorente de Nó termed its main regions the dentate gyrus, CA3, and CA1 (after *cornu ammonis*, or Ammon's horn, see Figure 1-5). The principal glutamatergic neurons of the hippocampus are embedded in a mainly

unidirectional trisynaptic circuitry (Andersen, *et al.*, 2006). Here, granule cells in the dentate gyrus receive inputs via the perforant path from layer II cells of the entorhinal cortex (EC). They relay the signal to CA3 pyramidal cells via their axonal projections, termed mossy fibres, which form their synapses in a narrow band above stratum pyramidale called *stratum lucidum*. From CA3, the signal is forwarded to CA1 pyramidal cells via Schaffer collaterals, which form the third synapse of the trisynaptic circuitry. Pyramidal cells from CA1 project back to layer V and VI of the EC. However, with the later discovery of direct EC-CA3, EC-CA1 and CA1-subiculum projections, it became clear that the trisynaptic circuit represents only a partial wiring diagram of the hippocampal formation.

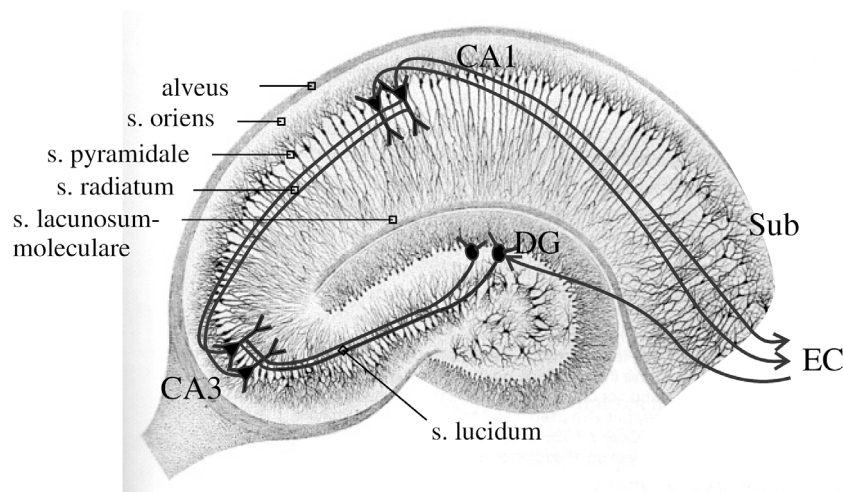


**Figure 1-5: Principal neurons of the hippocampal formation and their connectivity.**

A classical Golgi stain drawing of a sagittal hippocampal slice of a newborn kitten, overlaid with the excitatory trisynaptic circuitry of the principal neurons. DG: dentate gyrus, CA: *cornu ammonis*, Sub: subiculum, EC: entorhinal cortex, s.: *stratum*. Adapted from Camillo Golgi, first published in 1883, republished in Golgi, *et al.*, 2001).

The hippocampus has been a major area of research in neuroscience over decades for several reasons. Firstly, it is a fascinating object of study from a functional point of view, as it is crucially involved in episodic memory formation (Scoville and Milner, 1957), spatial navigation, and in the manifestation of pathophysiological conditions such as Alzheimer's disease and temporal lobe epilepsy. Secondly, compared to the seven-layered organisation of neocortical areas, the simple, three laminar structure comprising the *stratum radiatum* and *stratum lacunosum-moleculare* (apical dendrites), *stratum pyramidale* (cell bodies) and *stratum oriens* (basal dendrites) has greatly facilitated electrophysiological and morphological studies (see Figure 1-5). Several important neurophysiological discoveries have been made in the hippocampus, such as the identification of excitatory and inhibitory synapses, long-term

potentiation and depression, and the role of oscillations in neuronal networks (for review see Andersen, *et al.*, 2006).

Two very different preparations of hippocampal tissue were used for the work presented here, namely, acute hippocampal slice preparations of adult mice, and cell cultures of hippocampal neurons prepared from newborn mice and grown *in vitro* for up to three weeks. The synaptic connectivity of the hippocampus can be nicely preserved for several hours in acute brain slices and can be investigated using electrophysiological field recordings, whole cell patch clamp experiments and functional  $\text{Ca}^{2+}$  imaging. Hippocampal neurons in culture replicate basic *in vivo* synapse formation, and can be used for electrophysiological and biochemical experiments between 8 and 20 days *in vitro* (DIV). We primarily used the so-called autaptic culture preparation of isolated, self-innervating glutamatergic neurons (see 2.1.2) and focussed in particular on the differences between granule cells and pyramidal cells in these cultures (see 3.2.4).

### **1.5 Attempts to investigate neural circuitries by silencing specific neuronal populations**

Despite the simple anatomical organization of the hippocampus emphasized in the preceding paragraph, the hippocampal network is formed by interaction between multiple different neuronal cell types. These neurons, either excitatory or inhibitory, can generate complex patterns of activity, which depend on the behavioural state of the animal. The different forms of hippocampal network oscillations have been implicated in the formation and retrieval of hippocampus-dependent memory (Andersen, *et al.*, 2006). On the other hand, malfunction of the hippocampal network can lead to conditions such as temporal lobe epilepsy. For neuroscientists, elucidating the roles of the individual types of neurons in the hippocampal network is therefore of great interest. A classical experimental strategy to study complex biological systems is the deduction of a single component's functions by inactivation or ablation of the component. With the development of gene-knockout models, inactivation of genes has become a standard technique in modern biology. In comparison, the inactivation of individual cells or cell types in the CNS to study their function has proven more difficult (Wulff and Wisden, 2005; Luo, *et al.*, 2008). The ideal method to inactivate neurons for studying their role in the network and in the behaving animal should be a specific, rapid, and reversible silencing of the activity of a defined population of neurons, without invasive

---

manipulation of the animal. A number of studies attempted to achieve this by several approaches, particularly in the previous two decades (Table 1, see also for references). Apart from classical lesion studies, a commonly used method has been the local inactivation of neurons by drug infusion or cooling of tissue, which is rapid and reversible, but not specific. More specific is the expression of toxins in genetically defined neuronal populations to either kill neurons or inactivate transmitter release. However, once a toxin is expressed, its effect is usually not reversible, or, if an inducible system (such as tetracycline-regulated conditional expression) is used, only over very long time-scales. Furthermore, the slow onset of toxin expression and irreversible effects might lead to compensatory network rearrangements. Recent developments have focused on the combined use of targeted, transgenic expression of artificial receptors and subsequent, time-controlled, rapid activation of these by exogenous, receptor-specific ligands. The receptor-ligand systems described to date silence neuronal activity via hyperpolarization of the membrane potential, with exception of the MIST system (molecules for inactivation of synaptic transmission). These systems have several drawbacks. Firstly, their chemical ligands are usually difficult to apply, as they do not easily penetrate the blood-brain barrier, or, in the case of light-activated chloride pumps, require fibre optics implantations. Secondly, in most of these systems, the receptor needs to be expressed at very high levels and, in the case of the allatostatin receptor, high endogenous GIRK expression is also necessary, which is not the case in all neurons. These method-inherent disadvantages have prevented their widespread use. Recently, a novel, artificial GPCR was developed by molecular evolution, which was designed to overcome the limitations of the available methods for silencing neuronal activity (Armbruster, *et al.*, 2007). The so-called hM4D receptor (human muscarinic type 4-like designer receptor) is selectively activated by clozapine-N-oxide (CNO), which is a small, blood-brain barrier permeant molecule that has no activity on any known endogenous receptor. The hM4D receptor couples to inhibitory  $G\alpha_i/G\alpha_o$  proteins and was described as hyperpolarizing neurons by GIRK-channel activation. The features of the receptor described in the initial publications prompted us to study the neurophysiological action of hM4D in more detail, including its potential application in transgenic animals to investigate neuronal networks (see Chapter 3.3).

Table 1: Published methods to artificially silence neurons in the mammalian brain.

Method, References	Mechanism	Limitations
Local inactivation of brain tissue a) cooling b) drug infusion (for review see Lomber, 1999)	General inactivation of neuronal activity or signalling.	Not cell type-specific, targeting for deeper brain structures difficult, requires implants.
Genetically encoded toxins: a) Tetanus toxin (Yamamoto, <i>et al.</i> , 2003) b) Ca <sup>2+</sup> channel toxins (Ibanez-Tallon, <i>et al.</i> , 2004) c) Diphtheria toxin receptor-mediated cell ablation (Luquet, <i>et al.</i> , 2005)	Abolish transmitter release by a) cleavage of synaptobrevin or b) blocking of Ca <sup>2+</sup> influx. c) Injection of diphtheria toxin to kill neurons .	Slow onset, irreversible, compensation by network adaptation.
Genetically encoded inhibitory G-protein coupled receptors: a) Allatostatin receptor (Lechner, <i>et al.</i> , 2002) b) Selective expression of serotonin receptor 1A (Tsetsenis, <i>et al.</i> , 2007)	Activation of postsynaptic GIRK channels hyperpolarizes neurons.	a) Allatostatin not blood-brain barrier-permeable b) requires Htr1a KO mice. Transgene activated by endogenous serotonin.
Genetically encoded inhibitory ionotropic receptors: a) Glutamate gated chloride channel (GluCl) activated by Ivermectin (Slimko and Lester, 2003) b) Expression of the zolpidem-sensitive $\gamma$ 2-subunits of GABA <sub>A</sub> Rs in $\gamma$ 2-KO mice (Wulff, <i>et al.</i> , 2007) c) Halorhodopsin: light-driven chloride pump (Han and Boyden, 2007; Zhang, <i>et al.</i> , 2007)	Hyperpolarization of neurons by chloride ion influx (excitatory in the early postnatal brain).	a) Ivermectin modulates GABA <sub>A</sub> R and is toxic. GluCl is activated by endogenous glutamate. b) Only positive allosteric modulator of GABA <sub>A</sub> Rs, requires GABAergic inputs and co-expression of $\alpha$ 1- $\alpha$ 3. c) Requires high expression levels and fibre optic implantations.
Inhibition of transmitter release: Molecules for inactivation of synaptic transmission (Karpova, <i>et al.</i> , 2005)	Drug-induced dimerization of modified synaptobrevin and synaptophysin abolishes synaptic transmission.	Weak blood-brain barrier penetration of drugs, high over-expression of transgenes required.

---

## 1.6 Aims of this work

Our goal was the characterization of the molecular mechanisms underlying presynaptic inhibition additional to and independent of VDCCs in the hippocampus. As will be presented in the first part of the results section, we began by investigating the modulation of evoked and spontaneous glutamatergic transmission by GABA<sub>B</sub>Rs at Schaffer collateral synapses in CA1. We found evidence that this presynaptic inhibition consists of a VDCC-dependent and a second, VDCC-independent component. Based on the literature we hypothesized that G-protein signalling potentially interferes directly with SNAP-25 in the release machinery, as a molecular mechanism underlying the VDCC-independent pathway. To test this hypothesis, we established autaptic cultures of pyramidal neurons. We firstly studied how GABA<sub>B</sub>R signalling affects the energy barrier of vesicle fusion as an indicator for release machinery efficacy. Secondly, we tested whether SNAP-25 is the target of VDCC-independent presynaptic inhibition by cleaving the protein with botulinum neurotoxin A.

We further wanted to know whether VDCC-independent presynaptic inhibition by GABA<sub>B</sub>Rs also exists at other glutamatergic synapses. To address this question, we investigated hippocampal mossy fibre synapses, which are physiologically very different from Schaffer collateral synapses. Using slice preparations and by combining Ca<sup>2+</sup> imaging with electrophysiology, we studied the impact of GABA<sub>B</sub>R activation on presynaptic Ca<sup>2+</sup> influx and the field postsynaptic excitatory potential. We further established autaptic cell cultures of hippocampal granule cells and characterized morphological and physiological parameters of this cell culture model. These cultures allowed us to record pure mossy fibre mEPSCs, which we used to investigate the modulation of spontaneous vesicle fusion by GABA<sub>B</sub>Rs in the absence of Ca<sup>2+</sup>.

Part three of the results section illustrates the potential of presynaptic inhibition as a powerful biological principle to silence the output of neurons. We expressed the novel, artificially designed metabotropic receptor hM4D in autaptic cultures and found that it drastically reduces transmitter release when activated by a specific drug. We have begun developing a mouse model that will allow targeted expression of the receptor in genetically defined groups of neurons. In the future, this transgenic approach will enable acute inhibition of transmitter release from neurons in slice preparations or even in the behaving animal *in vivo*.



---

## 2 Materials and experimental methods

All experiments including animals were performed according to the regulations of Berlin animal experiment authorities and the animal welfare committee of the Charité Berlin.

### 2.1 Cell culture

#### 2.1.1 Media and solutions

Reagents and media were purchased from Gibco (Invitrogen, Carlsbad, CA, USA) and Sigma-Aldrich (St. Louis, MO, USA), if not stated otherwise. Standard cell culture flasks and dishes were purchased from TPP (Trasadingen, Switzerland) and Nunc (Thermo Fisher Scientific, Langenselbold, Germany). The following media and solutions were used for cell culture work:

##### Growth-permissive stamp solution

10 mM acetic acid  
0.85 mg/ml collagen  
0.1 mg/ml poly-d-lysine

##### Astrocyte growth medium

BME (basal medium eagle)  
10% fetal calf serum  
1 mM Glutamax  
0.2% penicillin-streptomycin  
10 mM Hepes  
5 mM glucose  
2.5 µg/ml insulin

##### Neurobasal A medium

Neurobasal A  
2 mM Glutamax  
0.2% penicillin-streptomycin  
2% B27 supplement

##### Papain solution (Papain Dissociation System, Worthington)

20 U/ml Papain  
1 mM L-cysteine  
0.5 mM EDTA  
100 U/ml Deoxyribonuclease I  
in EBSS

##### HEK cell medium

DMEM low glucose  
10% fetal calf serum  
1 mM Glutamax  
0.2% penicillin-streptomycin

### 2.1.2 Material

Microdot stamp	Custom made by the medical technical laboratories of the Charité, Universitätsmedizin Berlin
Surgical instruments	World Precision Instruments (WPI), Berlin, Germany
Coverslips, 30 mm	Hecht Assistant 1001, Sondheim, Germany
Papain dissociation system	Worthington, Lakewood, NJ, USA
Fugene transfection reagent	Fugene 6, Roche Applied Science, Mannheim, Germany
Cell culture microscope	Olympus CKX31, Olympus Hamburg, Germany
Life cell imaging microscope	Olympus IX61 with “Cell M” imaging system, Olympus Hamburg, Germany
Incubator	Heracell, Heraeus (now Thermo Fisher Scientific, Langenselbold, Germany)

### 2.1.3 Autaptic cultures

Microdot autaptic cultures were prepared according to modified protocols (Furshpan, *et al.*, 1976; Bekkers and Stevens, 1991; Pyott and Rosenmund, 2002). The cultivation of hippocampal neurons in autaptic cultures involved a number of preparation steps, described in the following paragraphs and illustrated in Figure 2-1 A.

#### 2.1.3.1 Preparation of coverslips

Coverslips of 30 mm diameter were cleaned in 1 M HCl overnight, rinsed twice with water and stored in 100% ethanol. Before transfer to six-well plates, they were briefly flamed to remove the alcohol, and afterwards coated with liquefied 0.15% agarose type IIa (Sigma-Aldrich). Agarose was dried for more than 48 h at room temperature, forming a thin film that prevents cell attachment. A custom-made stamp (0.2 mm spot diameter and 0.5 mm spot interspace, Figure 2-1 B) was used to print microdots of the growth-permissive stamp solution. Plates were UV-sterilised and stored at 4°C until further use.

#### 2.1.3.2 Astrocyte cultures

Newborn Sprague Dawley rats or C57/BL6-N mice were decapitated; the brains were removed and quickly transferred into ice-cold Earle’s balanced salt solution (EBSS) in a Petri dish. The cortical hemispheres were cleaned from meninges and vascular tissue with fine tip forceps and minced with a small scalpel. Throughout these preparation steps, care was taken

to maintain the low temperatures of the solution. Tissue pieces were digested enzymatically with 0.25% trypsin for 10 min at 37°C under mild shaking. Remaining pieces were slowly triturated with a 1 ml pipette tip to obtain a single-cell suspension. The cloudy supernatant was transferred to a new cup while avoiding undissociated tissue. Cells were centrifuged at 300x g for 7 min and resuspended in astrocyte growth medium. Cells were plated at densities of  $4 \times 10^4$  or  $8 \times 10^4/\text{cm}^2$  (rats or mice, respectively) in T75 flasks and cultivated for up to 7 days. Once astrocytes had reached confluency, they were trypsinized and  $4 \times 10^4$  cells/well were seeded on microdot plates in astrocyte growth medium. When cells fully covered the microislands (Figure 2-1 C), glia proliferation was attenuated by exchanging astrocyte medium with Neurobasal A medium.

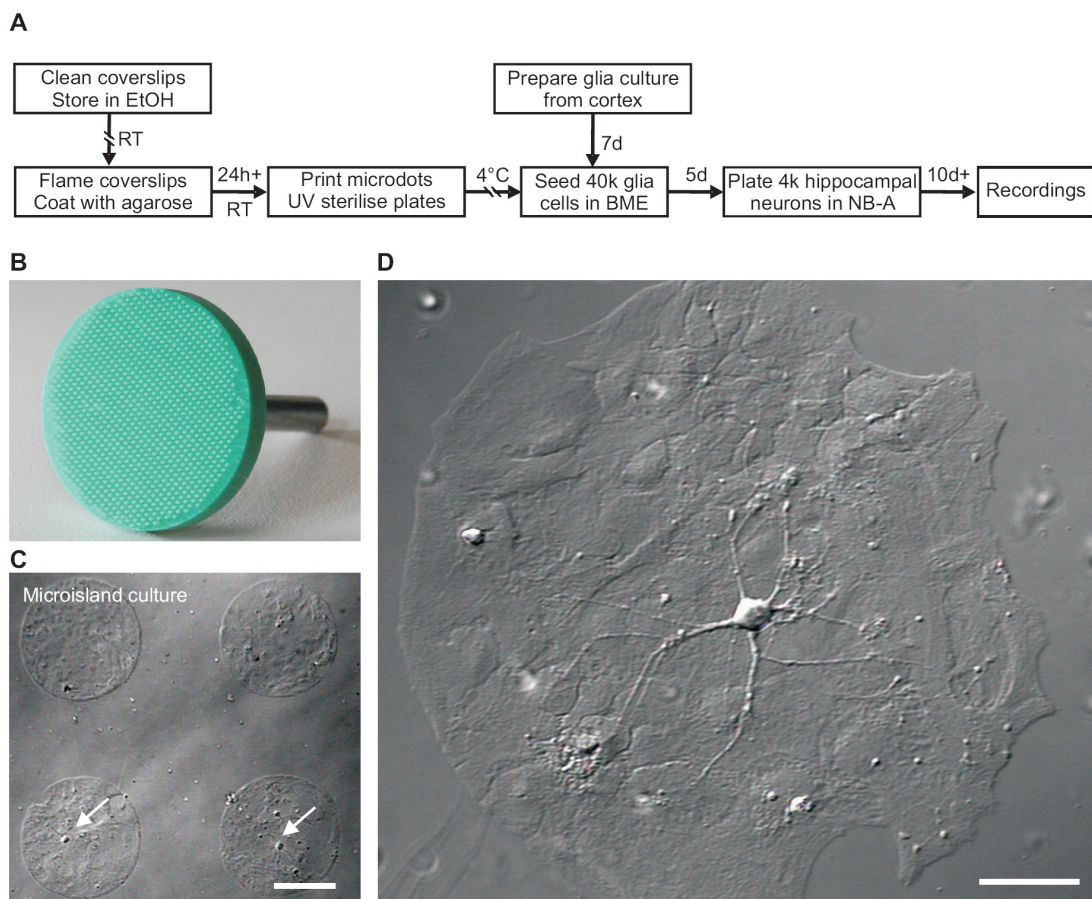


**Figure 2-1: Autaptic culture preparation.**

(A) Flow chart of the preparation steps of autaptic neuronal cell cultures, indicating minimum time requirements. (B) Microdot stamp used for prints of growth-permissive substrate. Stamp diameter is 30 mm, spot diameter is 0.2 mm and spot interspace is 0.5 mm. (C) Regularly spaced micro-islands formed by astrocytes. Single neurons are indicated by arrows (scale bar: 200  $\mu\text{m}$ ). (D) Higher magnification of a neuron on a glia island, observed with differential interference contrast microscopy (DIC) and Olympus LumPlan FI 20 $\times$ 0.5 water-immersion objective (scale bar 50  $\mu\text{m}$ ).

### 2.1.3.3 Neuronal cultures

Hippocampi were removed from P0 rats or mice and placed in cold EBSS. Neurons were isolated with the “*Papain Dissociation System*” according to the manufacturer’s instructions (Worthington, Lakewood, NJ, USA). Briefly, the tissue was placed in 2 ml of a papain solution and incubated for 1 h at 37°C under mild agitation. After trituration with a 1 ml pipette tip, cells were centrifuged at 300 x g for 5 min. Cells were resuspended in EBSS and layered on a mix of ovomucoid protease inhibitor and bovine serum albumin and centrifuged at 70 x g for 6 min. Debris and dead cells remained in the supernatant, while living cells were resuspended from the pellet.

For autaptic cultures we found that plating  $4 \times 10^3$  cells/well for mice and  $3 \times 10^3$  cells/well for rats in Neurobasal A medium yielded substantial numbers of islands with single neurons (Figure 2-1 C). For protein isolation we plated  $8 \times 10^6$  cells/well in six-well plates that were beforehand coated with growth-permissive stamp solution. Half of the Neurobasal A medium was replaced once a week to prevent proliferation of astrocytes. Cells were used for electrophysiology, immunocytochemistry and protein isolation between 10 and 20 days *in vitro* (DIV) to allow for full maturation of functional synapses (Basarsky, *et al.*, 1994; Gomperts, *et al.*, 2000).

To obtain autaptic cultures enriched for hippocampal granule cells (3.2.4), we separated the dentate gyrus from the hippocampal formation. Under a Zeiss stereo microscope a scalpel was moved longitudinally along the hippocampal fissure to peel away the CA3/CA1 region, which forms the outer and bigger curvature of the banana-shaped hippocampal formation (Figure 2-2 A). Granule cells were isolated using the Worthington dissociation system as described above and grown on glial microislands for 10 to 20 DIV. Using differential interference contrast (DIC) video-microscopy it became evident that autaptic hippocampal granule cells and pyramidal cells often differ in their morphology (Figure 2-2 B). Somata of granule cells are usually less prominent and have fewer primary dendrites than pyramidal cells, but this distinction alone was not conclusive. We therefore had to establish anatomical and functional markers to distinguish autaptic granule cells from non-granule cells in our cultures (see 3.2.4).

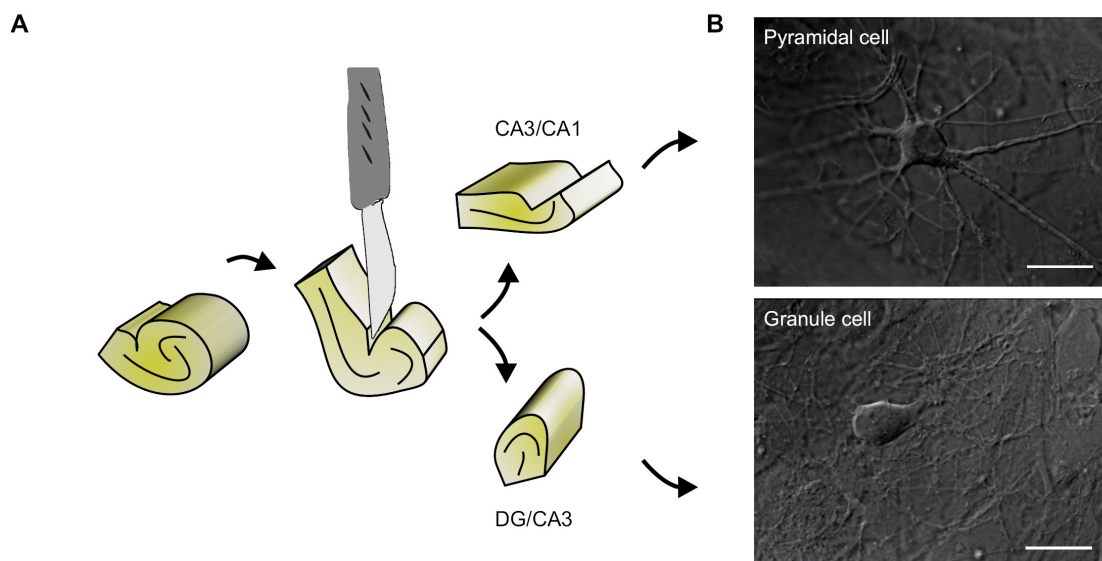


**Figure 2-2: Hippocampal granule cell preparation and morphological characterization of autaptic hippocampal neurons.**

(A) Enrichment of granule cells is achieved by separating the dentate gyrus (DG) from CA3 and CA1. A small blade is used to cut longitudinally along the hippocampal fissure. (B) Typical morphology of pyramidal and granule cells, observed with DIC optics (Olympus LumPlan FI 60×0.9 NA water-immersion objective). Cells were identified by electrophysiology and application of an agonist for metabotropic glutamate receptors 2/3 (see 3.2.4.1). Scale bars in B: 25  $\mu\text{m}$ .

#### 2.1.4 Expression of recombinant proteins in HEK293 cells

HEK293 (human embryonic kidney cells, purchased from Biocat, Heidelberg, Germany) were maintained in T75 flasks for up to 15 passages. For transient transfection they were detached with 0.25% trypsin and seeded into six-well plates at a density of  $2 \times 10^5$  cells/well. 24 h later (at ~70% confluence) they were transfected using Fugene 6 reagent according to the manufacturer's instructions: For each well, 2  $\mu\text{g}$  DNA was mixed with 3  $\mu\text{l}$  Fugene in a final volume of 100  $\mu\text{l}$  Optimem and incubated for 30 min at room temperature. The resulting DNA/lipid complexes were drop-wise added to the cultures; and cells were analyzed 48-72 hours later.

#### 2.1.5 Lentivirus production

For the expression of hM4D as recombinant protein in autaptic neurons (3.3.3) we were provided with lentiviral particles that were kindly produced by Dr. Ralf Nehring from the Rosenmund lab at Baylor College, Houston, TX, USA, according to published protocols (Lois, *et al.*, 2002; Xue, *et al.*, 2009).

## 2.2 Electrophysiology

### 2.2.1 Material

Vibratome	VT 1200 Leica, Wetzlar, Germany
Amplifier and digitizer	Axopatch 200A, Multiclamp 700 A or Multiclamp 700B, Molecular Devices, Toronto, Canada
Digitizer	BNC 2090 or USB 6229, both National Instruments, Austin, Texas, USA; or Digidata 1322a, Molecular Devices, Toronto, Canada
Extracellular stimulation unit	Iso Flex, A.M.P.I, Jerusalem, Israel
Stimulus generator	Master 8, A.M.P.I, Jerusalem, Israel
Oscilloscope	HG-1507-3, HAMEG Instruments, Mainhausen, Germany
Glass electrode puller	DMZ universal puller, Zeitz-Instrumente, Munich, Germany
Glass pipettes	Science products, Hofheim, Germany
Ag/AgCl electrode	Science products, Hofheim, Germany
Bath electrode	Science products, Hofheim, Germany
Upright microscopes	Olympus BX-51WI, equipped with Differential Interference Contrast (DIC) optics and video microscopy Olympus LumPlan FI 60x 0.9NA water immersion Olympus LumPlan FI 20x0.5 water-immersion Olympus UPlanFL N 4Xx0.13 PhP
Micromanipulators	Mini 25, 3 axes, Luigs & Neuman, Ratingen, Germany
Photodiode	Custom made by Jörg Breustedt and Dietmar Schmitz
Spinning disc system	Yokogawa CSU-22 , BFI Optilas, Puchheim, Germany
Spinning disc high speed camera	RedShirt NeuroCCD-SMQ camera, Life Imaging Services, Reinach, Switzerland
488 nm solid state laser	Sapphire 488 nm 50 mW Laser; Coherent, Utrecht, Netherlands
Ca <sup>2+</sup> indicators	Magnesium Green AM and Oregon Green Bapta-1 AM, both Molecular Probes/ Invitrogen, Carlsbad, CA, USA
Inverted microscope	IX50, Olympus Hamburg, Germany, equipped with video microscopy Olympus CPlan FI 10x/0.3 NA Olympus UiS2 LCAch N 40x/0.55 PhP
Valves and valve controller	8 channels Teflon valves unit with ValveLink 8 controller, Automate Scientific, Berkeley, CA, USA

---

Fast perfusion stepper	SF-77B Perfusion-Fast Step, Warner Instruments, Hamden, CT, USA
Quartz flow pipes	Polymicro Technologies, Phoenix, AZ, USA
Bath controller	MPCU, Lorenz Messgerätebau, Katlenburg-Lindau, Germany
Plastic syringes	B. Braun, Melsungen, Germany
Perfusion tubing	Carl Roth, Karlsruhe, Germany
<u>Software:</u>	
Axograph X 1.3	AxoGraph Scientific, Sydney, Australia
IGOR Pro 4.0	WaveMetrics Inc., OR, USA
pClamp 9.1	Molecular Devices, Toronto, Canada
Neuroplex	RedShirt, Life Imaging Services, Reinach, Switzerland
WinEDR and WinWCP	Strathclyde Institute of Pharmacy and Biomedical Sciences, University of Strathclyde, Glasgow G4 0NR, Scotland

## 2.2.2 Solutions for slice preparations and electrophysiological recordings

All standard salts were purchased from Sigma-Aldrich (St. Louis, MO, USA) and Carl Roth (Karlsruhe, Germany).

### Slicing solution

87 mM NaCl  
 26 mM NaHCO<sub>3</sub>  
 75 mM Sucrose  
 25 mM Glucose  
 2.5 mM KCl  
 1.25 mM NaH<sub>2</sub>PO<sub>4</sub>  
 0.5 mM CaCl<sub>2</sub>  
 7 mM MgCl<sub>2</sub>  
 saturated with 95% O<sub>2</sub>-5% CO<sub>2</sub>  
 350 mOsm

### Extracellular (“Ringer”) solution for slice recordings

119 mM NaCl  
 26 mM NaHCO<sub>3</sub>  
 10 mM Glucose  
 2.5 mM KCl  
 1 mM NaH<sub>2</sub>PO<sub>4</sub>  
 2.5 mM CaCl<sub>2</sub>  
 1.3 mM MgCl<sub>2</sub>  
 saturated with 95% O<sub>2</sub>-5% CO<sub>2</sub>  
 300 mOsm

### Intracellular solution for slice recordings

135 mM K-gluconate  
 20 mM KCl  
 2 mM MgATP  
 10 mM Hepes  
 0,5 mM EGTA  
 5 mM phosphocreatine  
 pH adjusted to 7.3 with KOH  
 300 mOsm

### “Stosiek” solution

150 mM NaCl  
 2.5 mM KCl  
 10 mM Hepes  
 pH 7.4

Extracellular solution for cell culture recordings

140 mM NaCl  
 2.4 mM KCl  
 10 mM Hepes  
 10 mM Glucose  
 2 CaCl<sub>2</sub> (2.5 CaCl<sub>2</sub> for granule cells)  
 4 MgCl<sub>2</sub> (1.3 MgCl<sub>2</sub> for granule cells)  
 pH adjusted to 7.3 with NaOH  
 300 mOsm

Intracellular solution for cell culture recordings I

146 mM K-Gluconate  
 17.8 mM Hepes  
 1 mM EGTA  
 4 mM Mg-ATP  
 0.3 mM Na-GTP  
 12 mM creatine phosphate  
 50 Units/ml phosphocreatine kinase  
 pH adjusted to 7.3 with KOH  
 300 mOsm

Intracellular solution for cell culture recordings II

136 mM KCl  
 17.8 mM Hepes  
 1 mM EGTA  
 4 mM Mg-ATP  
 0.3 mM Na-GTP  
 0.6 mM MgCl<sub>2</sub> x 6 H<sub>2</sub>O  
 12 mM creatine phosphate  
 50 Units/ml phosphocreatine kinase  
 pH adjusted to 7.3 with KOH  
 300 mOsm

Table 2: Drugs used for pharmacological manipulations

Drug, Company	Chemical name or <i>natural source</i>	Biological activity	Stock, solvent	Max. conc.
<b>Baclofen</b> , Tocris, Ellisville, Missouri, USA	(R)-4-Amino-3-(4-chlorophenyl) butanoic acid	GABA <sub>B</sub> R agonist	10 mM, in 10 mM NaOH	30 μM
<b>Clozapine-N-oxide (CNO)</b> , Enzo Life Science, Plymouth, PA, USA	8 -Chloro-11-(4-methyl-1-piperazinyl)-5H-dibenzo[b,e](1,4) diazepine N-oxide	Strong activator of hM4D-receptor, little or no activity at 5-HT receptors	10 mM, H <sub>2</sub> O	10 μM
<b>Cyclothiazide</b> , Tocris	6-Chloro-3,4-dihydro-3-(5-norbornen-2-yl)-2H-1,2,4-benzothiazidiazine-7-sulfonamide-1,1-dioxide	Positive modulator of AMPA receptors, inhibits receptor desensitization	100 mM, DMSO	100 μM

<b>DCG IV</b> , Tocris	(2S,2'R,3'R)-2-(2',3'-dicarboxycyclopropyl)glycines	Group II mGluR agonist	1 mM, H <sub>2</sub> O	1 μM
<b>Forskolin</b> , Tocris	<i>Coleus forskohlii</i>	Activator of adenylyl cyclase	50 mM, DMSO	50 μM
<b>Gabazine</b> (SR 95531 hydrobromide), Tocris	6-Imino-3-(4-methoxyphenyl)-1(6H)-pyridazinebutanoic acid hydrobromide	Competitive GABA <sub>A</sub> R antagonist	20 mM, H <sub>2</sub> O	2 μM
<b>Ionomycin</b> , USB, Cleveland, Ohio, USA	<i>Streptomyces conglobatus</i>	Ca <sup>2+</sup> -permeable ionophore	2 mM, H <sub>2</sub> O	2 μM
<b>L-CCG I</b> , Tocris	(2S,1'S,2'S)-2-(Carboxycyclopropyl)glycines	Group II mGluR agonist	10 mM, in 10 mM NaOH	10 μM
<b>NBQX</b> , Tocris	2,3-Dioxo-6-nitro-1,2,3,4-tetrahydrobenzo[f]quinoxaline -7-sulfonamide disodium salt	Competitive AMPA receptor antagonist	25 mM, H <sub>2</sub> O	10 μM
<b>Pertussis toxin</b> (PTX) Calbiochem/Merck, Darmstadt, Germany	<i>Bordetella pertussis</i>	Catalyzes ADP-ribosylation of Gα <sub>i</sub> , Gα <sub>o</sub> , Gα <sub>t</sub> proteins, blocks receptor coupling	100 μg/ml	0.5 μg/ml
<b>Tetrodotoxin</b> (TTX), Tocris	<i>Pseudoalteromonas tetraodonis</i>	Selective, use-dependent blocker of Na <sup>+</sup> channels	1 mM, H <sub>2</sub> O	1 μM

### 2.2.3 Hippocampal slice preparations

For field potential, whole-cell patch clamp and Ca<sup>2+</sup> imaging experiments, sagittal slices were prepared from C57/BL6-N mice aged P19-P29. Animals were briefly anesthetized with isoflurane. Immediately after decapitation, brains were rapidly removed into ice cold slicing solution equilibrated with 95% O<sub>2</sub> and 5% CO<sub>2</sub>, and chilled for 5 min. Hemispheres were separated and glued on the vibratome table that was mounted into a chamber filled with cold slicing solution. 300 μm slices were cut with a razor blade that was moved with a forward speed of 0.1 mm/s and lateral amplitude of 1 mm at 85 Hz, while care was taken to minimize vertical oscillations of the blade. Slices were incubated at 34°C for 30 min in slicing solution

before they were transferred to Ringer solution, where they were stored for 1-4 hours at room temperature.

#### **2.2.4 Field recordings and whole cell patch clamp experiments in hippocampal slices**

Whole cell voltage clamp and field excitatory postsynaptic potential (fEPSP) experiments were recorded with a Multiclamp 700A amplifier. Data were digitized at a sampling frequency of 5 kHz with a National Instruments board and stored using IGOR-Pro 4.0 software with custom made protocols. Slices were placed in the recording chamber of an upright microscope and superfused at 3 ml/min with Ringer solution saturated with 95% O<sub>2</sub>–5% CO<sub>2</sub>.

Whole cell recording electrodes were made from borosilicate glass capillaries with a DMZ universal puller. Pipette resistances ranged from 2 to 4 MΩ. During the recordings, access resistance and holding potential were constantly monitored, and no series resistance compensation was used. Only recordings with series resistance below 20 MΩ and holding currents smaller than -100 pA were accepted. For recordings of mEPSCs from CA1 pyramidal neurons in acute hippocampal slices, 1 μM TTX, 2 μM gabazine and 50 μM AP-V were added to the extracellular solution to block action potentials, GABA<sub>A</sub>R- and NMDA receptor-mediated currents. 100 μM cyclothiazide was added to prevent AMPA receptor desensitization.

For field potential recordings in CA1, low resistance pipettes filled with extracellular solution were placed in stratum radiatum. Schaffer collaterals were stimulated at 0.1 Hz for 0.1 ms with similar electrodes. Stimuli were generated with an A.M.P.I stimuflex box controlled by a Master-8. For the recording of mossy fibre fEPSPs, the stimulation electrode was placed in the granule cell layer or in the hilus region of the dentate gyrus, and the recording electrode was located in stratum lucidum of CA3. Stimulation frequency was 0.05 Hz for mossy fibre fEPSP experiments.

#### **2.2.5 Imaging experiments with photodiode and Nipkow spinning disc**

Slices were prepared as above. For photodiode measurements (Regehr and Tank, 1991; Gundlfinger, *et al.*, 2007) mossy fibres or Schaffer collaterals were labelled by injecting the low affinity Ca<sup>2+</sup> indicator Magnesium Green AM (dissociation constant (K<sub>D</sub>) of 6 μM;

100  $\mu\text{M}$  of dye dissolved in 20% Pluronic/DMSO) with a pressure stream into the fibre tracts. The final DMSO concentration in the injection solution was 5%. 30 min after labelling, epifluorescence was measured 200  $\mu\text{m}$  outside of the loading spot with a photodiode mounted on an upright microscope (BX51WI, with Olympus LumPlan FI 60 $\times$  0.9 NA water-immersion objective), while fibres were extracellularly stimulated with a patch pipette. Signals from the photodiode were low-pass filtered at 1 kHz, digitized at 5 kHz and captured with IGOR Pro. Action potential-triggered changes in fluorescence intensity ( $\Delta F$ ) relative to the baseline intensity of fluorescence ( $F$ ) were calculated as  $\Delta F/F$ .

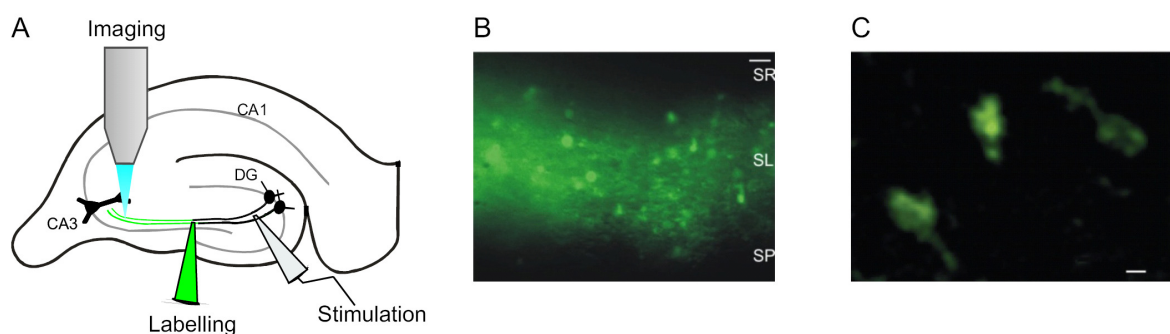


**Figure 2-3:  $\text{Ca}^{2+}$  imaging at mossy fibre terminals in hippocampal slices.**

(A) Schematic illustration of the experimental setup for mossy fibre imaging experiments. The mossy fibre tract was injected with an esterified  $\text{Ca}^{2+}$  indicator, which allowed uptake and trapping of the dye in the cells. The labelling pipette was always removed before the start of recordings and is indicated for illustration only. Imaging objective was 60 $\times$  0.9 NA water-immersion. (B) Mossy fibre terminals in stratum lucidum (SL) of CA3, labelled with the calcium indicator Magnesium Green AM. As the  $\text{Ca}^{2+}$  indicator can only diffuse inside the fibre tract over longer distances, the cellular structures in stratum radiatum (SR) and stratum pyramidale (SP) are not labelled (scale bar: 5  $\mu\text{m}$ ). (C) High magnification picture of three mossy fibre boutons loaded with the calcium indicator Oregon Green BAPTA-1 AM. Scale bar corresponds to 1  $\mu\text{m}$  (from Gundlfinger, *et al.*, 2007).

For high resolution time-lapse  $\text{Ca}^{2+}$  imaging experiments on single mossy fibre boutons, fibres were labelled in stratum lucidum with the cell-permeant AM-ester of the high affinity  $\text{Ca}^{2+}$  indicator Oregon Green BAPTA 1 AM ( $K_D$  of 170 nM). 50  $\mu\text{g}$   $\text{Ca}^{2+}$  dye was dissolved in 20  $\mu\text{l}$  Pluronic/DMSO and diluted in 180  $\mu\text{l}$  “Stosiek” solution (Stosiek, *et al.*, 2003), filled into a field electrode and injected by a light air-pressure into the fibre tract for 5 min. The spinning disc (Yokogawa CSU-22) coupled to a CCD camera (RedShirt Imaging) was mounted on an upright Olympus microscope (with LumPlan FI 60 $\times$ 0.9 NA water-immersion objective) equipped with a 488 nm *Sapphire 488-50* laser (Coherent). The high power of the laser as excitation source allowed us to identify cellular structures labelled with Oregon Green

BAPTA-1, which has very low basal fluorescence, but provides a high dynamic range of fluorescence, with an increase of up to 14-fold at saturating  $\text{Ca}^{2+}$  (compare transients in Figure 3-13 B1 with Figure 3-14 B). During the experiment, full frames were recorded at 125 Hz for 2 s every 60 s, and the focus was manually controlled between single acquisitions. Changes in fluorescence intensity ( $\Delta F/F$ ) were recorded and visualized using Neuroplex software (RedShirt Imaging). Only single boutons with little background fluorescence in the surrounding were chosen, and recordings were discarded if the exponential decay time constant of the  $\text{Ca}^{2+}$  transient increased for >20% over the experiment. Data were exported to Igor Pro for post-hoc analysis. In a first step, background fluorescence of a defined unlabeled region was subtracted from the  $\text{Ca}^{2+}$  signal.  $\Delta F/F$  was then calculated by normalizing the wave to the baseline signal recorded for 0.5 s before fibre stimulation. In order to reduce the signal jitter within the recording compared to a simple peak calculation, the maximal  $\text{Ca}^{2+}$  signal was estimated by fitting a mono-exponential function into the decay of the  $\text{Ca}^{2+}$  transient. The peak of this decay function at the time point of the highest fluorescence was then taken as  $\Delta F/F$ .

### **2.2.6 Recordings of autaptic neurons in culture**

Starting from DIV 10 of the culture, 30 mm coverslips were broken to suitable size with a diamond pen and transferred to the recording chamber mounted on an inverted microscope. Cells were superfused with HEPES buffered solution at 1-2 ml/min. Whole-cell recordings were performed at room temperature using a Multiclamp 700B or Axopatch 200A amplifier with borosilicate electrodes (3-4 M $\Omega$ ) filled with intracellular solution. In most of the experiments, membrane capacitance and 70% of the series resistance were compensated while changes in series resistance were monitored frequently throughout the experiments. Data were filtered at 2-5 kHz, digitised at 5-10 kHz and recorded with pClamp 9 or Axograph X. Unclamped action potentials were evoked by a 1 ms depolarisation step to 0 mV from holding potentials of -60 to -70 mV.

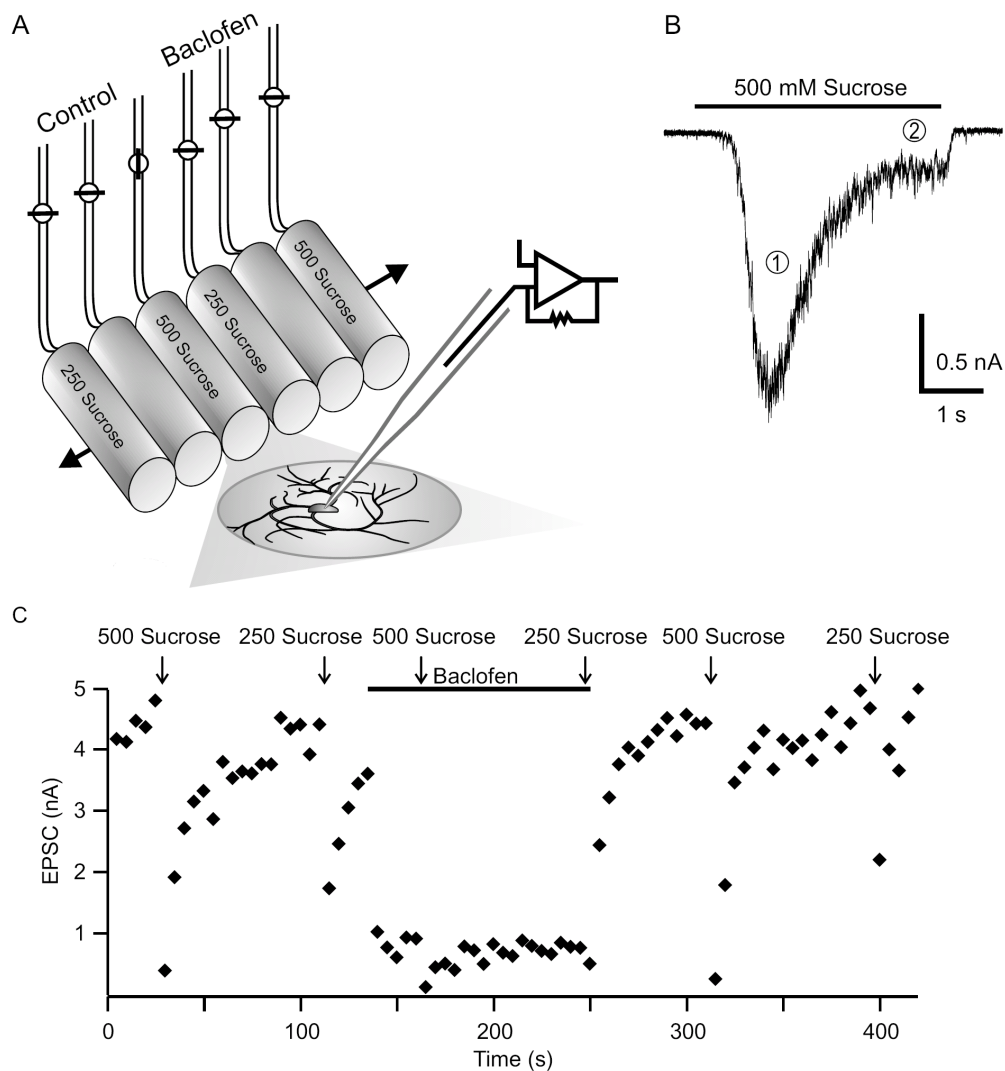


**Figure 2-4: A fast flow device enables rapid applications of hypertonic solutions and pharmacological manipulations in recordings of autaptic neuronal cultures.**

(A) The outflow of each barrel covers the whole micro-island (~300  $\mu\text{m}$  diameter). Flow pipes have an inner diameter of 480  $\mu\text{m}$  and are not drawn in scale. (B) Representative trace of a recording with fast application of hypertonic sucrose solution for 4 s on an autaptic neuron. During the initial transient (1) the RRP is depleted, which is followed (2) by a steady-state phase of continuous release. (C) Autaptic EPSCs recover within 90 s after depletion of the RRP. During a typical experiment, hypertonic solutions of different sucrose concentration (in mM) were applied repetitively, as indicated by arrows. 30  $\mu\text{M}$  baclofen was applied for 2 min and strongly suppressed EPSCs. Also hypertonic solutions applied during this time contained baclofen.

Fast drug application was performed using a modified perfusion system (Rosenmund, *et al.*, 1995; Pyott and Rosenmund, 2002). To achieve rapid solution exchange rates, we used a six barrel flow pipe made from quartz tubing (tube outer diameter 500  $\mu\text{m}$ , inner diameter 430  $\mu\text{m}$ ) mounted on a fast stepper device. The flow pipes were lowered into close position above the cells (~200  $\mu\text{m}$  distance). Solution flow from gravity fed reservoirs was controlled

by Teflon valves mounted in a valve bank. Both stepper and valve bank were simultaneously operated via a TTL signal triggered by the recording software, which allowed solution exchange in ~50 ms. In addition to the local perfusion, the recording chamber was constantly perfused with extracellular solution to prevent accumulation of drugs. The RRP was depleted by fast, 5 s applications of 500 mM sucrose dissolved in extracellular solution (Rosenmund and Stevens, 1996), while submaximal stimuli of 250 mM sucrose were applied for 10 s. A 60 to 90 s recovery interval was chosen between sucrose stimuli to allow refilling of the RRP, while the EPSC was monitored at 0.2 Hz (Figure 2-4). Recordings were excluded if the response to 500 mM sucrose showed a rundown over three applications.

### 2.3 Data analysis and statistics

In autaptic cultures, the readily releasable pool (RRP) of neurotransmitter vesicles can be calculated from the excitatory transient evoked by application of 500 mM sucrose ( $I_{\text{Sucrose}}$ ) after baselining to the steady state component ( $I_{\text{steady}}$ ), which represents the rate of refilling and release of recycled vesicles (see Figure 2-4 B). The charge of the RRP ( $Q_{500\text{Sucrose}}$ ) is then given by the integral from the onset to the end of the transient below 0.  $Q_{500\text{Sucrose}}$  is then divided by the charge of the average mEPSC ( $\bar{Q}_{\text{mEPSC}}$ ) for each neuron, which gives the number of vesicles in the RRP of the autaptic neuron:

$$(2) \text{ RRP} = \frac{Q_{500\text{Sucrose}}}{Q_{\text{mEPSC}}} = \frac{\int (I_{\text{Sucrose}}(t) - I_{\text{steady}}) dt}{\int \bar{I}_{\text{mEPSC}}(t) dt}$$

The probability ( $P_{\text{vr}}$ ) for a synaptic vesicle to be released after an action potential can be calculated as the ratio of the average EPSC charge ( $\bar{Q}_{\text{EPSC}}$ ) to the RRP charge:

$$(3) P_{\text{vr}}(\%) = \frac{\bar{Q}_{\text{EPSC}}}{Q_{500\text{Sucrose}}} \times 100 = \frac{\int I_{\text{EPSC}}(t) dt}{\int (I_{\text{Sucrose}}(t) - I_{\text{steady}}) dt} \times 100$$

Dose response curves were analysed using Graph Pad Prism 5.0 (La Jolla, CA, USA) to determine the half maximal inhibitory concentration ( $IC_{50}$ ) for presynaptic  $Ca^{2+}$  influx and inhibition of transmitter release, respectively. In this logistic equation,  $R_{\text{Min}}$  denotes the response in the presence of maximal inhibition, and  $\alpha$  is the Hill slope, which was kept variable. All responses were normalized to control conditions, set as 1:

---

$$(4) Y = R_{\text{Min}} + \frac{1 - R_{\text{Min}}}{1 + 10^{\alpha(\text{LogIC}_{50-x})}}$$

Decay time constants of sucrose transients were determined by fitting monoexponential decay functions to the responses using Axograph X, which adjusted the coefficient values by nonlinear least-square fitting based on a built-in simplex algorithm.

All results are given as mean  $\pm$  standard error of the mean, if not stated otherwise. Miniature EPSCs were analysed offline using WinEDR and WinWCP for slice recordings or Axograph X for autaptic recordings. Prism 5.0 was used for statistical analyses, and data were tested for significance using independent or paired Student's *t*-test for comparison of pairs of data, as appropriate. Significances ( $p < 0.05$ ) are indicated by stars (\*). K-means cluster analysis for two populations was performed using Mymstat software (Systat, Chicago, IL, USA).

## 2.4 Molecular biology and biochemistry

### 2.4.1 Materials

Centrifuges	Mikro 120, Hettich GmbH, Tuttlingen, Germany, with fix angle rotor 1242 (max 18000 x g) Heraeus Multifuge 1S-R, Thermo Fisher Scientific, with swing bucket rotor 75002002 F (max 4618 x g) Centrifuge 5417R, Eppendorf, Hamburg, Germany, with rotor F45-30-11 (max 25000 x g)
Mixer & stirrer	Eppendorf Thermomixer Compact Dos-10L, NeoLab, Heidelberg, Germany RTC basic stirrer, Ika Werke, Staufen, Germany Vortex genie, Scientific Industries, Bohemia, NY, USA
PCR machine	Sensoquest Labcycler, Göttingen, Germany
Agarose gel electrophoresis	Midi I Electrophoresis chamber (Carl Roth), with Consort EV power supply (Sigma Aldrich, St. Louis, MO, USA)
DNA spectrophotometer	ND 1000, Peqlab, now Thermo Fisher Scientific
Protein spectrophotometer	Novaspec Plus, Amerham / GE Healthcare, Chalfont, UK
Protein electrophoresis	X Cell II Blot Module chamber (Invitrogen), with Power Pac Basic (Biorad, München, Germany)
DNA extraction kits	QIAprep Spin Miniprep, Plasmid Midi and Plasmid Maxi Preparation kits (all Qiagen, Hilden, Germany)
DNA point mutations	Quickchange XL kit (Stratagene, now Agilent, Santa Clara, CA, USA)
DNA ladders	1 kb DNA ladder, Invitrogen 100 bp DNA ladder, Bioline, Luckenwalde, Germany
Software	Lasergene 8.0.2 package DNASTar, Madison, WI, USA Genamics Expression v1.1 (freeware)

### 2.4.2 Buffers and media

Buffer for heat shock competent <i>E. coli</i>	60 mM CaCl <sub>2</sub> , 15% Glycerol, 10 mM Pipes (pH adjusted to 7.0), filtered and sterilized.
LB media	10 g Bacto-Peptone, 5 g Yeast Extract, 10 g NaCl, 100 µl 5M NaOH (pH 7.2-7.4), in 1 l H <sub>2</sub> O
LB media agar plates	1 l LB media + 20 g Agar
PBS	137 mM NaCl, 2.7 mM KCl, 10 mM Na <sub>2</sub> HPO <sub>4</sub> , 1.76 mM

---

	KH <sub>2</sub> PO <sub>4</sub> , pH 7.4 (adjusted with NaOH or HCl)
SOC media	20 g bacto-trypton, 5 g yeastextract, 0.5 g NaCl in 950 ml H <sub>2</sub> O, autoclaved. Supplemented with 10 ml 250 mM KCl, 200 µl 5 M NaOH, 5 ml 2 M MgCl <sub>2</sub> , 10 ml 40% glucose, volume adjusted to 1 l, aliquots of 50 ml stored
50x DNA electrophoresis buffer	242.2 g/l TrisBase, 60 ml/l acetic acid, 37.2 g/l EDTA

### 2.4.3 Techniques to work with DNA

For cloning a DNA fragment of interest it is transferred into a bacterial plasmid that allows amplification in high copy numbers by *Escherichia coli* (E. coli) strains. The modified plasmid can be isolated from the bacteria and successful integration of the insert can be analysed using restriction enzymes and subsequent agarose gel electrophoresis. Fragments of DNA can also be amplified using the polymerase chain reaction (PCR). The techniques for amplification, manipulation and analysis of DNA are described in the following sections. The most commonly used enzymes are listed in Table 3.

Table 3: Enzymes used in the laboratory for molecular biology work.

Name	Buffer	Supplier
Restriction enzymes: Asi I, Avr II, BamH I, EcoR I, Nfe I, Not I, Sal I, Xho I	NEB: enzyme-specific Fermentas: universal FastDigest buffer	- New England Biolabs (NEB), Ipswich, MA, USA - Fermentas, Burlington, Ontario, Canada
CIP – calf intestine alkaline phosphatase	Restriction enzyme buffer	NEB
T4 ligase	T4 DNA Ligase Reaction Buffer	NEB
PfuUltra II HS high fidelity DNA polymerase	PfuUltra II Reaction buffer	Stratagene, now Agilent, Santa Clara, CA, USA
Expand Long Template PCR System (mix of polymerases)	Expand Long Template buffer	Roche, Basel, Switzerland

We used XL10 Gold (Stratagene) or TOP10 (Invitrogen) E. coli strains that were grown on agar plates or in liquid LB media at 37°C for amplification of DNA plasmids. The final concentration of antibiotics to select for positive clones was 60 µg/ml Ampicillin or 30 µg/ml Kanamycin. For plasmids encoding viral sequences, the incubation temperature was reduced to 32°C to avoid spontaneous recombination.

For generating large quantities of heat-shock competent bacteria, the selected strain was cultured without antibiotics in a small volume of LB media over night. This preculture was transferred into 500 ml LB media and grown at 37°C under mild agitation. Optical density at 550 nm was checked regularly. Cultures with an OD of 0.6 were cooled on ice for 10 min and pelleted at 3000 x g for 15 min at 4°C. Pellets were washed three times with decreasing volumes (100, 50, 25 ml) of heat shock buffer. Cells were finally resuspended in 5 ml of heat shock buffer and frozen in aliquots of 100 µl at -80°C.

For heat shock transformation, 100 µl E.coli were slowly thawed on ice and 10-50 ng plasmid DNA added to the cup. After 30 min on ice, the suspension was incubated at 42°C for 40 s, which causes (by an unknown mechanism) efficient uptake of the DNA by the cells. After 2 min on ice, bacteria were transferred to 2 ml SOC media (only in case of Kanamycin selection) before plating them on agar plates supplemented with antibiotics.

#### **2.4.3.1 DNA purification**

For small scale (“mini”) preparations, single colonies of bacteria were picked using a sterilized tip and transferred into 2.5 ml LB supplemented with appropriate antibiotics. After overnight incubation at 37°C under mild agitation, cells were pelleted at 6000 x g and resuspended in P1 buffer of the QIAprep Spin Miniprep Kit (Qiagen). Plasmid DNA was isolated according to the manufacturer’s protocol and finally eluted with H<sub>2</sub>O.

For medium or large scale preparations, we used Plasmid Midi or Plasmid Maxi preparation kits (both Qiagen). 100-500 µl of a mini culture were transferred to 100 or 250 ml LB media and cultivated over night at 37°C at 280 rpm agitation. Bacteria suspension was centrifuged in 50 ml tubes at 3500 x g, 4°C for 30 min, washed with PBS, pooled and centrifuged again. Cells were resuspended in P1 buffer and further processed to isolate plasmid DNA according to the manufacturer’s protocols. We finally precipitated purified DNA by adding 3.5 ml isopropanol and 830 µl 3 M sodium-acetat to 5 ml DNA solution. After incubation for 10 min at room temperature, samples were centrifuged at maximal speed for 30 min at 20°C. Pellets were washed twice with 2 ml cold (-20°C) 70% ethanol, dried at room temperature and resuspended in 100 to 500 µl H<sub>2</sub>O.

---

#### **2.4.3.2 Digestion of DNA with restriction enzymes**

Restriction endonucleases recognize and cut specific, most often palindromic DNA sequences, thereby creating DNA fragments of defined length. These enzymes can be used for the analysis of recombinant plasmids or preparative digestions of DNA. We usually incubated 0.5 or 2 µg plasmid DNA with restriction enzymes and the appropriate buffer (all NEB or Fermentas “fast digest” enzymes) in 20 or 50 µl final volume at 37°C for up to 2 h. The resulting fragments were separated and visualized by agarose gel electrophoresis.

#### **2.4.3.3 Agarose gel electrophoresis and fragment isolation**

Because of their negatively charged phosphate groups it is possible to separate DNA molecules by size in agarose gels when applying an electrical field. By using the intercalating dye ethidium bromide with a final concentration 0.25 µg/ml (Carl Roth), it is possible to later visualize bands of DNA under UV light. Dependent on the fragment size, we used agarose gels of 0.7 to 1.5%. Agarose was dissolved in TAE buffer by heating and poured into the gel chamber. After solidification of the gel, DNA samples were mixed with a 5x sample buffer (Bioline, Luckenwalde, Germany), loaded into the gel pockets and separated by applying a constant voltage of 60 to 120 V. As a size reference, we used commercially available DNA ladders (1 kb DNA ladder, Invitrogen; or 100 bp DNA ladder, Bioline), which were always run in parallel with the DNA samples. DNA bands were visualized and photo-documented under UV light. To isolate a fragment, it was cut out from the gel with a fresh scalpel blade on a low intensity UV light table. DNA was isolated from gel fragments using the QIAquick extraction kit (Qiagen) according to the manufacturer’s instructions.

#### **2.4.3.4 Ligation**

When the vector backbone was opened with only one restriction enzyme, we dephosphorylated the open ends using calf intestine alkaline phosphatase (CIP) to prevent re-ligation. 20 µl of DNA were incubated with 1 µl CIP at 37°C for 30 min. The phosphatase was inactivated by heating the sample to 65°C for 15 min. In case of digestion with two restriction enzymes, DNA fragments were separated by agarose gel electrophoresis and purified as described above. We used 50 ng of vector DNA and 5 fold the number of molecules of insert fragment for ligation with 1 Weiss unit T4 ligase. The reaction was performed at room temperature for 1 h or at 4°C over night. After heat inactivation of the ligase (10 min, 65°C), 2-4 µl of the ligation were used for bacterial heat shock transformation.

### 2.4.3.5 Polymerase chain reaction (PCR)

Short stretches of DNA can be amplified by the PCR method, which exploits the ability of heat insensitive DNA polymerases to synthesize new DNA complementary to a template strand. The three major steps in a PCR cycle are the following: (1) DNA denaturation at 95°C for 30 s to separate the double-stranded DNA. (2) Annealing of DNA oligomers of ~20 base pair length (“primers”) to complementary sequences on the single strand DNA. In every PCR reaction, two primers are necessary, one for the leading strand and one for the complementary strand. The annealing temperature is specific for every PCR reaction and was set usually 5°C lower than the melting temperature ( $T_m$ ) of the primers, which depends on their GC content and length. (3) Elongation of the DNA at 72°C. Starting from the primers, the DNA polymerases synthesise DNA in the 5’ to 3’ direction, resulting in a new double stranded DNA molecule. For Taq polymerase the elongation time is calculated as 60 s/1000 base pairs. A standard PCR mix of 25  $\mu$ l contained PCR-buffer diluted to 1x, 200  $\mu$ M nucleotides, 40 pM of each primer, 1 U polymerase and ~20 ng DNA template. Primers used in this work are listed in Table 4.

A typical PCR protocol is given below:

Step	Temperature	Time	
1	95°C	5 min	Heat activation of the inactive polymerase
2	95°C	30 s	Denaturation
3	specific	30 s	Annealing
4	72°C	x s	Elongation
} Repetition for 30-40 cycles			
5	72°C	5 min	final elongation of partial sequences
6	12°C	$\infty$	Cooling

Single point mutations were introduced into a stretch of DNA by a modified PCR protocol using the Quickchange kit XL (Stratagene). A long PCR with a low number of cycles using Pfu DNA polymerase was run around the complete plasmid, with a complementary pair of primers containing the point mutation in the middle of the oligomers, flanked by 10-15 bases of correct sequence on both sides. By this, new circular plasmids are synthesized containing the desired mutation. The parental plasmid is different from the newly generated DNA by its DNA methylation, which was introduced during the amplification step in *E. coli*. Therefore, it is possible to specifically digest parental DNA by Dpn I, a DNA endonuclease that only

recognizes methylated DNA. The new DNA containing the point mutation was afterwards transformed into XL10 Gold competent cells.

Table 4: Primers used for DNA amplification by PCR.

Name	Sequence	T <sub>m</sub> (°C)	Application
T7	TAATACGACTCACTAT AGGG	49.9	Amplification of hM4D from pcDNA3.1
hM4D-rev-Xba I	GAACATCGGCACTGCC AGGTCTAGATCT	67.0	As above, introduces Xba I restriction site
mKate-S162T-fw	CCTGGAAGGCAGAACC GACATGGCCCT	73.5	Point mutation in mKate to generate mKateT
mKate-S162T-rev	AGGGCCATGTCGGTTC TGCCTTCCAGG	73.5	s. above
hM4D-fw-Sac I	GAGCTCGGATCCACCA TGGCCAACTTCACACC TGTC	74.7	Amplification of hM4D from pcDNA3.1 to insert in front of mKateT with Sac I
hM4D-rev-EcoR I	GAATTCTATGGTGATG GTGATGATGACCGG	64.4	As above, inserts EcoR I site
Mfe I-Stop-cassette-fw	GAATCAATTGTTAATT AATTAAGTCCCTCAGG TGCAGGCTG	63.4	Amplification of Stop-Cassette from pCALN. Introduces Mfe I restriction site and three stop codons.
Mfe I-Stop-cassette-rev	CATTCAATTGTTAATT AATTAAGTGCAGGTCG AGGGATCTTC	63.2	As above
GT001 PGK3'-fw	CACGCTTCAAAGCGC ACGTCTG	63.8	PCR screen for 5' integration of hM4D construct into ROSA26 acceptor locus: 280 bp product
GT002 Neo5'-rev	GTTGTGCCAGTCATA GCCGAATAG	62.8	As above
GT005 PolyA-fw	TTCCTCCTCCTGACT ACTCC	58.3	PCR screen for 3' integration of hM4D construct into ROSA26 acceptor locus: 258 bp product
GT006 Rosa3'-rev	TAAGCCTGCCAGGAAG ACTC	58.3	As above
GT013 hM4D3'rec-rev	CAGATACTGCGACCTC CCTA	59.2	Tests FLEX switch of hM4D in Rosa26: 826 bp with GT006

#### 2.4.4 Protein isolation, SDS polyacrylamide gel electrophoresis and western blots

Proteins can be separated by size in a sodium dodecyl sulfate polyacrylamide gel electrophoresis (SDS-PAGE), may subsequently be transferred onto nitrocellulose membranes (Western blot) and detected by specific antibodies and a chemiluminescence reaction. The following buffers and reagents are required during the purification and analysis steps:

TNN buffer:	50 mM Tris-HCl pH7.5, 120 mM NaCl, 5 mM EDTA, 0.05% Nonident-P40, 100 mM NaF, 2 mM Na <sub>3</sub> VO <sub>4</sub> (activated); sterile filtered. Supplemented before use with 1 mM PMSF (phenylmethyl-sulphonyl fluoride) and 1 “tablet complete mini EDTA free protease inhibitor” (Roche) per 10 ml buffer.
4x protein loading buffer:	50% glycerol, 0.5% (w/v) bromphenol blue, 10% SDS, 250 mM Tris pH 6.8, 100 mM DTT (dithiothreitol), stored at -20°C
Tris buffered saline (TBS):	50 mM Tris, 150 mM NaCl, pH adjusted to 7.5 with HCl
TBST:	TBS supplemented with 0.05% Tween
Stacking gel buffer:	1.5M Tris HCl pH 8.8
Separating gel buffer:	0.5M Tris HCl pH 6.8
Stacking gel:	0.75 ml 40% acrylamide (final conc. 5%), 1.5 ml stacking gel buffer, 60 µl 10% SDS, 3.6 ml H <sub>2</sub> O, 60 µl 10% APS (Ammonium persulfate), 6 µl Temed (N, N, N', N'-tetramethylethylenediamine)
Separating gel 10%:	2.5 ml 40% acrylamide (final concentration 10%), 2.5 ml separating gel buffer, 100 µl 10% SDS, 4.8 ml H <sub>2</sub> O, 100 µl 10% APS, 10 µl Temed
Nitrocellulose membrane:	Whatmen Protran Nitrocellulose Membrane, 0.2 µm pore size, GE Healthcare, Chalfont, UK

Cells were washed with PBS in the culture dish, eventually frozen at -80°C and finally lysed using TNN-buffer by repetitive scraping and incubation on ice. Samples were cleared by 10 min centrifugation at 4000 x g, 4°C. The supernatant was mixed with the appropriate amount of 4x protein loading buffer and boiled at 95°C for 15 min. This step in denaturing and reducing conditions causes unfolding of the proteins, break of disulfide bonds and coating with negatively charged SDS molecules. The electrophoretic mobility of the negatively charged proteins is then only dependent on the protein size when exposed to an electrical field in a gel matrix. Protein samples together with a size standard were loaded into the pockets of a discontinuous polyacrylamide gel, consisting of a stacking gel (5% acrylamide) and a

---

separating gel (10% acrylamide), which offers improved resolution. Samples were focussed by applying 60 V for 30 min, before voltage was increased to 120 V to separate protein samples. 10% acrylamide gels were chosen to separate proteins in the range of 20 to 70 kDA.

Proteins were transferred to nitrocellulose membranes by 1 h 25 V wet transfer in blotting buffer. In general we used TBST as buffer during the following procedures. To block unspecific binding in the subsequent antibody reaction, the membranes were incubated in 5% milk powder at 4°C over night. After washing, the primary antibody (for SNAP-25: 1:2000 in 5% BSA) was applied for 1 h at RT. Membranes were washed 3 times and incubated with the horseradish peroxidase conjugated secondary antibody (1:1000 in 5% milk). To visualize the antigen-antibody complexes we used the enhanced chemiluminescence system (ECL; Perkin Elmer, Waltham, MA, USA). Membranes were incubated for 1 min with a 1:1 mixture of ECL reagent 1 and 2, before exposure of X-ray film to detect light emitted by the chemiluminescence reaction.

#### **2.4.5 Immunofluorescence stainings**

Cultured cells were washed with PBS, fixed with 4 % paraformaldehyde, permeabilized with 0.1 % Triton X-100 (Carl Roth), washed twice and blocked with 3% BSA or 5 % FCS for 1 h at room temperature. Cells were incubated with primary antibodies (see Table 5) in blocking solution at room temperature for 1 h, washed again twice and incubated with secondary antibodies for 1 h at room temperature. Nuclei were visualised by 1 mg/ml DAPI (Roche, Basel, Switzerland) applied for 30 sec. Samples were mounted using Gel Mount™ Aqueous Mounting Medium (Sigma-Aldrich) and fixed to the microscope slide with nail polish. Immunofluorescence was observed with Leica ACS Apo 40x/1.15 oil and 63x/1.3 oil objectives on a confocal microscope (DM 2500, Leica, Wetzlar, Germany) equipped with 405, 488, 532 and 635 nm solid-state lasers.

Table 5: Antibodies used for immunocytochemistry (ICC), Western blots (WB) and secondary antibodies (2nd):

Antigen	Company	Donor species	Dilution	Application
MAP-2	Millipore, MAB3418, Billerica, MA, USA	Mouse monoclonal	1:500	ICC
SNAP-25	Covance, SMI-81R, Princeton, NJ, USA	Mouse monoclonal	1:10000	WB
Synaptoporin	Synaptic Systems, 102 002, Göttingen, Germany	Rabbit polyclonal	1:1000	ICC
Mouse IgG HRP-coupled	Dianova 115-035-146, Hamburg, Germany	Goat polyclonal	1:10000	2nd WB
Mouse IgG Cy5 coupled	Dianova 715-175-151	Donkey polyclonal	1:100	2nd ICC
Rabbit IgG FITC coupled	Sigma-Aldrich F9887, St. Louis, MO, USA	Donkey polyclonal	1:100	2nd ICC





---

## 3 Results

### 3.1 Presynaptic inhibition by GABA<sub>B</sub>Rs in hippocampus area CA1

To study the modulation of glutamatergic transmission at Schaffer collateral-CA1 synapses by presynaptic GABA<sub>B</sub>Rs we conducted electrophysiological and functional imaging experiments in mouse hippocampal slices (3.1.1). These experiments spurred our interest in the underlying molecular mechanisms, which we investigated using autaptic cultures of principal hippocampal neurons (3.1.3). We also confirmed some of these results for mossy fibre-CA3 synapses, which differ in several aspects from Schaffer collateral synapses in CA1 (see 3.2).

#### 3.1.1 Presynaptic inhibition by GABA<sub>B</sub>Rs cannot be explained by reduced calcium influx alone

As outlined in the introduction, transmitter release strongly depends on the amount of Ca<sup>2+</sup> influx that occurs once an action potential invades the presynaptic terminal. A reduction of the opening probability of voltage-dependent Ca<sup>2+</sup> channels (VDCCs) by G-proteins is therefore a powerful way to inhibit the fusion of synaptic vesicles, which ultimately leads to a reduction of the postsynaptic response. The dependency of the field excitatory postsynaptic potential (fEPSP) on presynaptic Ca<sup>2+</sup> concentration ( $[Ca^{2+}]_i$ ) can be described with a power function that is specific for every type of synapse in the brain (Dittman and Regehr, 1996; Kamiya and Ozawa, 1998):

$$(5) \text{ fEPSP} = k \cdot [Ca^{2+}]_i^n$$

The exponent  $n$  of the above equation is seen as an empirical value that is often referred to as the biochemical Ca<sup>2+</sup> cooperativity of neurotransmitter release and could be interpreted as a lower bound on the number of Ca<sup>2+</sup> ion-binding events involved in exocytosis (Matveev, *et al.*, 2009). Processes that modulate the effective Ca<sup>2+</sup> concentration at the vesicular sensor or change the affinity of the individual Ca<sup>2+</sup> binding sites at the sensor itself will change the postsynaptic signal according to the defined power function. Conversely, alterations of the

release process occurring independently of presynaptic  $\text{Ca}^{2+}$  handling can result in changes of the theoretical minimal number of  $\text{Ca}^{2+}$ -binding sites that have to be filled to trigger vesicle fusion (Koh and Bellen, 2003), and will be reflected by a change of the exponent. Experimentally, the exponent  $n$  can be estimated by artificially changing the intracellular  $\text{Ca}^{2+}$ , for example by lowering extracellular  $\text{Ca}^{2+}$  in order to decrease AP-triggered  $\text{Ca}^{2+}$  influx. By plotting the normalized postsynaptic response against the normalized presynaptic  $\text{Ca}^{2+}$  signal on double logarithmic scales, one can calculate the exponent of the power function from the steepness of a line fitted to the data (see Figure 3-1 C2).

We hypothesised that  $\text{GABA}_B$ Rs might inhibit transmitter release in a process that directly affects the vesicular fusion, in parallel to the well described inhibition of  $\text{Ca}^{2+}$  channel opening. This should be reflected by a change of the exponent of the power function for transmitter release in baclofen, compared to control experiments where transmitter release was decreased by reducing extracellular  $\text{Ca}^{2+}$ . We first assessed the effect of presynaptic  $\text{GABA}_B$ Rs activated by baclofen on the presynaptic  $\text{Ca}^{2+}$  transient and on the postsynaptic excitatory response in CA1. Baclofen (30  $\mu\text{M}$ ) nearly abolished the fEPSP ( $9\pm 1\%$  of control) and reduced the presynaptic  $\text{Ca}^{2+}$  transients to maximally  $72\pm 3\%$  (Figure 3-1 A1 to A3). In a parallel set of experiments, we stepwise reduced the  $\text{Ca}^{2+}$  concentration in the external solution and monitored presynaptic  $\text{Ca}^{2+}$  signals or fEPSPs, while  $\text{CaCl}_2$  was replaced by equimolar concentrations of  $\text{MgCl}_2$  to keep the total concentration of divalent cations constant (Figure 3-1 B). In 0.5 mM  $\text{Ca}^{2+}$ , the fEPSP was reduced to  $1.5\pm 0.3\%$  of control, while the remaining presynaptic  $\text{Ca}^{2+}$  transients amounted to  $41\pm 2\%$  of control. We found that changes in extracellular  $\text{Ca}^{2+}$  and Baclofen did not alter the fibre volley in fEPSP recordings, indicating no general change of the fibre excitability (not shown). A nonlinear regression fitted to the data obtained with reduced extracellular  $\text{Ca}^{2+}$  gave an exponent of  $n=4.1$  for the power function of transmission at Schaffer collateral synapses ( $R^2=0.99$ ; Figure 3-1 D). In comparison to this, the data for baclofen revealed a much stronger effect by  $\text{GABA}_B$ Rs on the fEPSP than on the presynaptic  $\text{Ca}^{2+}$  influx (Figure 3-1 C). This becomes most obvious in the double logarithmic plot, where the exponent of the power function for the baclofen data could be calculated as  $n=6.1$  ( $R^2=0.98$ ; Figure 3-1 D). These experiments gave a first indication arguing for an additional inhibitory mechanism utilised by presynaptic  $\text{GABA}_B$ Rs to reduce transmitter release beside the well known reduction of  $\text{Ca}^{2+}$  influx.

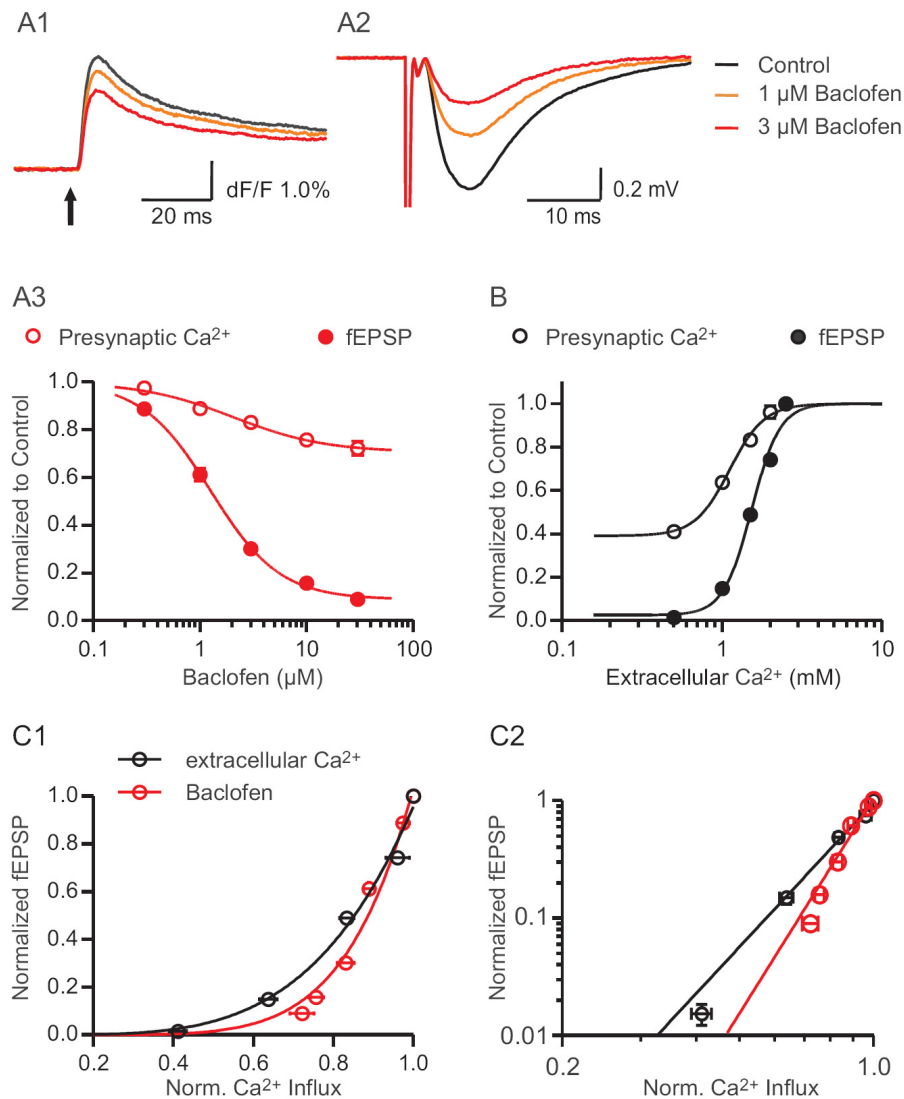


**Figure 3-1: Evidence for  $\text{Ca}^{2+}$ -independent inhibition of transmitter release by presynaptic  $\text{GABA}_B\text{Rs}$  at hippocampal Schaffer collateral synapses.**

(A1) Baclofen causes a dose-dependent decrease of the presynaptic  $\text{Ca}^{2+}$  influx after an action potential (indicated by arrow). (A2) fEPSPs in CA1 are reduced by  $\text{GABA}_B\text{R}$  activation with baclofen. (A3) Baclofen dose response curves for presynaptic  $\text{Ca}^{2+}$  influx and fEPSP (0.3, 1.0, 3.0, 10, 30 mM baclofen). The  $\text{IC}_{50}$  values are 2.05  $\mu\text{M}$  for the  $\text{Ca}^{2+}$  influx and 1.26  $\mu\text{M}$  for fEPSPs. (B) Presynaptic  $\text{Ca}^{2+}$  signals and fEPSPs recorded in different concentrations of extracellular  $\text{Ca}^{2+}$  (2.5, 2.0, 1.5, 1.0, 0.5 mM). (C1) Relation of presynaptic  $\text{Ca}^{2+}$  influx and postsynaptic response for Schaffer collaterals, plotted on linear scales. The effect of baclofen (red circles) on the fEPSP amplitude exceeds the effect of an equivalent reduction of presynaptic calcium influx alone (black circles; all  $n=5-6$ ). (C2) In double logarithmic scales, the power of the transmitter release function is given by the steepness of the fitted line. The fit of the baclofen data is obviously steeper than the data-fit for the changes of extracellular  $\text{Ca}^{2+}$  concentrations.

### 3.1.2 GABA<sub>B</sub>Rs inhibit spontaneous neurotransmitter release in CA1 in presence and absence of extracellular calcium

Neurotransmitter vesicles docked in the active zone of nerve terminals do not only release their content after action potential triggered Ca<sup>2+</sup> influx, but also fuse spontaneously with the presynaptic plasma membrane. This form of release has been attributed to be largely independent of Ca<sup>2+</sup> (Scanziani, *et al.*, 1992, but see also Xu, *et al.*, 2009; Groffen, *et al.*, 2010), and their frequency has been correlated with the general “fusion willingness” of vesicles (a figurative term first introduced by Lou, *et al.*, 2005). Inhibition of spontaneous glutamate release by GABA<sub>B</sub>Rs has been investigated in hippocampal cell cultures (Scanziani, *et al.*, 1992; Scholz and Miller, 1992) and in recordings from purkinje cells in cerebellar slice preparations (Dittman and Regehr, 1996). In these studies baclofen reduced the frequency of mEPSCs, which was interpreted as an inhibitory action of GABA<sub>B</sub>Rs downstream of VDCCs. In our recordings of mEPSCs from CA1 pyramidal neurons in hippocampal slices we too found that application of 30 μM baclofen significantly decreased the frequency of mEPSCs (from 0.86±0.1 Hz to 0.59±0.07 Hz,  $p=0.004$ ; Figure 3-2 A), without changing the quantal amplitude (control: 15.9±1.3 pA, baclofen: 15.2±1.1 pA,  $p=0.2$ ). In a second set of experiments, we removed extracellular Ca<sup>2+</sup> after establishing stable recording conditions to reduce possible background Ca<sup>2+</sup> currents in the presynaptic terminals that might be modulated by GABA<sub>B</sub>Rs. Already the change to Ca<sup>2+</sup>-free conditions (0 Ca<sup>2+</sup>, 1 mM EGTA) led to a profound decrease in mEPSC frequency (from 0.83±0.1 Hz to 0.58±0.12 Hz,  $p=0.0008$ ; Figure 3-2 B), while mEPSC amplitudes remained unchanged (2.5 mM Ca<sup>2+</sup>: 19.4±2.5 pA, 0 Ca<sup>2+</sup>: 20±2.4 pA,  $p=0.45$ ). Additional application of baclofen further reduced mEPSC frequencies (from 0.58±0.12 Hz to 0.41±0.1 Hz,  $p=0.007$ ; Figure 3-2 C), also without affecting quantal amplitudes (Baclofen in 0 Ca<sup>2+</sup>: 21.5±3 pA,  $p=0.32$ ). The relative decrease of mEPSC frequencies by GABA<sub>B</sub>Rs activation was very similar in the presence or absence of extracellular Ca<sup>2+</sup> (reduction in 2.5 mM Ca<sup>2+</sup>: 31.4%, in 0 Ca<sup>2+</sup>: 29.3%).

In summary, the data from experiments in area CA1 of hippocampal slice preparations indicate that GABA<sub>B</sub>R activation may have an additional effect on transmitter release that acts independently of the modulation of VDCC.

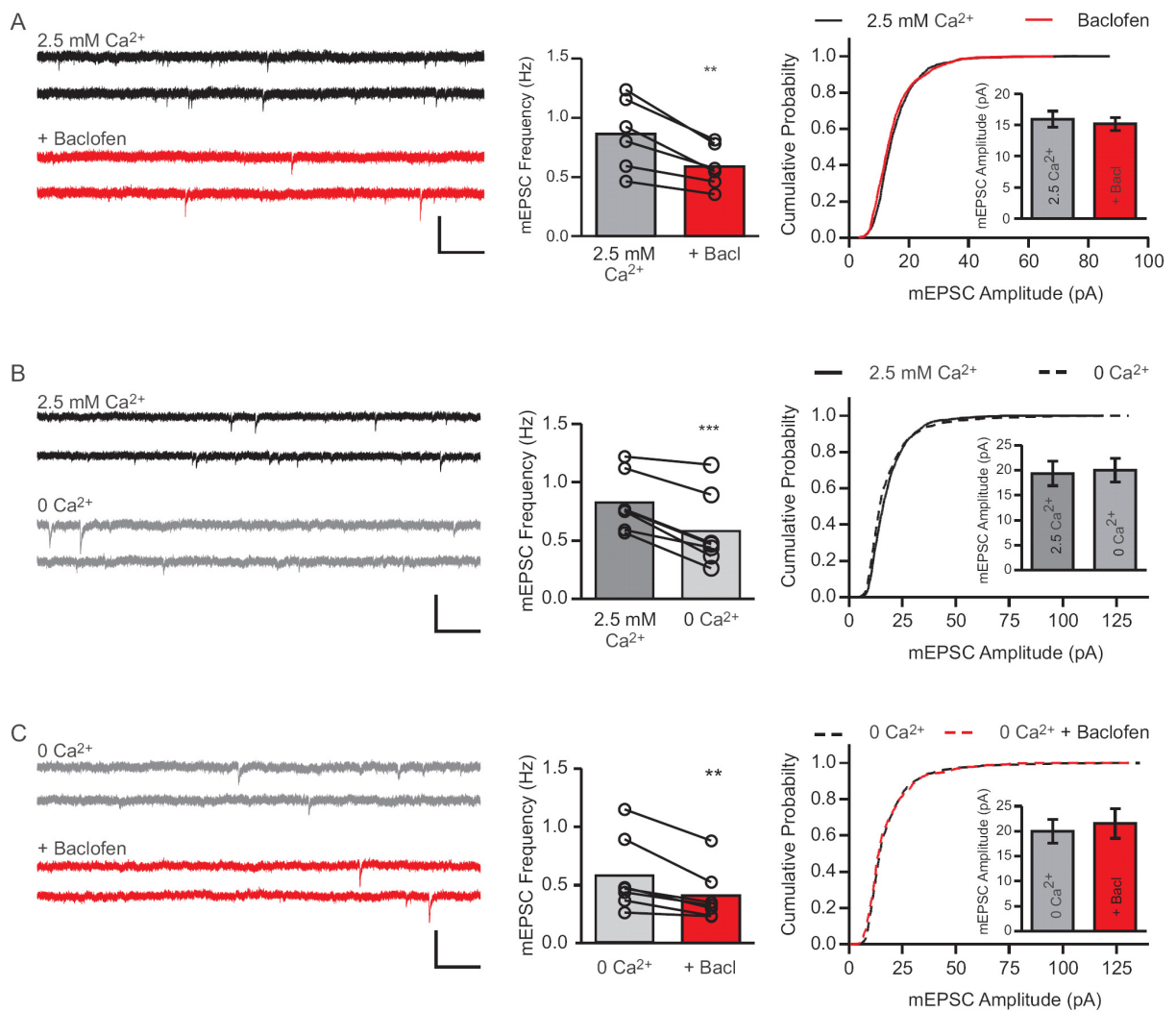


**Figure 3-2: Baclofen reduces the mEPSC frequency, but does not alter the amplitude of quantal events in CA1 pyramidal neurons.**

(A) GABA<sub>B</sub>R activation by baclofen causes a decrease in mEPSC frequency, without changing mEPSC amplitudes ( $n=6$ ). (B) Removal of extracellular Ca<sup>2+</sup> leads to a reduction of mEPSC frequency, without significantly changing the quantal amplitude ( $n=7$ ). (C) 30  $\mu$ M baclofen applied after removal of Ca<sup>2+</sup> further decreases the mEPSC frequency ( $n=7$ ). Scale bars are 1 s and 50 pA in all panels.

### 3.1.3 Investigation of GABA<sub>B</sub>R-mediated inhibition in autaptic cultures

To investigate a possible inhibitory mechanism of GABA<sub>B</sub>Rs acting downstream of VDCCs, we established autaptic cultures of hippocampal pyramidal neurons (see 2.1.2). With these isolated, self-innervating neurons it is possible to control the pre- and postsynaptic element with only one patch pipette. The cultures also enable us to incubate neuron with different toxins over longer time periods, an experimental option that is not feasible in acute slice experiments. Further, rapid applications of hypertonic sucrose solutions on autaptic neurons allow eliciting transmitter release by a Ca<sup>2+</sup>-independent stimulus (Rosenmund and Stevens, 1996). As modulatory changes of presynaptic Ca<sup>2+</sup> influx alone does not alter the sucrose triggered response, these cultures offer ideal experimental conditions to study the modulation of vesicle exocytosis by GABA<sub>B</sub>Rs, while bypassing Ca<sup>2+</sup> triggering of neurotransmitter release. In total, it is possible to record three different forms of transmitter release from an autaptic neuron within one experiment: AP-triggered EPSCs (Ca<sup>2+</sup>-dependent), spontaneous mEPSCs (eventually Ca<sup>2+</sup>-dependent) and sucrose-evoked release (Ca<sup>2+</sup>-independent). We first determined the sensitivity of autaptic EPSCs to baclofen treatment, showing similar effects as obtained from the fEPSP recordings in hippocampal slices. Baclofen inhibited autaptic EPSCs with an IC<sub>50</sub> of 0.86 μM and suppressed the autaptic EPSC by maximally 82±8% (Figure 3-3 A, B). Next, we applied short pulses of 30 μM baclofen to investigate the kinetics of the GABA<sub>B</sub>R effect on spontaneous neurotransmission (Figure 3-3 C). A reduction of mEPSC frequency was already present within the first second of drug application, with comparable latencies as the postsynaptic activation of GIRK currents, which we measured simultaneously in the same neuron. Similar to the observations from acute slices, we found that GABA<sub>B</sub>R activation decreased the incidence of spontaneous transmitter release to the same extent in standard extracellular Ca<sup>2+</sup> as in Ca<sup>2+</sup>-free (+1 mM EGTA) conditions (decrease in 2 mM Ca<sup>2+</sup>: 49.7±8%; in 0 Ca<sup>2+</sup>: 51.0±8%). mEPSC amplitudes were not altered in baclofen compared to control conditions (Figure 3-3 D).

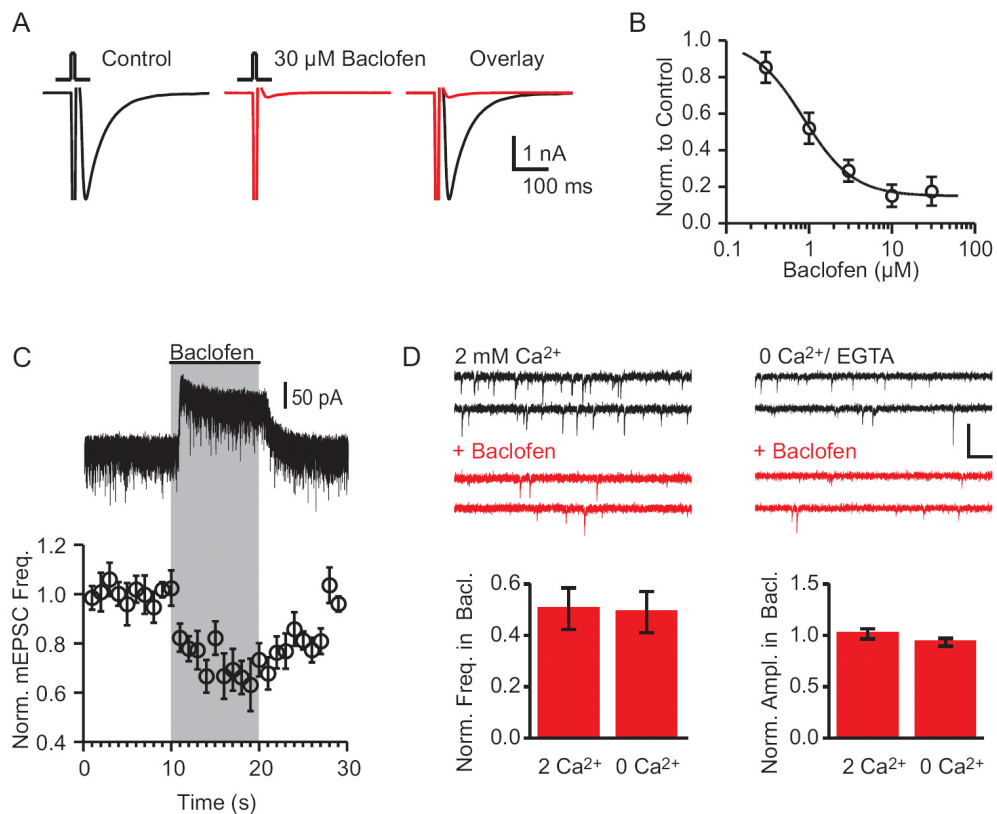


**Figure 3-3: Autaptic cultures of hippocampal pyramidal neurons are useful tools to study mechanisms of presynaptic inhibition by GABA<sub>B</sub>Rs.**

(A) Strong inhibition of EPSCs by baclofen application in autaptic cultures. Action potentials were evoked by square pulse depolarisations to 0 mV for 1 ms at 0.2 Hz. (B) Dose-response curve for baclofen effects on autaptic EPSCs ( $n=4$  to  $7$ ). (C) GABA<sub>B</sub>Rs decrease mEPSC frequencies in a comparable time course as the activation of postsynaptic GIRK conductances, shown as an outward current in the upper trace ( $n=9$ ). (D) mEPSC recordings in autaptic neurons in 2 mM Ca<sup>2+</sup> and Ca<sup>2+</sup>-free conditions. Scale bar is 100 ms, 100 pA. mEPSC frequencies are decreased to a similar extent by 30 μM baclofen in Ca<sup>2+</sup>-containing and Ca<sup>2+</sup>-free solution, while mEPSC amplitudes are not affected by baclofen (2 mM Ca<sup>2+</sup>:  $n=7$ ; 0 Ca<sup>2+</sup>:  $n=8$ ).

At the reticulospinal synapse of the lamprey spinal chord it was found that presynaptic, VDCC-independent inhibition by serotonergic receptors causes a reduction in mEPSC amplitudes (Photowala, *et al.*, 2006), and a later study described changes in the decay kinetics of evoked EPSCs caused by activation of presynaptic 5-HT receptors (Schwartz, *et al.*, 2007). These observations were interpreted as indicative for a change of the transmitter release mode, which alters transmitter concentration dynamics in the synaptic cleft and the postsynaptic response. It was therefore suggested that presynaptic G-protein coupled receptors can inhibit full fusion of neurotransmitter vesicles via Gβγ subunits, causing incomplete (“kiss and run”) transmitter release. We analysed the amplitude, rise time, half width and

decay time constant of mEPSCs both in  $\text{Ca}^{2+}$ -containing and  $\text{Ca}^{2+}$ -free extracellular solution and found no significant difference between control conditions and baclofen application (Table 6). Since no mEPSC parameter beside the frequency was altered in baclofen as would be expected for transient, “kiss and run” fusion, our findings argue against an alteration of the fusion mode by direct inhibition of the release process.

Table 6: GABA<sub>B</sub>R-induced changes of frequency, amplitude and kinetics of mEPSCs measured in autaptic cultures in  $\text{Ca}^{2+}$ -containing and  $\text{Ca}^{2+}$ -free conditions.

	2 mM $\text{Ca}^{2+}$ , $n=7$			0 $\text{Ca}^{2+}$ , $n=8$		
	Control	Baclofen	t-test*	Control	Baclofen	t-test*
Frequency (Hz)	17.51±3.9	8.6±2.8	$p=0.02$	9.1±2.8	5.3±2.2	$p=0.001$
Amplitude (pA)	21.6±2.6	22.1±2.9	n.s.	18.1±1.4	16.9±1.5	n.s.
Rise time (ms)	0.35±0.03	0.33±0.02	n.s.	0.35±0.02	0.35±0.02	n.s.
Half width (ms)	2.62±0.10	2.59±0.11	n.s.	2.62±0.06	2.65±0.11	n.s.
Decay time constant (ms)	4.61±0.35	4.31±0.19	n.s.	4.28±0.21	4.35±0.24	n.s.

\* Statistics were evaluated using paired two-tailed Student's t-test.

### 3.1.4 Presynaptic inhibition by GABA<sub>B</sub>Rs depends on Gα<sub>i</sub>/Gα<sub>o</sub>-proteins

Early studies on GABA<sub>B</sub>Rs proposed that the inhibition of glutamate release by GABA<sub>B</sub>Rs in CA1 was independent of Gα<sub>i</sub>/Gα<sub>o</sub>-proteins, while GIRK-mediated hyperpolarization of the postsynaptic element by GABA<sub>B</sub>Rs was abolished by treatment of neurons with Pertussis toxin (PTX) (Dutar and Nicoll, 1988; Thompson and Gahwiler, 1992). As a G-protein-independent mechanism of presynaptic inhibition appears contradictory to the common view of GPCR signalling, we addressed the issue by incubating autaptic cultures with 500 ng/ml PTX for 48 h before testing the function of presynaptic GABA<sub>B</sub>Rs. In all PTX-pretreated neurons tested, 30 μM baclofen failed to inhibit EPSCs to the same extent as in untreated neurons (90.1±2.6% of control vs. 16.3±3.2% of control in untreated cells; Figure 3-4 A, B). Likewise, mEPSC frequencies were not reduced by baclofen in PTX-treated neurons in  $\text{Ca}^{2+}$ -containing or  $\text{Ca}^{2+}$ -free conditions (in  $\text{Ca}^{2+}$ : 98.6±2.6% of control; in 0  $\text{Ca}^{2+}$ : 111.2±8.2% of control; Figure 3-4 C, D). We therefore conclude that presynaptic inhibition of AP-triggered

EPSCs and mEPSCs in  $\text{Ca}^{2+}$ -containing and  $\text{Ca}^{2+}$ -free conditions depends on the PTX-sensitive  $\text{G}\alpha_i/\text{G}\alpha_o$ -proteins.

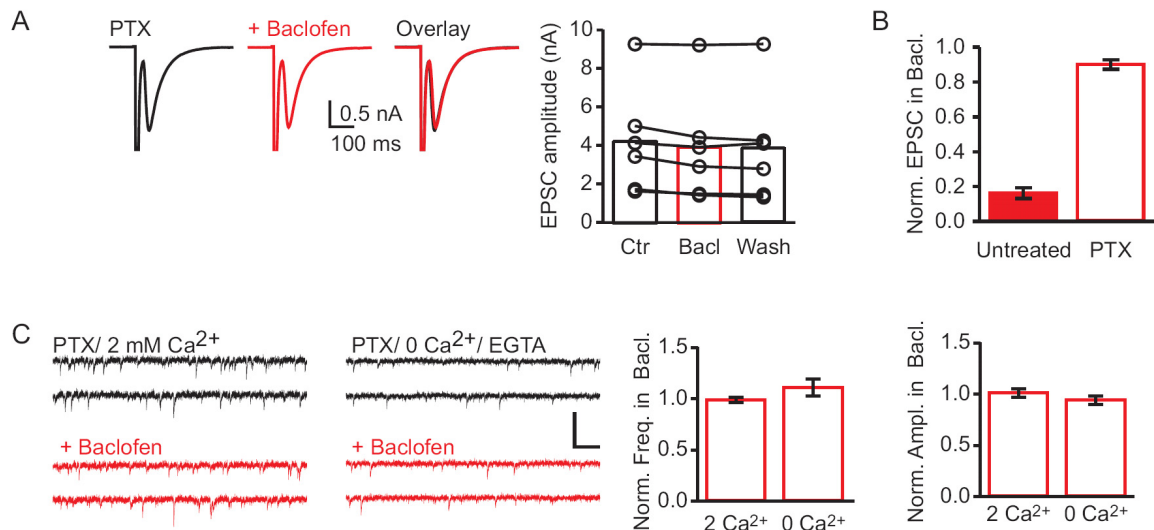


**Figure 3-4: Pertussis toxin treatment of autaptic cultures abolishes presynaptic inhibition by  $\text{GABA}_B$ Rs.**

(A)  $\text{GABA}_B$ Rs activated by baclofen fail to inhibit action potential evoked release in neuronal cultures incubated with Pertussis toxin (PTX,  $n=6$ ) (B) Comparison of the baclofen effect on autaptic EPSCs in untreated and PTX treated neurons. (C) Example traces of mEPSC recordings in PTX treated autaptic neurons. Scale bar is 100 ms, 100 pA. (D) Frequency and amplitude of mEPSCs are not significantly altered by baclofen in PTX-treated cultures (2 mM  $\text{Ca}^{2+}$ :  $n=8$ ; 0  $\text{Ca}^{2+}$ :  $n=7$ ).

### 3.1.5 $\text{GABA}_B$ Rs inhibit transmitter release evoked by hypertonic stimuli

As already described before, the combination of autaptic cultures with electrophysiological recordings and fast applications of hypertonic solutions allows to study transmitter release that occurs independent of  $\text{Ca}^{2+}$  influx. It also allows to assess the total number of fusion competent vesicles, which are referred to as the readily releasable pool (RRP). Vesicles that constitute the RRP completed the docking and priming steps and are in principle available for  $\text{Ca}^{2+}$ -triggered transmitter release (Rosenmund and Stevens, 1996). The amount of transmitter released by hypertonic stimuli depends on the hypertonic strength: it saturates around 500 mM sucrose, whereas 250 mM sucrose only depletes a fraction of the RRP consisting of those vesicles that face a low energy barrier for fusion (see Figure 3-5 A and Figure 3-7 D).

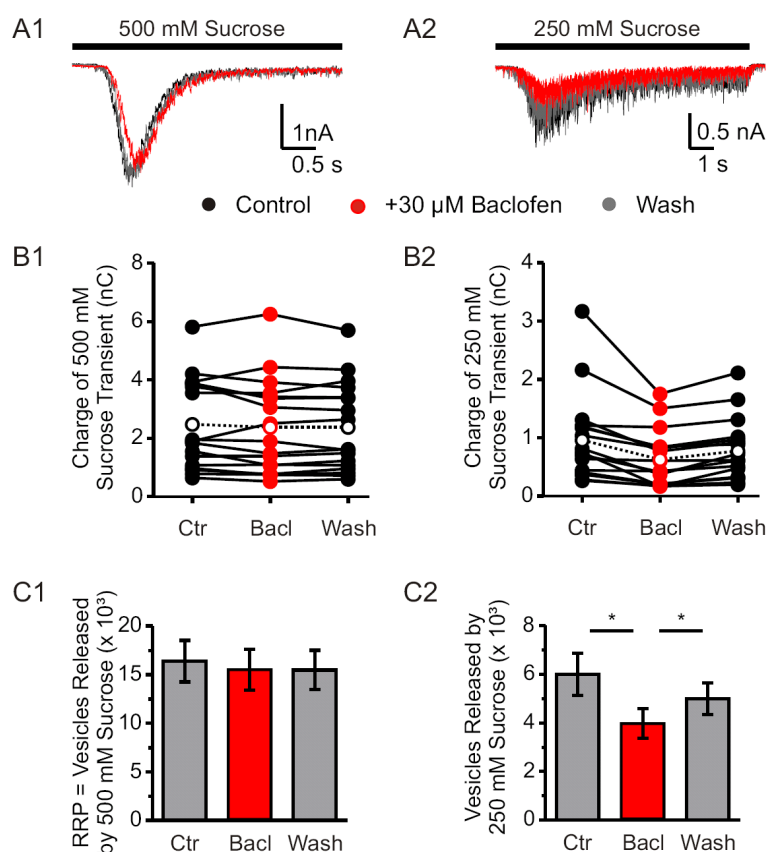


**Figure 3-5: GABA<sub>B</sub>R activation does not change the size of the RRP, but decreases the number of vesicles released by hypertonic stimuli of intermediate strength.**

Hypertonic solutions of 500 mM (A1) or 250 mM sucrose (A2) were applied in absence or presence of baclofen. (B1) No alteration of the charge of the 500 mM sucrose response in 30  $\mu$ M baclofen, whereas (B2) the charge of the 250 mM sucrose transient is significantly smaller in the presence of baclofen. Averages are indicated by open circles and dashed lines ( $n=17$  for all panels). (C1) GABA<sub>B</sub>R activation does not alter the number of vesicles in the RRP. (C2) The number of vesicles released by the intermediate sucrose concentration is significantly smaller in baclofen ( $p<0.001$ ).

In this experimental setting where transmitter release occurs independent of Ca<sup>2+</sup> influx and therefore inhibition of VDCCs does not play a role, we investigated the efficiency of vesicle exocytosis by repetitively applying 500 and 250 mM sucrose stimuli in absence or presence of 30  $\mu$ M baclofen (Figure 3-5 A1, A2 and see also Figure 2-4 C). By these means we were able to directly probe whether GABA<sub>B</sub>R signalling influences the energy barrier for vesicle fusion. The charge of the excitatory transient evoked by 500 mM sucrose was not changed in baclofen (Figure 3-5 B1, 500 mM-control:  $2.48\pm 0.38$  nC vs. + baclofen:  $2.38\pm 0.39$  nC), thus GABA<sub>B</sub>R activation did not alter the total number of vesicles in the RRP (Figure 3-5 C1, 500 mM-control:  $16.3\pm 2.2\cdot 10^3$  vs. +baclofen:  $15.4\pm 2.1\cdot 10^3$  vesicles,  $n=17$ ,  $p>0.05$ ). However, responses to 250 mM sucrose were significantly smaller in baclofen (Figure 3-5 B2,

---

250 mM-control:  $0.96 \pm 0.18$  nC vs. +baclofen:  $0.63 \pm 0.12$  nC), which means that GABA<sub>B</sub>R activation resulted in a reduced number of vesicles released by the intermediate hypertonic stimulus (Figure 3-5 C2, 250 mM-control:  $5.9 \pm 0.8 \cdot 10^3$  vesicles vs. +baclofen:  $3.9 \pm 0.6 \cdot 10^3$ ,  $n=17$ ,  $p < 0.001$ ). Consequently, the fraction of vesicle released from the RRP by 250 mM sucrose significantly decreased from  $38.8 \pm 3.5\%$  to  $26 \pm 2.5\%$  by GABA<sub>B</sub>R activation, a reduction of about 33%. In a couple of control experiments, sucrose stimuli were applied first in the presence of baclofen and then in control solutions. We found that the order of drug applications had no influence on the results.

### **3.1.6 Kinetics of sucrose-evoked release are slowed by GABA<sub>B</sub>R activation**

The above analyses of the effect of baclofen on the number of vesicles released by hypertonic solutions revealed that GABA<sub>B</sub>R activation does not change the total number of docked and primed vesicles in synaptic terminals, but reduces the likeliness of transmitter release triggered by intermediate hypertonicities. This implies a reduction of the vesicular “fusion willingness”, which is caused by an increase in the energy barrier for vesicle fusion. If this is the case, it should manifest in a decrease of the maximal release rate during the sucrose responses, a delayed onset as well a slowed decay of the transients.

We analysed the peak vesicular release rates for all conditions by plotting the cumulative number of vesicles released by hypertonic stimuli over time and determining the peak release rate as maximal slope of the curve (Figure 3-6 A). We found that in the presence of baclofen the peak vesicular release rates of the transients elicited by 500 mM sucrose were significantly reduced, on average from  $30032 \pm 4448$  to  $23521 \pm 3221$  vesicles/s ( $n=17$ ,  $p=0.0025$ ), a reduction of  $19.5 \pm 3\%$  (Figure 3-6 B). The peak release rates of the 250 mM sucrose-evoked transients were reduced by  $45.8 \pm 3.7\%$ , from  $3704 \pm 622$  to  $1909 \pm 310$  vesicles/s ( $n=17$ ,  $p < 0.0001$ ).

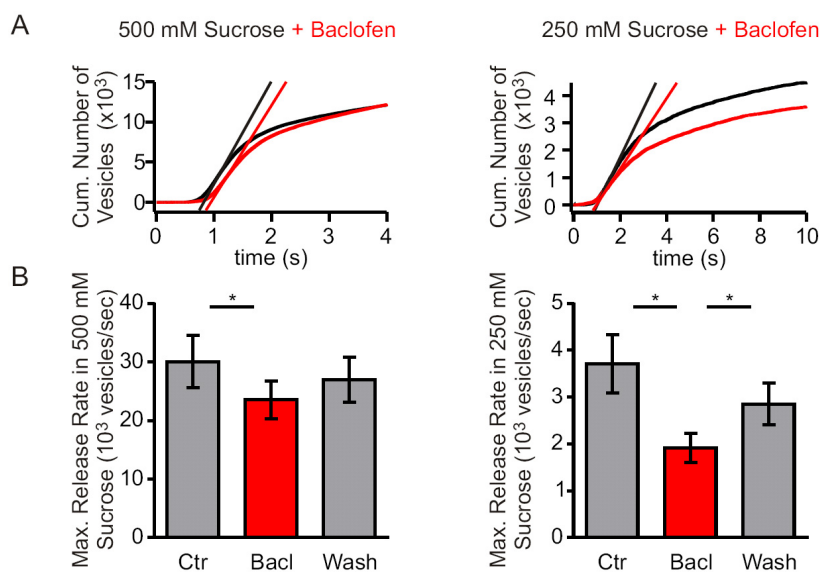


**Figure 3-6: Peak release rates of sucrose-evoked release are slowed in baclofen.**

(A) Cumulative plots of vesicles released by 500 and 250 mM sucrose from a single experiment. Release kinetics are slowed and the total number of vesicles released by 250 mM sucrose decreases in the presence of baclofen. Linear fits indicate the maximum slope of the curves as peak release rates. (B) GABA<sub>B</sub>R activation significantly decreases peak release rates in both sucrose concentrations ( $p < 0.01$ , repeated measures ANOVA with Bonferroni's post test; all  $n = 17$ ).

In addition, the onset kinetics of the sucrose transients were significantly delayed upon GABA<sub>B</sub>R activation (Figure 3-7 A, 500 mM-control:  $0.52 \pm 0.01$  s vs. +baclofen:  $0.64 \pm 0.02$  s,  $n = 17$ ,  $p < 0.0001$ ; 250 mM-control:  $0.91 \pm 0.06$  s vs. +baclofen:  $1.2 \pm 0.10$  s,  $n = 17$ ,  $p < 0.001$ ). Also the decay kinetics of the sucrose-evoked current transients were slower for both 500 and 250 mM sucrose (Figure 3-7 B, 500 mM-control  $0.42 \pm 0.03$  s vs. +baclofen  $0.51 \pm 0.02$  s,  $n = 17$ ,  $p < 0.0001$ ; 250 mM-control:  $1.58 \pm 0.08$  s vs. +baclofen:  $1.82 \pm 0.13$  s,  $n = 17$ , n.s.). A correlation of the decay time constants with the onset latencies illustrates this shift towards slower kinetics in baclofen (Figure 3-7 C). The vesicular fusion rate increases with the amount of osmotic energy supplied in a dose-dependent manner, while the total number of vesicles released is limited and therefore saturates at 500 mM sucrose, as indicated by the data fit in Figure 3-7 D. GABA<sub>B</sub>R activation slows the release and decreases the number of vesicles released along that fit. These observations are indicative for an increase in the energy barrier for vesicle fusion by GABA<sub>B</sub>Rs. While at 500 mM sucrose the effect is not strong enough to decrease the number of vesicles but only slows the release kinetics, the increase in the energy barrier leads to both a reduced number of released vesicles and a slowing of the fusion rate at intermediate hypertonic strength.

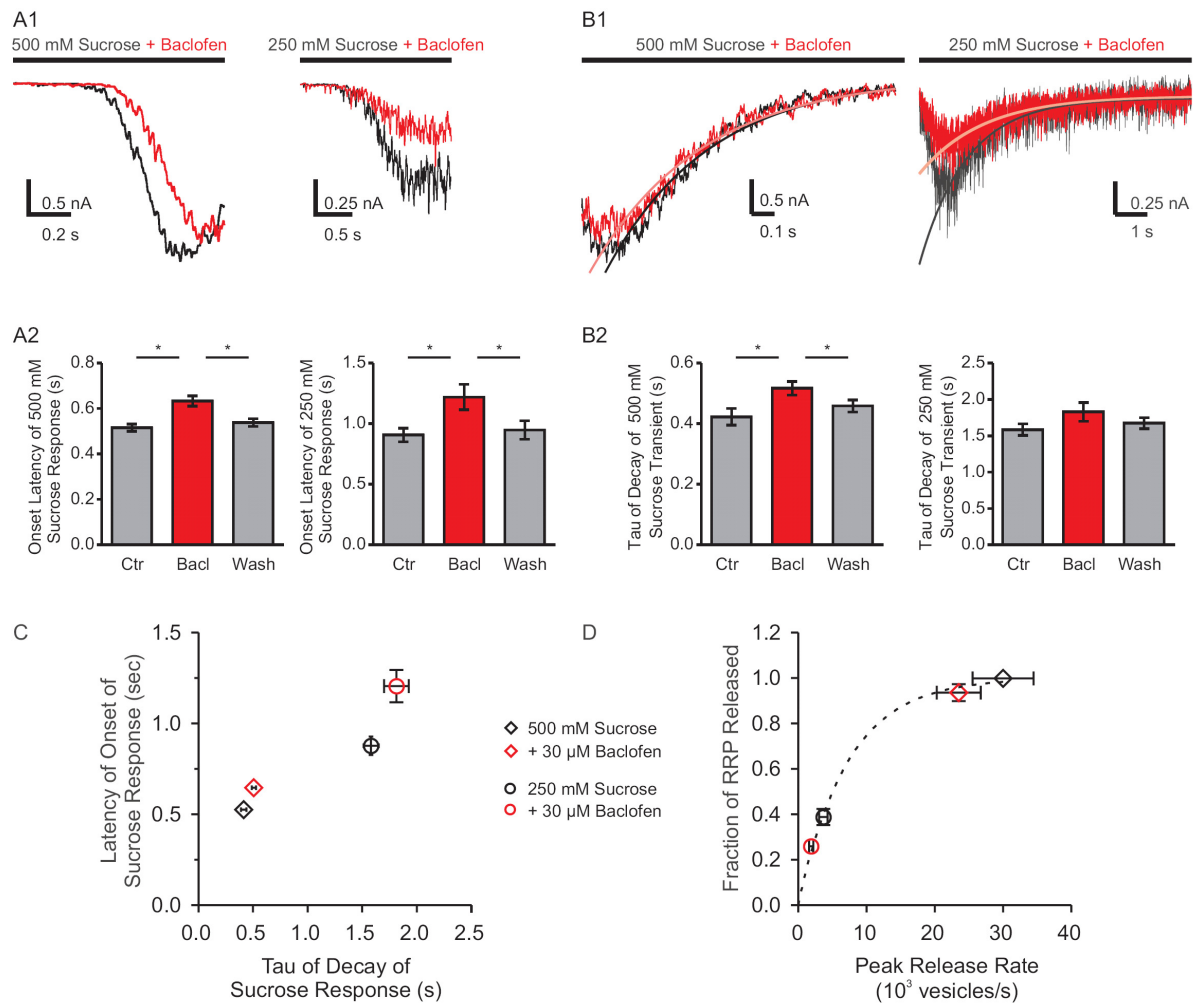


**Figure 3-7: GABA<sub>B</sub>R activation slows the kinetics of transmitter release evoked by hypertonic stimuli.**

(A1) Onset kinetics of responses to 500 mM and 250 mM sucrose. For illustration, traces were filtered with a digital low pass filter at 50 Hz. (A2) Addition of 30  $\mu$ M baclofen significantly delays the onset of the sucrose responses ( $p < 0.01$ , repeated measures ANOVA with Bonferroni's post test). (B1) Overlay of responses with monoexponential fits to estimate decay time constants. 500 mM sucrose traces were aligned at peak for illustration. Washout traces not shown. (B2) The decay of the 500 mM sucrose transients is slowed in the presence of baclofen ( $p < 0.01$ ; change of 250 mM responses n.s.). (C) Correlation of decay time constants and onset latencies from above. The prolonged decay time constant of the sucrose response by baclofen is paralleled by a delayed response onset. (D) Correlation of the fraction of vesicles released from the RRP and the peak release rate in the absence or presence of baclofen. As GABA<sub>B</sub>R activation decreases the peak release rate, it also decreases the fraction of vesicles released from the RRP during submaximal hypertonic stimuli. The dashed line indicates a data fit representing the saturating response to increasing concentrations of sucrose ( $n = 17$  for all panels).

### 3.1.7 BoNT-A treatment does not abolish direct inhibition of transmitter release by GABA<sub>B</sub>Rs

The data so far argues for a scenario in which metabotropic GABA<sub>B</sub>R signalling affects the release machinery in a way that increases the energy demand for overcoming the fusion barrier for vesicle release. The question arises which specific molecular components of the release apparatus might be targets of presynaptic GABA<sub>B</sub>Rs inhibition. Recent studies in the lamprey spinal cord and on dense core vesicle release in PC12 cells (a rat cell line derived from a pheochromocytoma of the adrenal medulla) implicated that Gβγ subunits might compete with synaptotagmin I for the interaction with the C-terminus of SNAP-25 (Blackmer, *et al.*, 2005; Gerachshenko, *et al.*, 2005). As synaptotagmin is the high affinity Ca<sup>2+</sup> sensor of the release machinery, this might be an effective way of inhibiting Ca<sup>2+</sup> triggered vesicle fusion directly at the release step. Botulinum neurotoxin A (BoNT-A) cleaves off the last nine amino acids from the C-terminus of SNAP-25 that supposedly represent the binding site for Gβγ; and treatment of neurons with this neurotoxin was shown to abolish direct inhibition of vesicle fusion (Gerachshenko, *et al.*, 2005).

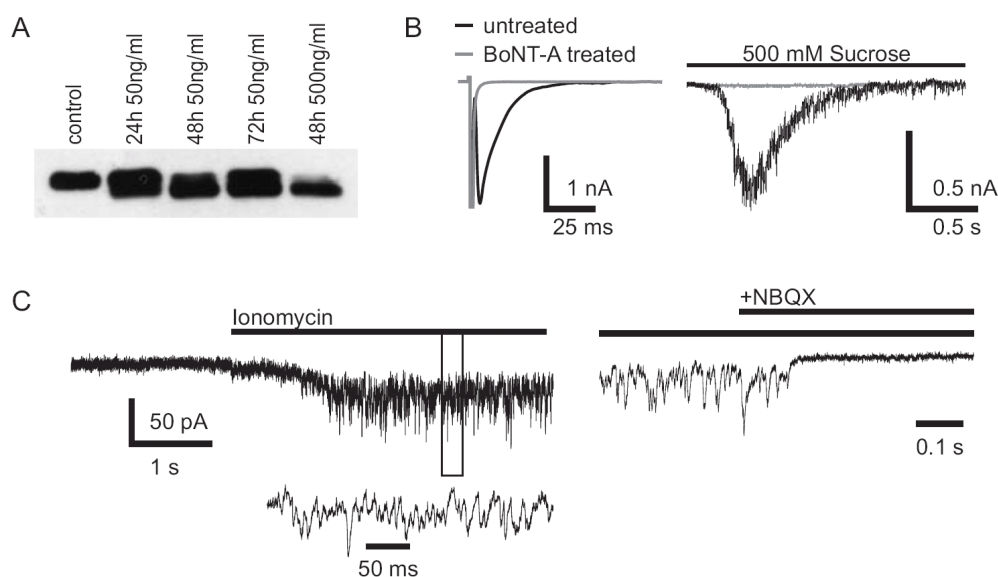


**Figure 3-8: Full cleavage of SNAP-25 by extensive treatment of neuronal cultures with BoNT-A.**

(A) 48 h incubation of neuronal cultures with 500 ng/ml of BoNT-A is sufficient for full cleavage of SNAP-25. The toxin cleaves the C-terminal nine amino acids, thereby reducing the molecular mass from 25 to 22.5 kDa, as confirmed by western blots. (B) BoNT-A treatment totally abolishes AP-triggered transmitter release in autaptic cultures. Likewise, transmitter release by hypertonic solutions is abolished in BoNT-A treated neurons. (C) 2 μM ionomycin was used to restore transmitter release in BoNT-A treated cells. Inset shows quantal nature of the evoked release. 10 μM NBQX fully blocks ionomycin-induced excitatory currents.

We treated autaptic cultures with BoNT-A in order to test a possible block of GABA<sub>B</sub>R-mediated inhibition of vesicle release by SNAP-25 cleavage. To achieve full cleavage of the protein, a 48 hour incubation of neuronal cultures with 500 ng/ml BoNT-A was required, as observed by western blot detection of SNAP-25 (Figure 3-8 A). This resulted in complete silencing of transmission with respect to AP-triggered release, release evoked by hyperosmotic solutions and spontaneous transmitter release (Figure 3-8 B, C). In the case of a remaining EPSC, recordings were discarded. In order to trigger neurotransmitter release from these neurons, we applied 2  $\mu$ M ionomycin in standard extracellular solution containing 2 mM Ca<sup>2+</sup>. Ionomycin introduces artificial Ca<sup>2+</sup>-permeable pores into the membrane and raises the intracellular Ca<sup>2+</sup> concentration (Liu and Hermann, 1978), and was used to restore release in BoNT-A treated cultures (Capogna, *et al.*, 1997). Ionomycin evoked a steady inward current consisting of multiple superimposed release events (Figure 3-8 C). All ionomycin-induced currents were completely blocked by 10  $\mu$ M NBQX, confirming that this procedure evoked no other conductances except for AMPA receptor-mediated currents (Figure 3-8 C and Figure 3-11 A).

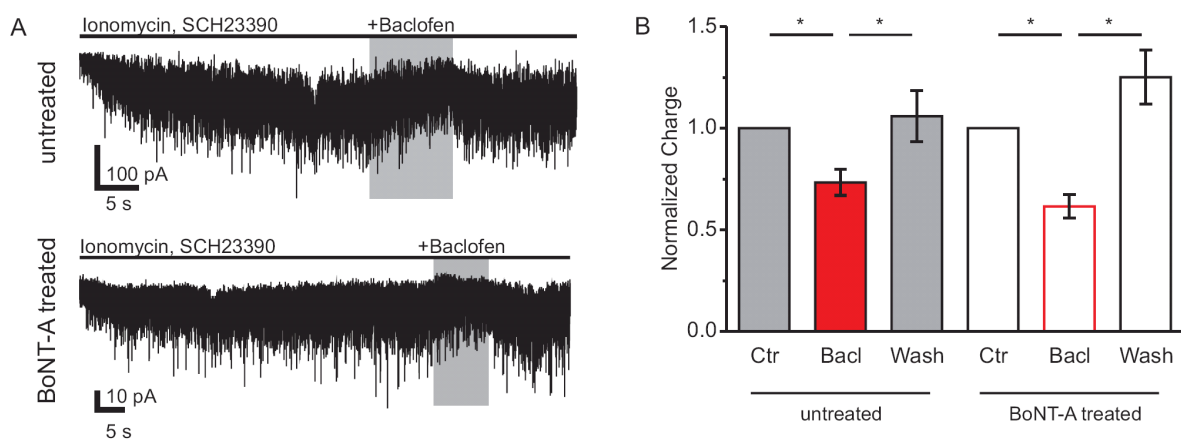


**Figure 3-9: Cleavage of SNAP-25 with BoNT-A does not abolish presynaptic inhibition by GABA<sub>B</sub>Rs.**

(A) Baclofen applied during the steady state of ionomycin-induced vesicle fusion inhibits transmitter release in both untreated and BoNT-A treated cultures. Note that the ionomycin evoked release is much weaker in BoNT-A treated cultures than in control cultures. 20  $\mu$ M SCH23390 was applied at least 90 s before start of the ionomycin application and was present throughout the recordings. (B) Similar effects of baclofen in untreated and treated neurons ( $p < 0.05$ , repeated measures ANOVA with Bonferroni's post test; untreated:  $n=11$ , BoNT-A treated:  $n=9$ ).

We waited until a steady state of ionomycin-induced release was reached, and then applied additionally 30  $\mu$ M baclofen for 10 s (Figure 3-9 A). As analysis of individual miniature

EPSCs was not feasible in these recordings, we calculated the total charge of release over 4 s before, during and after baclofen application. In order to block GIRK channels that could be activated by postsynaptic GABA<sub>B</sub>Rs and confound the analysis of release by charge calculation, these experiments were performed in the continuous presence of 20 μM SCH23390, and the effectiveness of the block was controlled by short baclofen applications in all recordings (Figure 3-10). We found that GABA<sub>B</sub>R activation by baclofen reversibly reduced the ionomycin-evoked charge to  $73.4 \pm 6.5\%$  of control in untreated cultures. In the BoNT-A treated cultures, baclofen reduced the ionomycin evoked transmitter release to  $61.5 \pm 5.7\%$  of control (Figure 3-9 B). Importantly, this effect was not significantly different between the two conditions ( $p=0.2$ ), indicating that cleavage of SNAP-25 does not abolish direct presynaptic inhibition by GABA<sub>B</sub>Rs.

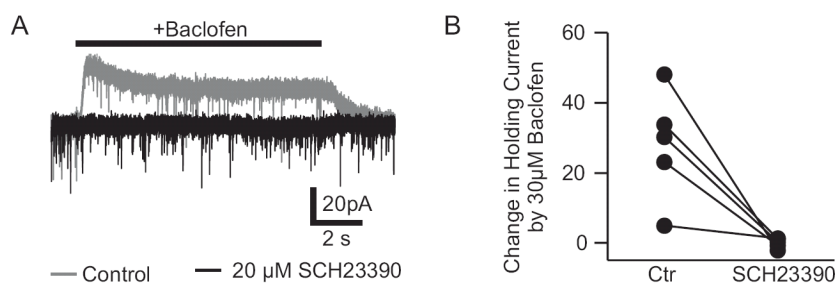


**Figure 3-10: SCH23390 can be used to block GIRK-mediated currents activated by postsynaptic GABA<sub>B</sub>Rs.**

(A) 30 μM baclofen induces hyperpolarizing currents in control neurons (grey trace). When the same neuron is preincubated with 20 μM SCH23390 for 90 s, these currents are completely abolished (black trace). (B) Summary of five neurons incubated with 20 μM SCH23390, which blocked baclofen-induced changes of the holding current.

In order to validate these observations we designed another set of experiments not requiring a block of postsynaptic GIRK currents by SCH23390: During the ionomycin evoked release transient we first applied baclofen alone, and subsequently again in the presence of 10 μM NBQX, which blocks all AMPA receptor-mediated currents and unmask the GIRK current (Figure 3-11 A). This enabled us to subtract the GIRK currents from the baclofen-induced change of the ionomycin transients (Figure 3-11 B, C). Again, we found a significant and reversible decrease of the ionomycin-induced transmitter release by baclofen after the GIRK current subtraction both in untreated as well as BoNT-A treated autaptic cultures (untreated:  $66.6 \pm 7.2\%$  of control,  $n=9$ ,  $p<0.001$ ; BoNT-A treated:  $75.6 \pm 10.8\%$  of control,  $n=10$ ,  $p<0.05$ ).

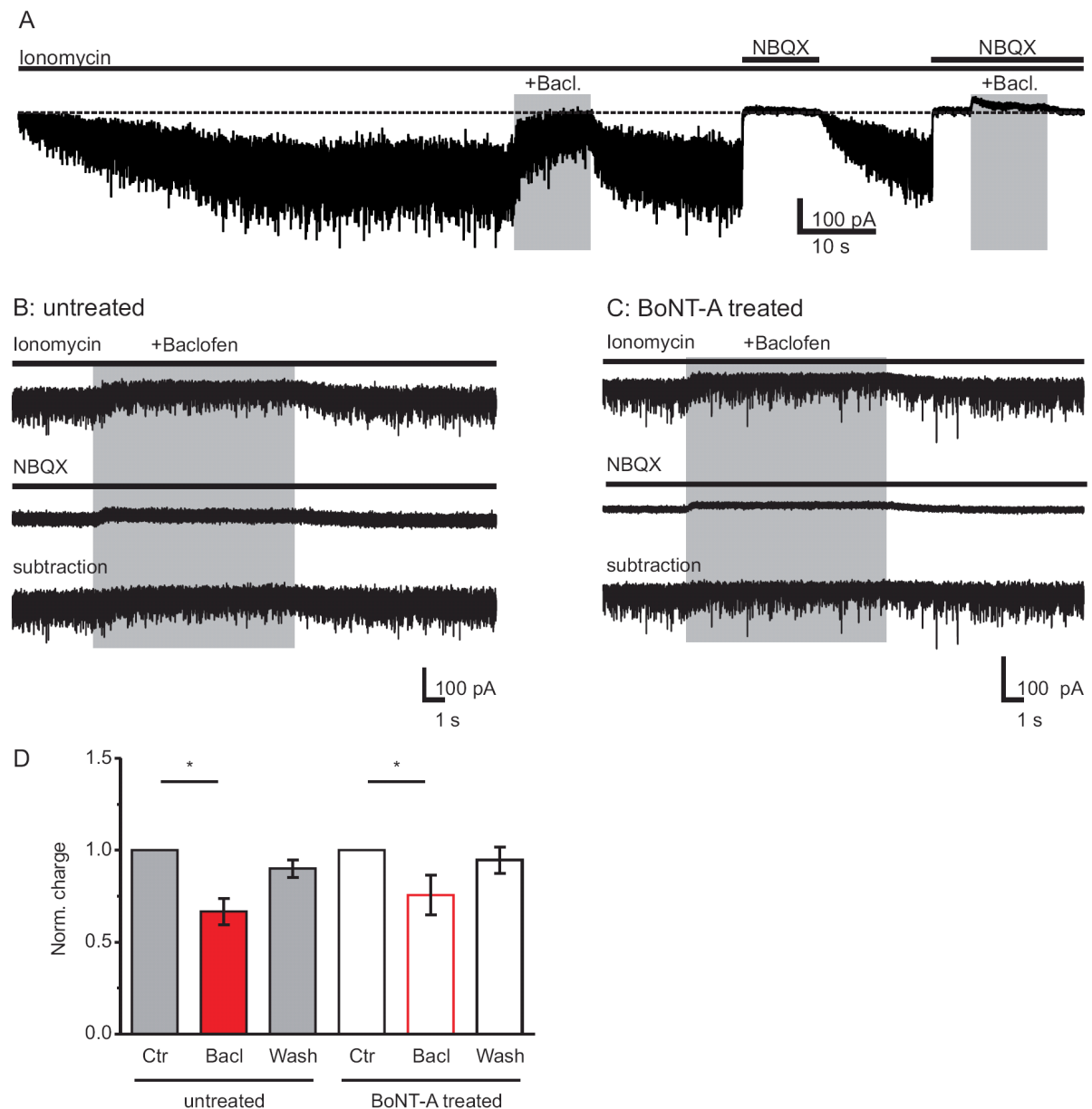


**Figure 3-11: Subtraction of non-AMPA receptor currents during baclofen application from the ionomycin-induced release events confirms that cleavage of SNAP-25 by BoNT-A does not occlude direct inhibition of transmitter release by GABA<sub>B</sub>Rs.**

(A) Representative experiment with ionomycin application on a control cell and subsequent application of 30  $\mu$ M baclofen, 10  $\mu$ M NBQX and baclofen in the presence of NBQX. Block of AMPA receptor-mediated currents by NBQX shifts the holding current back to baseline (dashed line). (B) Baclofen was applied for 10 s during the steady-state of ionomycin-triggered release. GIRK-mediated currents activated by postsynaptic GABA<sub>B</sub>Rs are unveiled by application of baclofen in the presence of NBQX. Post-hoc subtraction of the GIRK-mediated current reveals a decrease of transmitter release during baclofen application. (C) After cleavage of SNAP-25 with BoNT-A, GABA<sub>B</sub>R activation still decreases ionomycin-induced transmitter release. (D) GABA<sub>B</sub>R-mediated inhibition of ionomycin-induced release in untreated and BoNT-A treated neurons ( $p < 0.05$ , repeated measures ANOVA with Bonferroni's post test;  $n = 9$  and  $n = 10$ ). Direct comparison of the effect shows no significant difference between control cells and neurons treated with BoNT-A ( $p = 0.51$ ).

The two sets of experiments using ionomycin add some important aspects to our understanding of presynaptic inhibition by GABA<sub>B</sub>R. First, they verify the findings by Capogna and co-workers that transmitter release triggered by Ca<sup>2+</sup> influx through ionomycin pores can be inhibited by presynaptic GPCRs (Capogna, *et al.*, 1996). Here the source of Ca<sup>2+</sup> is independent of presynaptic VDCCs, and it is highly unlikely that G-protein-signalling interferes with Ca<sup>2+</sup> influx through the ionomycin pores. Thus one may conclude that presynaptic GPCRs do interfere with Ca<sup>2+</sup> evoked transmitter release downstream of the VDCCs. We excluded postsynaptic GIRK currents as a confounding aspect of GABA<sub>B</sub>R signalling, and also show that ionomycin induces no other currents beside the AMPA receptor-dependent synaptic EPSCs; two controls that have not been performed in former studies. Finally, in combination with BoNT-A preincubation of the autaptic cultures, we found the C-terminus of SNAP-25 not necessary for direct inhibition of the fusion process by presynaptic GABA<sub>B</sub>Rs.

In summary, we have found evidence that GABA<sub>B</sub>Rs affect transmission via two G-protein-dependent pathways, one involving classical reduction of Ca<sup>2+</sup> influx through VDCCs, and a second, downstream pathway that leads to an increase of the energy barrier for vesicle fusion. The second signalling pathway seems not to involve the C-terminus of SNAP-25, because it is not abolished by pre-incubation with BoNT-A. It remains the scope of future studies to define the exact molecular mechanism of direct inhibition at the release machinery.

---

### 3.2 GABA<sub>B</sub>R-mediated inhibition at mossy fibre terminals and characterization of autaptic hippocampal granule cells

In the previous chapter, our investigations on the modulation of glutamatergic transmission by GABA<sub>B</sub>Rs based on experiments on Schaffer collateral synapses in CA1 of hippocampal slice preparations. At these synapses, we found evidence for a VDCC-independent mechanism of transmitter release inhibition, in parallel to the VDCC-dependent form of presynaptic inhibition. Obviously it was of interest for us to know whether VDCC-independent presynaptic inhibition by GABA<sub>B</sub>Rs is a general mechanism that can also be found at other glutamatergic terminals. To address this question, we decided to investigate mossy fibre (MF) synapses onto CA3 pyramidal cells, which are remarkably different from Schaffer collateral synapses in CA1 (for reviews, see Henze, *et al.*, 2000; Nicoll and Schmitz, 2005). Forming the second glutamatergic synapses in the trisynaptic hippocampal circuitry, they exhibit (i) an unusually low basal release probability, (ii) a strong presynaptic suppression of transmitter release by group II metabotropic glutamate receptors (mGluR 2/3), and (iii), a presynaptic form of long-term plasticity that is independent of NMDA receptor activation. The morphological features of these synapses are similarly remarkable: The presynaptic elements form so-called boutons, which are very large in diameter (2-5 µm), and contact CA3 pyramidal neurons in stratum lucidum only. Unlike many other terminals, MF boutons contain multiple release sites, and can be identified by synaptopodin (synaptophysin 2) as a molecular marker. They express presynaptic metabotropic group II glutamate receptors (mGluR 2/3) as glutamatergic autoreceptors, while the postsynaptic side harbours ionotropic kainate receptors, which add a slow component to the fast AMPA receptor-mediated EPSP.

Investigations on MF synaptic transmission are challenged by a number of technical obstacles that need to be overcome. First, granule cells are only sparsely connected to CA3 pyramidal cells. Selective stimulation of MF inputs is difficult due to the complexity of the circuitry in the CA3 region, so evoked postsynaptic responses are easily contaminated by other inputs stimulated unintentionally, namely associational/commissural fibres (Henze, *et al.*, 2000). Second, due to multiple inputs by other glutamatergic synapses onto CA3 pyramidal cells, it is practically impossible to record pure MF mEPSCs from CA3 pyramidal cells. However, the analysis of mEPSC amplitude and frequency is regarded inevitable for investigating basic characteristics of a synapse (Del Castillo and Katz, 1954; Redman, 1990), imposing the need

for alternative strategies to record MF mEPSCs. We decided to develop autaptic cultures of hippocampal granule cells, which enabled us to record pure mossy fibre mEPSCs from neurons that receive only MF inputs (see 3.2.4).

To adequately address the problem of selective stimulation of MF inputs in slices, a recording of synaptic responses in CA3 has to fulfil a number of criteria to be reckoned as “pure” mossy fibre experiment (Nicoll and Schmitz, 2005): First, one should test short-term plasticity behaviour of the input, which is remarkably strong for MFs. When the stimulation frequency is increased from low (0.05 Hz) to moderate (1 Hz), the postsynaptic response should increase by >300% (Figure 3-12 B). This is not the case for the neighbouring associational/commissural or perforant path synapses, which show only mild frequency facilitation. Low basal release probability and strong short-term plasticity are accompanied by a high paired pulse ratio, which is >2 for interstimulus intervals of 50 ms (Figure 3-12 C). Second, MF responses are extremely sensitive to agonists of mGluR 2/3 (Figure 3-12 D). 10  $\mu$ M L-CCG I or 1  $\mu$ M DCG IV, which at these concentrations are selective for mGluR 2/3, should completely abolish any postsynaptic response in a mossy fibre experiment. In case of an incomplete block of the postsynaptic response by these drugs, the recording should be regarded as contaminated by other inputs and discarded.

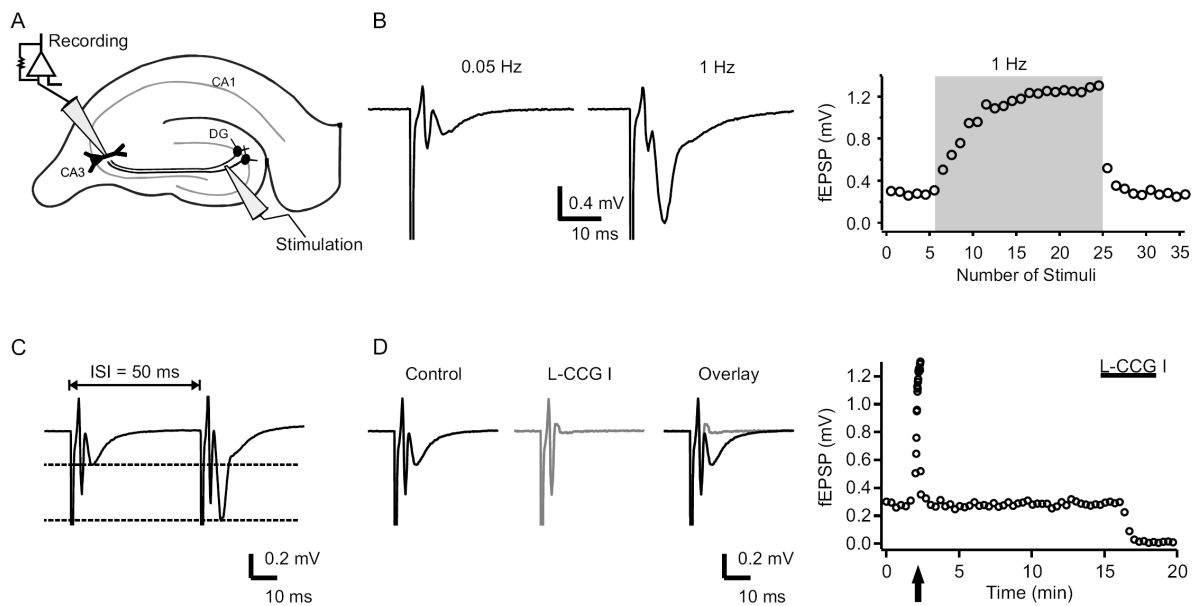


**Figure 3-12: Configuration and quality standards for electrophysiological field recordings of mossy fibre synaptic transmission.**

(A) Recording configuration for mossy fibre field experiments. The stimulation electrode is placed in the hilus of the dentate gyrus, and the recording electrode in stratum lucidum of CA3. (B) fEPSPs plotted over stimulus number. The stimulation frequency was increased from 0.05 to 1 Hz. Traces are from the same experiment and represent averages of 5 sweeps. (C) Mossy fibre transmission shows strong paired pulse facilitation. Paired pulse ratio is typically  $>2$  for an inter-stimulus interval of 50 ms. (D) Application of 10  $\mu\text{M}$  L-CCG I completely blocks postsynaptic responses in pure mossy fibre recordings. Time plot on the right shows fEPSP amplitudes plotted over time. The black arrow indicates 1 Hz stimulation for 20 seconds.

### 3.2.1 Modulation of fEPSPs and presynaptic calcium signals at mossy fibre synapses by GABA<sub>B</sub>Rs

We first characterized the impact of GABA<sub>B</sub>R-mediated inhibition on MF fEPSPs in CA3. Postsynaptic responses were completely blocked by 30  $\mu\text{M}$  baclofen ( $6.6 \pm 0.9\%$  of control; Figure 3-13 A). Using photodiode imaging of presynaptic Ca<sup>2+</sup> transients visualized by Magnesium Green-AM (Invitrogen) we found that baclofen likewise decreased the presynaptic Ca<sup>2+</sup> influx into MF terminals with a maximal effect of  $14.5 \pm 2.2\%$  (Figure 3-13 B). We determined an IC<sub>50</sub> of 0.2  $\mu\text{M}$  baclofen for fEPSPs and 0.8  $\mu\text{M}$  baclofen for presynaptic Ca<sup>2+</sup> influx, indicating that transmitter release from MF is even more sensitive to baclofen than release from Schaffer collateral synapses (1.26  $\mu\text{M}$  for fEPSPs and 2.05  $\mu\text{M}$  for Ca<sup>2+</sup> influx; see Figure 3-1).

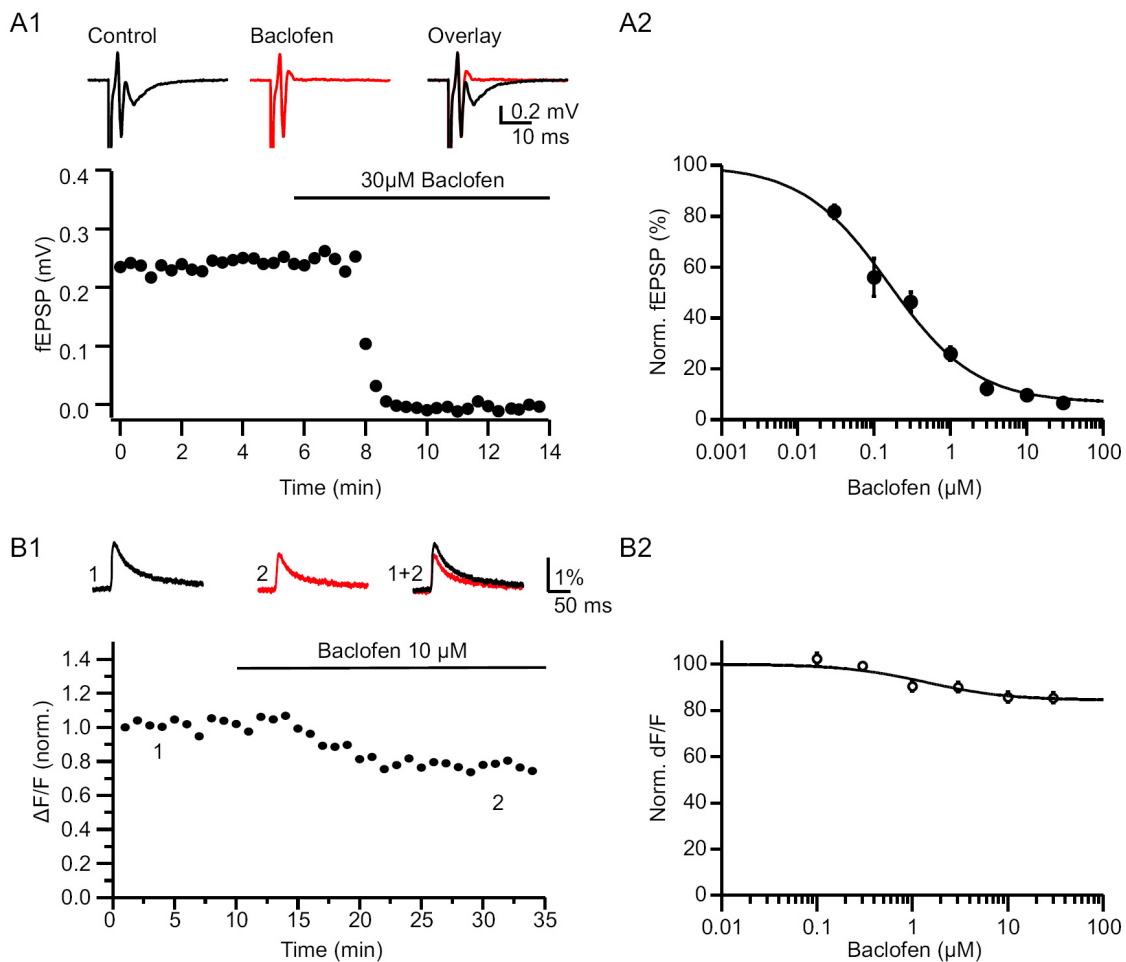


**Figure 3-13: Activation of presynaptic  $\text{GABA}_\text{B}$ Rs strongly inhibits transmitter release from mossy fibres and decreases presynaptic  $\text{Ca}^{2+}$  influx.**

(A1) Bath application of 30  $\mu\text{M}$  baclofen profoundly decreases MF fEPSPs in CA3. (A2) Dose-response curve for increasing concentrations (0.03, 0.1, 0.3, 1, 3, 10 and 30  $\mu\text{M}$ ) of baclofen (all  $n=5-6$ ). (B1)  $\text{Ca}^{2+}$  transients elicited by extracellular tract stimulation were visualized with Magnesium green and measured using a photodiode. Baclofen reliably caused a reduction of the  $\text{Ca}^{2+}$  signal in mossy fibre terminals. (B2) Dose response curve for the effect of baclofen on presynaptic  $\text{Ca}^{2+}$  influx.

### 3.2.2 Baclofen decreases calcium transients in single mossy fibre boutons

$\text{Ca}^{2+}$  imaging experiments using a photodiode lack spatial resolution and could be confounded by signals from other labelled structures than presynaptic terminals, as the diode detects the sum of all fluorescence in the field of view. We therefore performed confocal time-lapse recordings using a Nipkow spinning disc system with a sensitive CCD camera and a laser as source of excitation light (see methods 2.2.5 for details). The main advantage of this system is that it allows to record  $\text{Ca}^{2+}$  signals at a high speed in a confocal manner, with a lateral pixel size of 0.4  $\mu\text{m}$ . The high spatial resolution enabled us to identify individual, dye-labelled

boutons that were monitored throughout the experiment (Figure 3-14 A). As the mossy fibre forms a very laminar tract in stratum lucidum of CA3 it was possible to label fibres from extracellular with a cell-permeant AM-ester of Oregon Green BAPTA-1 and to identify boutons outside of the loading spot, where they were surrounded by unstained tissue (Figure 3-14 A). For analysis of the signal, background fluorescence from unstrained structures was subtracted from the signals recorded from labelled boutons, and peaks of exponential functions fitted into the decay of  $\text{Ca}^{2+}$  signals were used to determine the AP-triggered  $\text{Ca}^{2+}$  transients relative to baseline  $\text{Ca}^{2+}$  signals ( $\Delta\text{F}/\text{F}$ ). By the use of this high resolution imaging at the level of single terminals we found that 30  $\mu\text{M}$  baclofen reduced presynaptic  $\text{Ca}^{2+}$  influx into MF boutons to  $86.3\pm 6.2\%$  of control, very similar to the value obtained with the photodiode imaging ( $85.5\pm 2.2\%$ ).

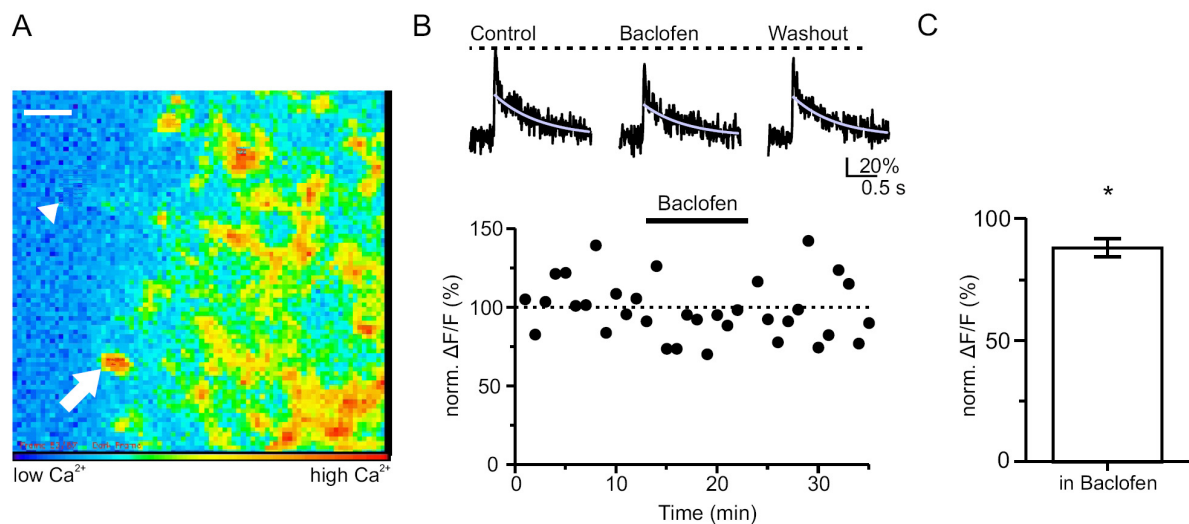


**Figure 3-14: Baclofen effect on presynaptic  $\text{Ca}^{2+}$  transients in mossy fibre boutons recorded by high resolution confocal Nipkow spinning disc imaging.**

(A) False colour picture generated by the Neuroplex software during acquisition of AP-triggered  $\text{Ca}^{2+}$  signals, captured with the “RedShirt NeuroCCD-SMQ” camera. Image shows average of five frames of highest fluorescence intensities, of which a dark frame image was subtracted. Arrow indicates the identified bouton recorded throughout the session, while arrowhead indicates background area. Scale bar represents 4  $\mu\text{m}$ . (B) Traces and time plot from the same bouton as in (A). Traces are averages of five sweeps each.  $\Delta\text{F}/\text{F}$  was calculated after background subtraction from the peak of an exponential function fitted into the decay, as indicated in the example traces. (C) Average represents the mean  $\text{Ca}^{2+}$  signal in baclofen over 5 min from 18 identified boutons ( $p=0.0043$ , one sample t-test against 100%).

### **3.2.3 Presynaptic GABAergic inhibition at mossy fibre terminals cannot be explained by a decrease of calcium influx alone**

As in all other synapses, changes in presynaptic  $\text{Ca}^{2+}$  influx into mossy fibre boutons affect transmitter release and hence the postsynaptic signal in a non-linear manner. Whether at this synapse the  $\text{GABA}_B\text{R}$  triggered inhibition of transmitter release could be fully explained by changes in  $\text{Ca}^{2+}$  influx can therefore only be estimated by comparing the baclofen effect on presynaptic  $\text{Ca}^{2+}$  influx and fEPSP with a power function describing the relation of the  $\text{Ca}^{2+}$  signal to the postsynaptic fEPSP. By lowering extracellular  $\text{Ca}^{2+}$  and recording presynaptic  $\text{Ca}^{2+}$  signals or, in a separate set of experiments, fEPSPs, we determined the power function for mossy fibre transmission by the same experimental approach as for Schaffer collateral synapses (see 3.1.1). A nonlinear regression fitted to the data revealed a power of 3.7 ( $R^2=0.97$ ; Figure 3-15), which is slightly lower compared to the power value of 4.1 obtained for Schaffer collateral synapses. Activation of  $\text{GABA}_B\text{Rs}$  with increasing baclofen concentrations (see also Figure 3-13) caused a much more pronounced reduction of the fEPSP in relation to the presynaptic  $\text{Ca}^{2+}$  signal. For this set of data we obtained a power value of 9.7 ( $R^2=0.63$ ), clearly indicating additional inhibitory mechanisms acting independent of the inhibition at the level of  $\text{Ca}^{2+}$  influx. Due to the lower power of the release function for mossy fibre-CA3 synapses and the higher power of the baclofen data fit found here, the offset corresponding to VDCC-independent inhibition of transmitter release is even larger than in CA1. This indicates that at mossy fibre terminals the impact of VDCC-independent inhibition by  $\text{GABA}_B\text{Rs}$  might be even more pronounced than at CA3-CA1 synapses.

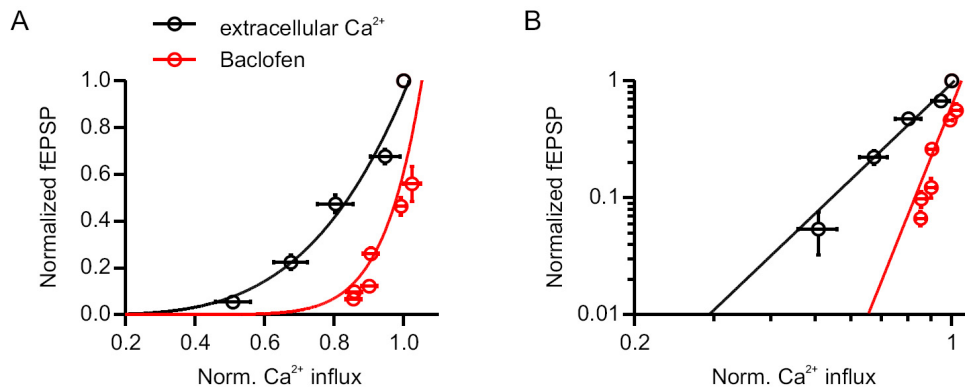


**Figure 3-15: Comparison of changes in Ca<sup>2+</sup> influx and fEPSP by manipulation of extracellular Ca<sup>2+</sup> or by GABA<sub>B</sub>R activation.**

(A) Correlation of Ca<sup>2+</sup> influx into MF terminals and the postsynaptic response. Extracellular Ca<sup>2+</sup> was changed from 2.5 mM to 2, 1.5, 1 and 0.5 mM (black circles). Increasing concentrations of baclofen (red circles; 0.1, 0.3, 1, 3, 10, 30 μM) were applied in 2.5 mM Ca<sup>2+</sup>. Note the difference of the baclofen data compared to the Ca<sup>2+</sup> data, showing a stronger effect on the fEPSP than expected for an equivalent reduction of presynaptic calcium influx (all  $n=5-6$ ). (B) Double logarithmic plot of the power function of transmitter release for mossy fibre synapses and the baclofen data. The slope of the baclofen data fit reveals a much higher exponent for the power function than for the fit of the control data.

### 3.2.4 Establishing autaptic cultures of hippocampal granule cells to study mossy fibre mEPSCs

As already stated above, recordings of mossy fibre mEPSCs are complicated in slice preparations. To investigate MF mEPSCs, some studies restricted quantal analysis of CA3 pyramidal cell recordings on kainate receptor-mediated events, isolated by their slow decay kinetics (Cossart, *et al.*, 2002; Epsztein, *et al.*, 2005), or by investigating asynchronous release in the presence of extracellular strontium (Bekkers and Clements, 1999; Marchal and Mulle, 2004; Breustedt, *et al.*, 2009). However, both approaches do not present a direct and unbiased measurement of mEPSCs. Still, in light of the results from slice experiments it was of interest to us whether GABA<sub>B</sub>Rs on MF boutons inhibit mEPSCs in the absence of extracellular Ca<sup>2+</sup>. We therefore established autaptic cultures of hippocampal granule cells, in which all synaptic contacts are formed by MF terminals and therefore guarantee recordings of isolated MF mEPSCs (see 2.1.3.3). Most of the results presented in the following section have been published in the European Journal of Neuroscience (Rost, *et al.*, 2010).

### 3.2.4.1 Morphological and pharmacological characterization of autaptic granule cells

To distinguish granule cells from non-granule cells in autaptic cultures, we first had to establish anatomical and morphological markers to identify granule cells in cultures. As already described for slice preparations and dissociated neuronal cultures (Grabs, *et al.*, 1994; Grosse, *et al.*, 2003), we found that autaptic granule cells express synaptoporin in their presynaptic terminals (Figure 3-16). This allowed us to reliably distinguish them from non-granule cells and to evaluate the purity of our dentate gyrus preparations. During the course of our studies we assessed the fraction of synaptoporin positive neurons of 296 microislands in total from four different preparations and found on average  $38.3 \pm 5.5\%$  isolated autaptic neurons stained positive for synaptoporin.

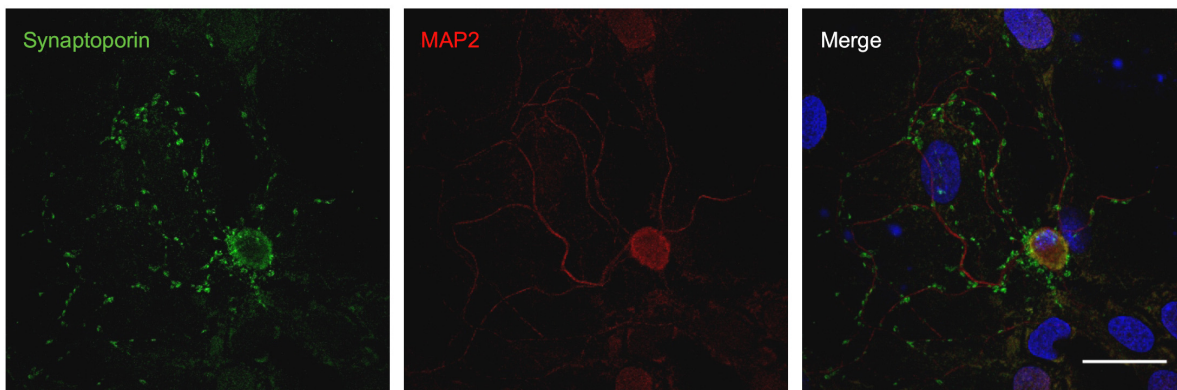


**Figure 3-16: Synaptoporin is a marker specific for hippocampal granule cells.**

Granule cells grown on glia microislands for 20 days *in vitro* express synaptoporin (green) in the presynaptic terminals. Cells were double-stained with anti-MAP2 (red), labelling the dendrites. Nuclei are visualised by blue DAPI staining, indicating also the location of glial cells in the overlay (scale bar: 25  $\mu\text{m}$ ).

Besides defining a morphological marker for autaptic granule cells it was necessary to also functionally identify autaptic granule cells in an ongoing electrophysiological experiment. We therefore sought to test the pharmacological criteria established for mossy fibre recordings in rodent hippocampal slices (see 3.2) in our recordings of autaptic granule cells. Indeed we found that 10  $\mu\text{M}$  L-CCG I inhibited EPSCs recorded from autaptic neurons to a variable extent, ranging from no effect to nearly full block of transmission (Figure 3-17 A, B). We performed a K-means cluster analysis for two populations of cells on 121 recorded neurons, using both EPSC amplitude and suppression by L-CCG I as criteria (Figure 3-17 A; error bars indicate standard error). The mean EPSC amplitude of the first cluster was  $2.62 \pm 2.056$  nA and

---

mean normalised EPSC under L-CCG I was  $28.1 \pm 14.3\%$  of control. EPSC amplitudes in this cluster were in the range of 0.284 to 8.924 nA, and normalised EPSCs under L-CCG I ranged from 0.9 to 55.0% of control. The second cluster comprised cells with a mean EPSC amplitude of  $5.176 \pm 4.947$  nA, and a mean normalised EPSC under L-CCG I of  $83.6 \pm 16\%$ . EPSC amplitudes ranged from 0.466 to 24.142 nA, and normalised EPSCs under L-CCG I were between 57.3 and 115.3% of control. Based on these results and in light of an earlier study on guinea pig granule cells (Tong, *et al.*, 1996), we considered neurons with  $<40\%$  remaining EPSC amplitude under L-CCG I to be granule cells (average:  $22 \pm 3\%$ ,  $n=53$ ; Figure 3-17 B). Conversely, those neurons exhibiting  $>80\%$  EPSC after application of L-CCG I were considered pyramidal cells (average:  $93.6 \pm 16.8\%$ ,  $n=31$ ). Cells with intermediate levels of EPSC suppression by L-CCG I were not included in further analyses, representing a “safety margin” between the two populations of interest. In general, granule cells were found to have smaller amplitudes ( $2.327 \pm 0.32$  nA) compared to pyramidal cells ( $4.852 \pm 0.871$  nA), whereas the paired pulse ratio was not significantly different for the two cell types (granule cells:  $1.053 \pm 0.073$ ,  $n=23$ ; pyramidal cells:  $0.913 \pm 0.04$ ,  $n=22$ ;  $p=0.095$ ). In granule cells, application of  $10 \mu\text{M}$  L-CCG I significantly increased the paired pulse ratio of two EPSCs triggered at 50 ms interval, underlining the presynaptic action of mGluR 2/3 (Figure 3-17 C).

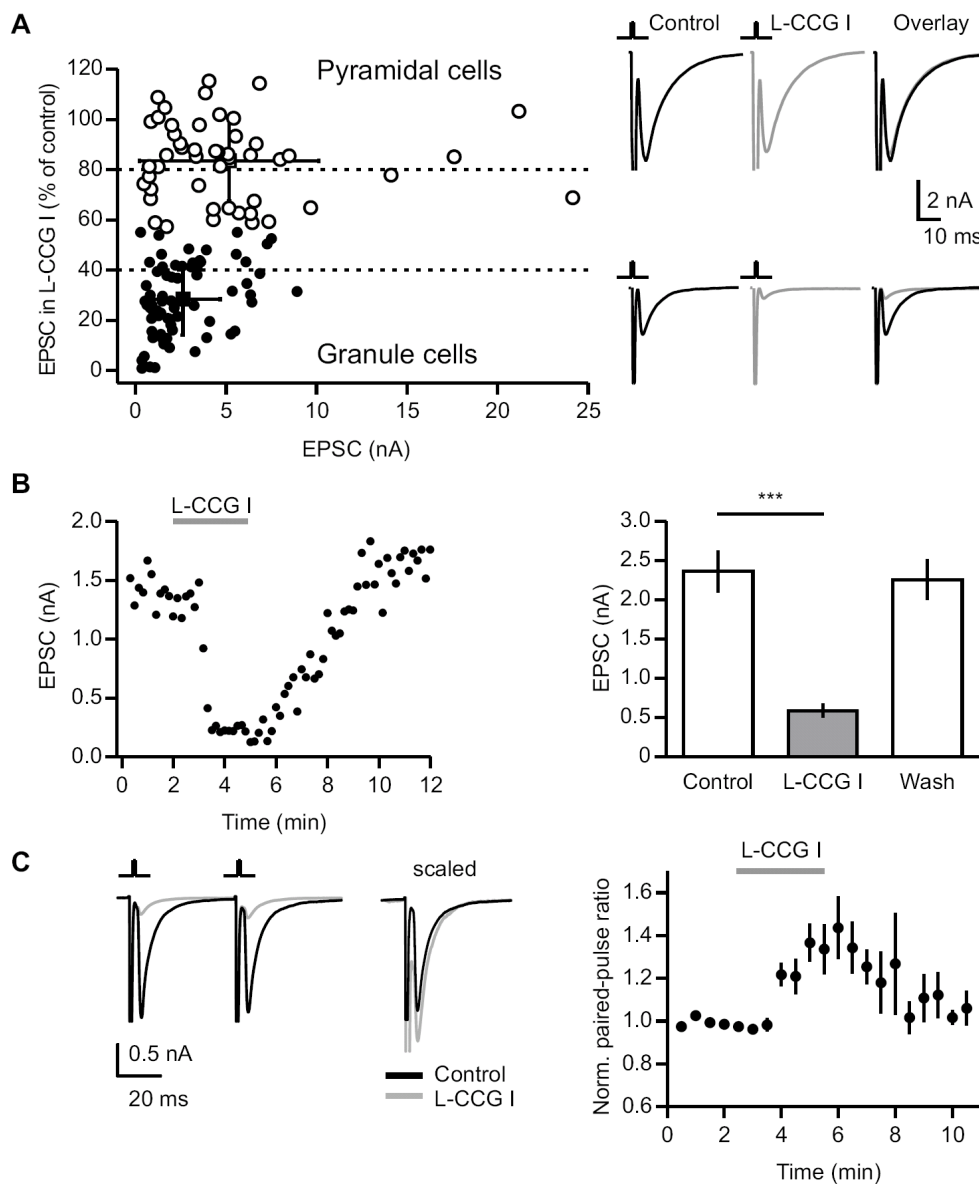


**Figure 3-17: Inhibition of transmitter release by activation of presynaptic mGluR 2/3 can be used to identify granule cells in autaptic cultures.**

(A) In autaptic cultures of DG/CA3 preparations, glutamatergic neurons show a wide range of sensitivity to presynaptic inhibition by mGluR 2/3. EPSC amplitudes correlate with the sensitivity of transmitter release to application of 10  $\mu$ M L-CCG I. The remaining EPSC under L-CCG I normalised to control was used to define granule cells (<40% EPSC) and pyramidal cells (>80% EPSC), indicated by dashed lines. Granule cells have generally smaller amplitudes than pyramidal cells. Means of two clusters of cells with standard errors are represented by closed and open squares. (B) Time course of the L-CCG I effect on autaptic EPSCs from granule cells using the bath perfusion for drug application. 10  $\mu$ M L-CCG I reversibly suppresses transmitter release. The summary bar graph comprises both experiments with bath perfusion and L-CCG I administration via a fast applications system ( $n=53$ ,  $p<0.0001$ , paired Student's t-test). (C) L-CCG I causes an increase of the paired-pulse ratio (50 ms interstimulus interval,  $n=22$  cells). For scaled traces, the peak of the first EPSC under L-CCG I was normalized to the peak of the first EPSC in control conditions; only the second EPSC is shown.

We also aimed at combining the morphological and pharmacological characterization of autaptic neurons within the same experiment. Therefore, we filled a number of autaptic neurons with the fixable polar tracer Cascade Blue (Invitrogen) during whole cell recordings and L-CCG I applications. After post hoc immunocytochemistry for synaptoporin and MAP-2 we were able to retrieve 11 cells (Figure 3-18). These analyses revealed a good correlation of our pharmacological criteria with synaptoporin expression. Of 4 cells showing <40% remaining EPSC amplitude under L-CCG I, 3 neurons were synaptoporin positive (Figure 3-18 A), whereas 4 cells identified as pyramidal neurons were all synaptoporin negative (Figure 3-18 B). From the cell population exhibiting >40% and <80% EPSC under L-CCG I, 1 cell was synaptoporin positive and 2 cells were synaptoporin negative.

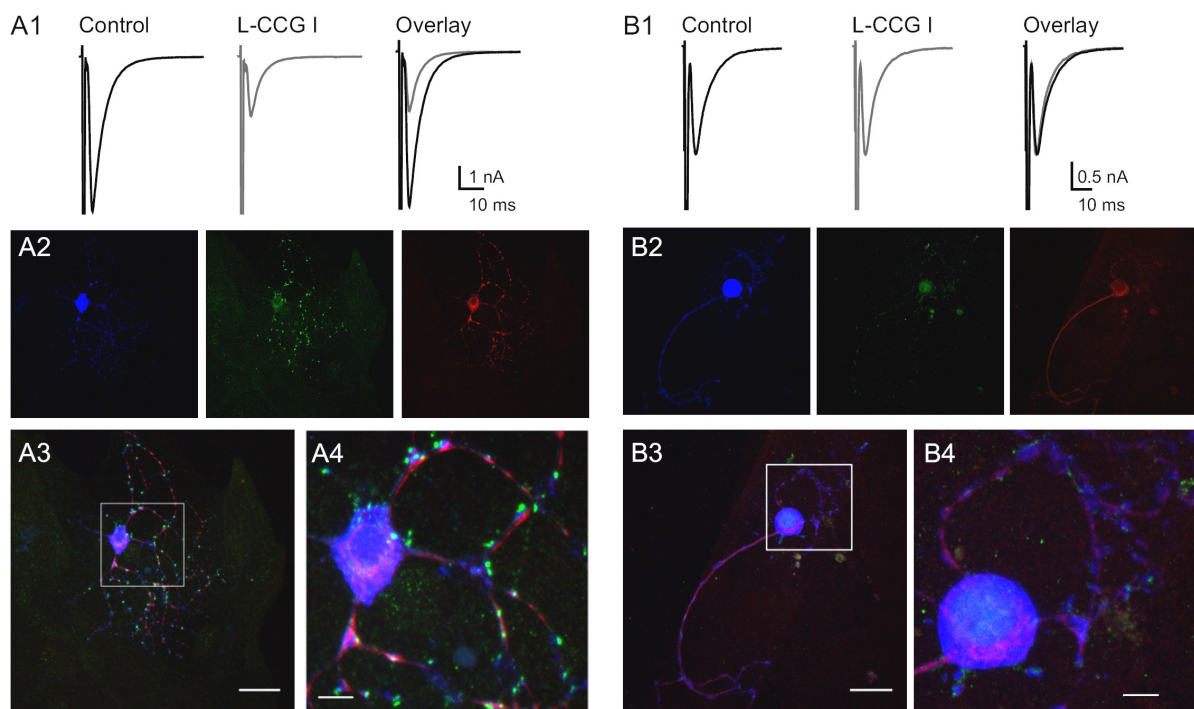


**Figure 3-18: Pharmacological characterization by L-CCG I application and subsequent immunocytochemistry for synaptoporin expression in the same autaptic neurons.**

(A1) Granule cell identified by a pronounced L-CCG I effect on the autaptic EPSC. The cell was filled with Cascade Blue during the recording. (A2) The blue fluorescence of the tracer enabled us to retrieve the recorded neuron after post-hoc immunocytochemistry for synaptoporin (green) and MAP-2 (red). Shown are maximal projections of a confocal z-stack for the three fluorescence channels. (A3) Overlay of the channels, displaying the complete cell. (A4) Magnification of inset in A3. Synaptoporin positive presynaptic terminals are clearly visible, targeting the dendrites. (B1) L-CCG I insensitive pyramidal cell. (B2) Immunocytochemical processing was performed as for the granule cell in A. (B3) Overlay indicating blue fluorescence of the tracer and MAP-2 immunoreactivity, but no synaptoporin expression. (B4) Magnification reveals some unspecific artefacts of green staining, but no specific synaptic labelling as seen for the granule cell. Scale bars in A3/B3 and A4/B4 are 20  $\mu\text{m}$  and 5  $\mu\text{m}$ .

### 3.2.4.2 Detailed characterization of granule cell in autaptic cultures

In the process of a more detailed characterization of autaptic granule cell cultures, we also compared L-CCG I with DCG IV, a more potent agonist for mGluR 2/3. We also analysed the readily releasable pool and the release probability of granule cells in comparison to pyramidal cells and their release during short trains of 1 Hz stimulation, and finally tested chemically-induced long-term plasticity of granule cells.

At concentrations of 100  $\mu\text{M}$  and higher, L-CCG I has been reported to activate also other metabotropic glutamate receptors that inhibit transmission in the hippocampus, mostly mGluR group III receptors at A/C fibre terminals (Kirschstein, *et al.*, 2004). In recordings on autaptic granule cells (Figure 3-19), we tested 10  $\mu\text{M}$  L-CCG I in direct comparison with another mGluR group II agonist, DCG IV, which is routinely used at concentrations of  $\leq 1 \mu\text{M}$  to verify pure mossy fibre recordings in hippocampal slice preparations (Nicoll and Schmitz, 2005). 0.1  $\mu\text{M}$  DCG IV reduced the autaptic EPSC to  $53.6 \pm 4.1\%$  in L-CCG I-sensitive neurons. 1  $\mu\text{M}$  DCG IV inhibited synaptic transmission to  $28.0 \pm 2.8\%$ , very similar to the effect of 10  $\mu\text{M}$  L-CCG I in the same cells ( $25.0 \pm 2.8\%$ ). The effect was not significantly different between the two drugs ( $n=7$ ,  $p=0.22$  paired Student's t-test), indicating that at the given concentrations, both substances can be equally used to pharmacologically identify autaptic granule cells.

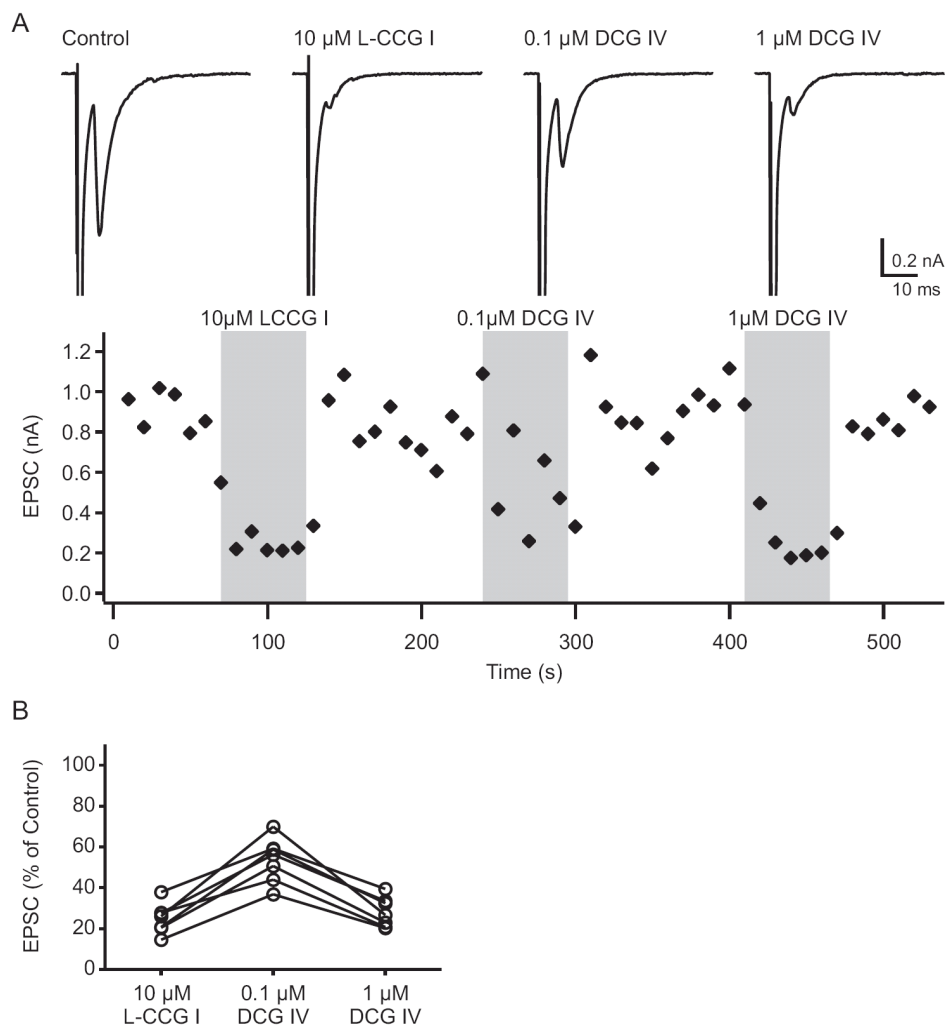


**Figure 3-19: Comparable efficacy of 1  $\mu$ M DCG IV and 10  $\mu$ M L-CCG I to suppress autaptic granule cell EPSCs.**

(A) The effect of 10  $\mu$ M L-CCG I on autaptic EPSCs was compared with 0.1 and 1  $\mu$ M DCG IV in the same recording. Traces are averages of 5 sweeps each, and time plot shows EPSCs amplitudes during the recording. (B) Summary of  $n=7$  cells. EPSC amplitudes were normalized to control EPSCs.

Using fast applications of 500 mM sucrose solved in extracellular solution, we determined the RRP and the vesicular release probability ( $P_{vr}$ ) of autaptic granule cells and pyramidal cells. The size of the RRP was found to be significantly different between granule cells and pyramidal cells (Figure 3-20 B, granule cells:  $2231 \pm 542$  vesicles,  $n=11$ ; pyramidal cells:  $5570 \pm 1320$  vesicles,  $n=15$ ;  $p=0.038$ , independent Student's t-test). Knowing the number of vesicles that are available for release, it was also possible to calculate the  $P_{vr}$  of action potential triggered fusion events (Rosenmund and Stevens, 1996; Basu, *et al.*, 2007). For pyramidal cells we found a  $P_{vr}$  of  $9.08 \pm 1.27\%$  (Figure 3-20 C,  $n=15$ ), which is in the range of  $P_{vr}$  values reported for wild type hippocampal autaptic cultures in previous studies (Junge, *et*

*al.*, 2004; Basu, *et al.*, 2007; Gerber, *et al.*, 2008). For granule cells we obtained a  $P_{vr}$  of  $8.34 \pm 1.4\%$  ( $n=11$ ), which was not significantly different from the  $P_{vr}$  value of autaptic pyramidal cells ( $p=0.7$ , independent Student's t-test).

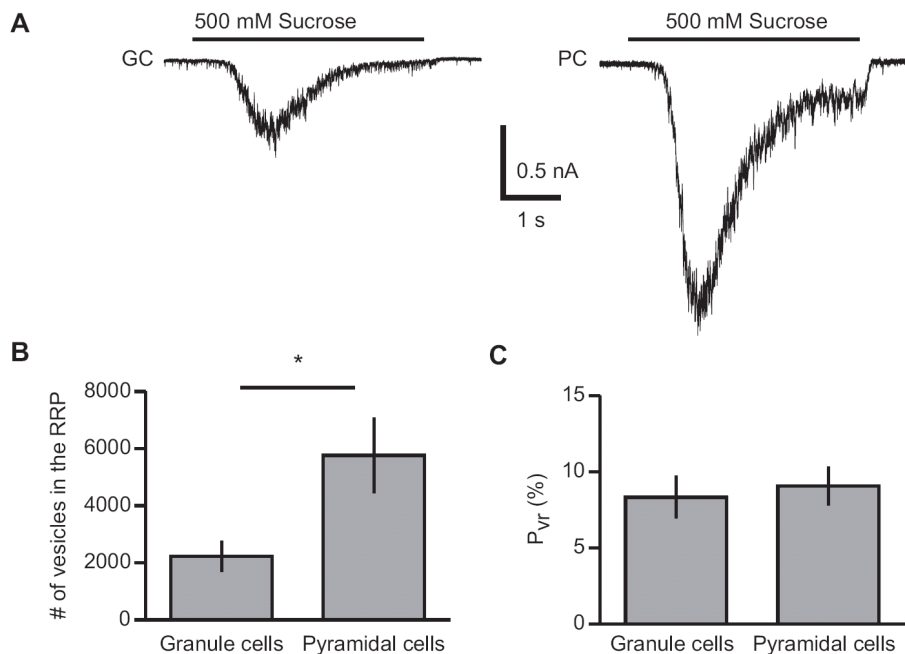


**Figure 3-20: Hippocampal granule cells have a smaller readily releasable pool but similar vesicular release probability compared to pyramidal neurons.**

(A) 500 mM sucrose applied for 4 s onto a granule cell and pyramidal cell. (B) For granule cells ( $n=11$ ), the number of vesicles in the RRP is much smaller than for pyramidal cells ( $n=15$ ,  $p<0.05$ ). The probability of vesicular release triggered by an action potential was calculated as the ratio of the EPSC charge to the charge of the sucrose transient. No difference in the  $P_{vr}$  was found between granule and pyramidal cells.

In line with the finding that cultured hippocampal pyramidal and granule cells have similar  $P_{vr}$  values, we found comparable initial depression of the EPSC when applying a train of 20 stimuli at 1 Hz. However, EPSCs of autaptic granule cells recovered during the 20 stimuli, whereas EPSCs of pyramidal neurons remained constantly smaller as control EPSCs (Figure 3-21), which suggests that granule cells might be able to more efficiently refill their vesicle pool at the active zone during high frequency stimulation.

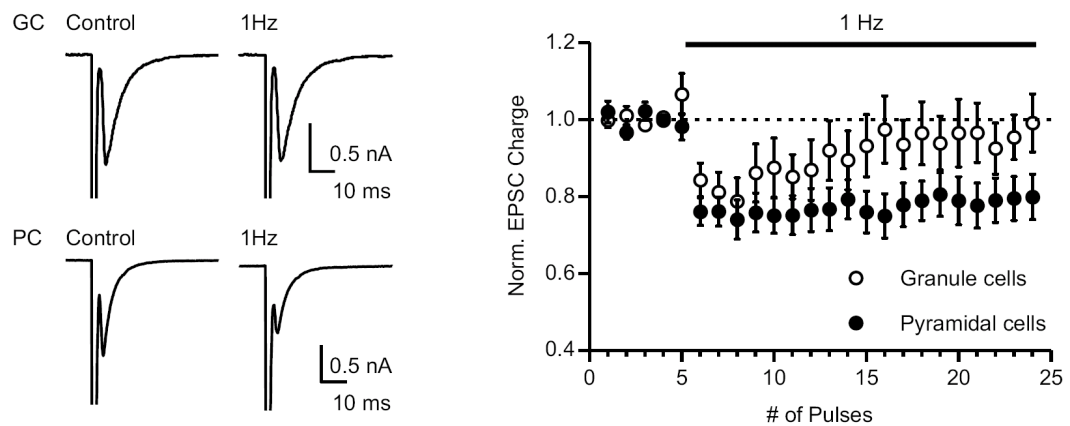


**Figure 3-21: Short-term plasticity of EPSCs during 1 Hz stimulation in autaptic neurons.**

To test short-term plasticity, 20 stimuli were applied at 1 Hz. Traces represent averages of four sweeps before and at the end of the stimulus trains. Granule cell EPSCs show a recovery after initial depression during the train ( $n=8$ ), while EPSCs in pyramidal cells remained depressed throughout the train ( $n=7$ ).

Finally, we were interested whether we could find a forskolin (FSK)-induced potentiation of transmitter release in autaptic granule cell cultures, as was described for cultures of guinea pig hippocampal granule cells (Tong, *et al.*, 1996). FSK activates adenylyl cyclase and thereby increases cAMP levels, which was shown to induce long-term potentiation (LTP) of mossy fibre transmission in slice preparations (Weisskopf, *et al.*, 1994). In recordings from our autaptic cultures of murine hippocampal granule cells we found that application of 50  $\mu$ M FSK robustly increased EPSCs (to  $215 \pm 18\%$  of control,  $n=5$ ; Figure 3-22 A). By the same time FSK application decreased the paired pulse ratio of two EPSCs triggered at 50 ms interstimulus interval (to  $70.6 \pm 5\%$ ; Figure 3-22 B), indicating a presynaptic form of potentiation as described for mossy fibre LTP.

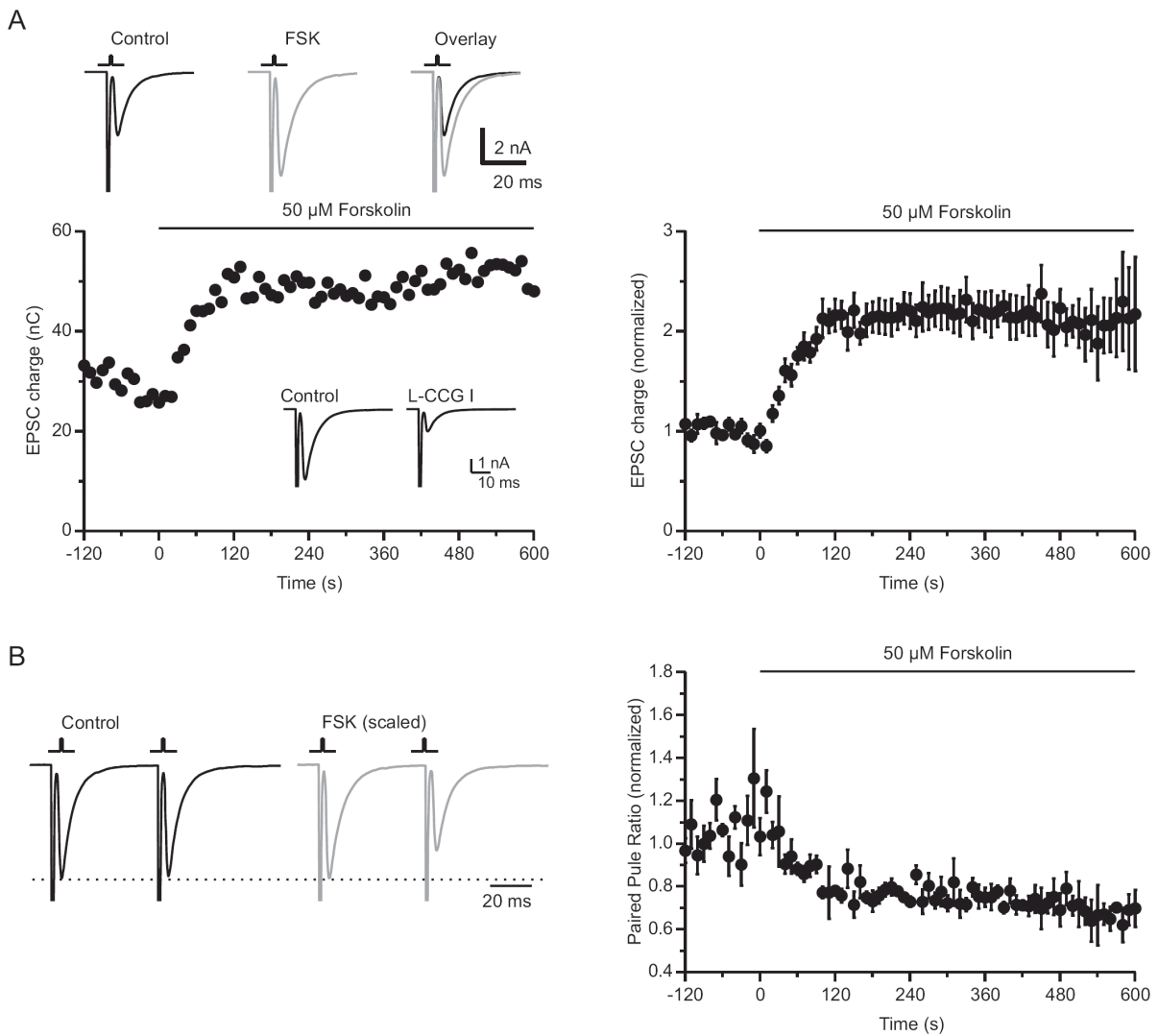


**Figure 3-22: Application of FSK leads to a presynaptic potentiation of transmitter release in autaptic granule cells.**

(A) Representative traces from a granule cell recordings before and 10 min after application of 50  $\mu$ M FSK. Traces represent averages of six sweeps. Time plot from the same cell, depicting the rapid onset of potentiation. Inset shows the effect of 10  $\mu$ M L-CCG I on the EPSC in this cell. FSK leads to a doubling of EPSCs in autaptic granule cells ( $n=5$ ). (B) Paired pulse traces from the same cell as in (A). The FSK trace is scaled to the first EPSC amplitude of control. Paired pulse ratio decreases after FSK application ( $n=5$ ).

---

### **3.2.5 Baclofen decreases the frequency of mossy fibre mEPSCs in the absence of extracellular calcium**

The above characterisation of autaptic hippocampal granule cells revealed that these neurons retain some important molecular features described from MF slice experiments, even when the granule cells were grown on glia microislands for 2 to 3 weeks in culture. Therefore they present a useful tool to record pure mossy fibre mEPSCs, although one has to keep in mind that their synapses do not represent classical mossy fibre synapses between granule cell terminals and CA3 pyramidal neurons. To investigate GABA<sub>B</sub>R-triggered inhibition of spontaneous vesicle fusion, we applied baclofen in nominally Ca<sup>2+</sup>-free conditions (+1 mM EGTA) in recordings of autaptic neurons that were beforehand identified as granule cells by application of 10 μM L-CCG I (Figure 3-23 A,B). Indeed we found that 30 μM baclofen significantly decreased mEPSC frequency to 37.8±5% compared to the frequency in 0 Ca<sup>2+</sup> (*n*=6, *p*<0.0001, two-tailed one sample t-test), while the amplitude did not change significantly (94±3.2% of control, *p*=0.12; Figure 3-23 C). Taken together, this experiment further supports our notion that presynaptic GABA<sub>B</sub>Rs utilize two inhibitory signalling pathways to inhibit transmitter release, both at MF synapses in CA3 and Schaffer collateral synapses in CA1 of the mouse hippocampus.

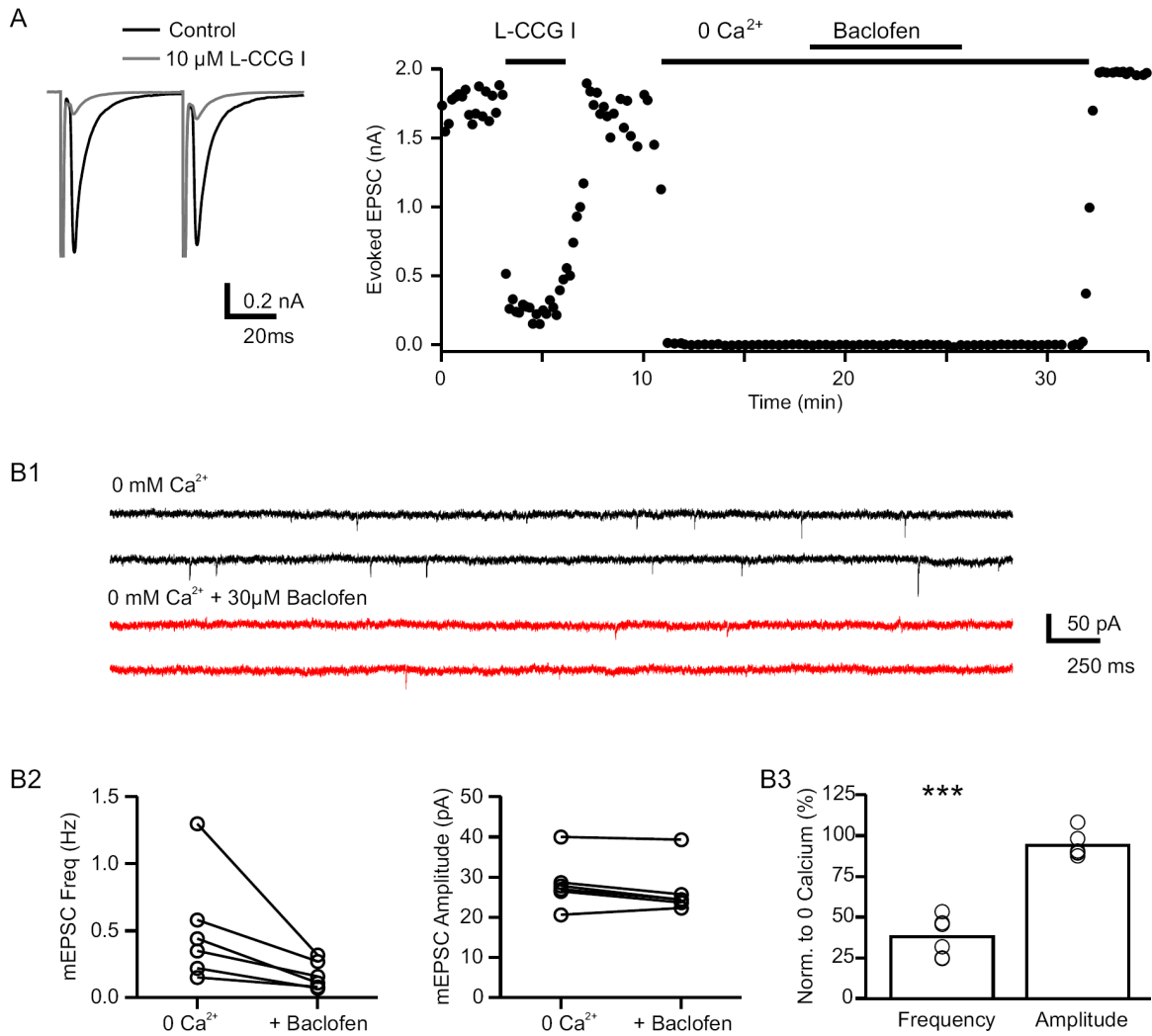


**Figure 3-23: Baclofen reduces frequency but not amplitude of mossy fibre mEPSCs.**

(A) Typical experiment to investigate GABA<sub>B</sub>R-mediated Ca<sup>2+</sup>-independent inhibition in cultured autaptic hippocampal granule cells. Traces show effect of 10  $\mu$ M L-CCG I applied to characterize the cell type. Time plot indicates time requirements for multiple wash-in and wash-out steps with slow bath perfusion. (B1) mEPSCs recorded from an identified granule cell in 0 Ca<sup>2+</sup> and in 0 Ca<sup>2+</sup> +30  $\mu$ M baclofen. Traces represent continuous recordings within each condition. (B2) The incidence of mEPSCs is decreased by baclofen, whereas the amplitude is not altered. (B3) When normalized to 0 Ca<sup>2+</sup>, the mEPSC frequency is significantly reduced in baclofen ( $n=6$ ,  $p<0.0001$ ), whereas the mEPSC amplitude is not significantly changed ( $p=0.12$ ).

---

### 3.3 Presynaptic inhibition by an artificial receptor as a tool to silence neuronal output

So far, we have studied mechanisms of presynaptic inhibition by endogenous GABA<sub>B</sub>Rs, both at Schaffer collateral and mossy fibre synapses. We have also used presynaptic inhibition of transmitter release by metabotropic glutamate receptors to identify granule cells in autaptic cell cultures. In the following, I will present presynaptic inhibition by an artificial G-protein coupled receptor as a method to experimentally silence neuronal output. When the receptor is selectively expressed in genetically defined neuronal population, it will allow to silence the transmitter output of these neurons, and to investigate their role in neuronal network activity.

#### 3.3.1 Development of hM4D, a designer receptor activated by a designer drug

In 2007, the group of Bryan Roth from the University of North Carolina, in Chapel Hill, USA, published the creation of a group of “designer receptors activated by a designer drug” (DREADDs), which they had developed by directed molecular evolution in yeast (Armbruster, *et al.*, 2007). Starting from the human muscarinic acetylcholine receptor type 3 (hM3), they created a large library of randomly mutated receptors, which were selected for their ability to be activated by Clozapine-N-oxide (CNO), an orally bioavailable small molecule with no known activity on any endogenous receptor in mammals (Figure 3-24).

In multiple rounds of mutagenesis and selection, they were able to isolate a mutant that showed high affinity to CNO in the nanomolar range, a severely reduced ability to respond to its natural ligand acetylcholine, and a reduced antagonism by atropine (Conklin, *et al.*, 2008). Surprisingly, only two amino acid exchanges (Y149C and A239G) were needed to convert the ligand-specificity of the hM3 receptor, without changing its signalling properties via G $\alpha_q$ -proteins. To generate an artificial receptor that activates G $\alpha_i$ /G $\alpha_o$ -proteins, these two point mutations were transferred to the corresponding amino acids in the human muscarinic receptor type 4 (Y113C und A202G), which created hM4D (Figure 3-24 C). hM4D was shown to activate GIRK channels in HEK293 cells and to hyperpolarize hippocampal neurons in cell culture (Armbruster, *et al.*, 2007). An *in vivo* study on hM3D demonstrated that oral administration of CNO led to activation of neurons by intracellular Ca<sup>2+</sup> mobilization only in hM3D-expressing mice, as shown by electrophysiological recordings and behaviour monitoring (Alexander, *et al.*, 2009). The study further confirmed that CNO has no effects on

neuronal activity in wildtype mice, that it can efficiently cross the blood brain-barrier and activates receptors expressed in the intact brain, and therefore promoted the use of this receptor family for neuroscience studies.

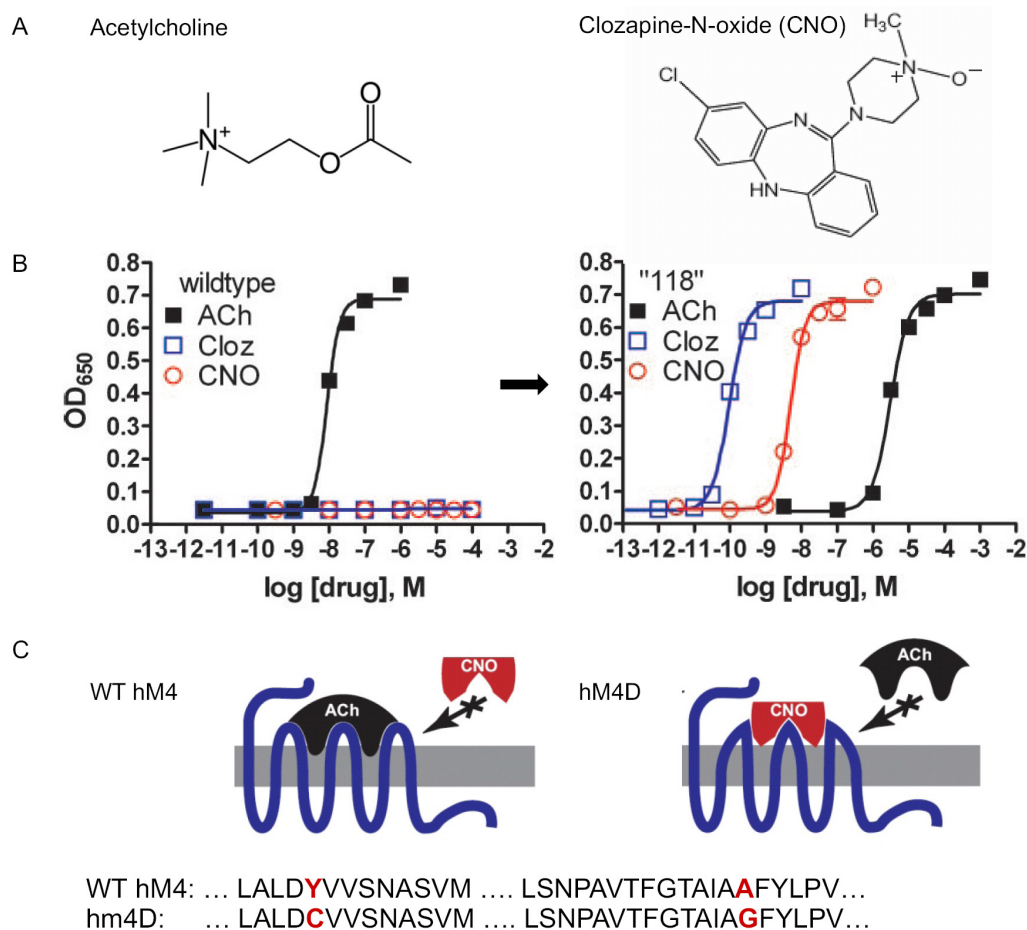


**Figure 3-24: Development of the hM4D receptor family.**

(A) Molecular structure of Acetylcholine and CNO. (B) Main result of the direct evolution approach by Armbruster et al.: The wildtype muscarinic acetylcholine receptor is only activated by its natural ligand, whereas clone 118 (founding member of the artificial receptor family) shows reduced activation by acetylcholine compared to wildtype, strong activation by CNO and highest activation by Clozapine. (C) Two point mutations are sufficient to alter agonist binding properties of the receptor and transform WT hM4 into hM4D (modified from Armbruster, *et al.*, 2007; Conklin, 2007).

### 3.3.2 Cloning of hM4D receptor constructs for functional testing

The sequence of hM4D in pcDNA3.1 was kindly provided by the lab of Brian Roth. Since hM4D is highly homologous to mouse muscarinic acetylcholine receptor type 4, detectability of the artificial receptor was a major concern. Therefore, hM4D was PCR-amplified with T7 and hM4D-rev-Xba1 primers and subcloned into pcDNA3.1/V5-His A using BamH I and

Xba I sites, which generated a C-terminal V5-His tag. We further designed two constructs that allow for visual identification of living cells expressing the hM4D receptor: hM4D coexpressed by an IRES-cassette (internal ribosomal entry site) with the soluble far red (635 nm) fluorescent protein Katushka, or hM4D directly fused to the far red fluorescent protein mKate (Shcherbo, *et al.*, 2007). Katushka and mKate are highly similar, as they were derived from the same red fluorescence protein and were optimized for expression as a soluble dimeric fluorescent marker or as fluorescent monomeric tag, respectively. For the wildtype muscarinic receptor type 4 it was described that direct tagging with the green fluorescent protein (GFP) decreases the receptor's affinity to its ligand carbachol (Madziva and Edwardson, 2001), so we were concerned whether a direct tag of hM4D would interfere with receptor function, and wanted to test both constructs in electrophysiological experiments (3.3.3) and fluorescence imaging (3.3.5).

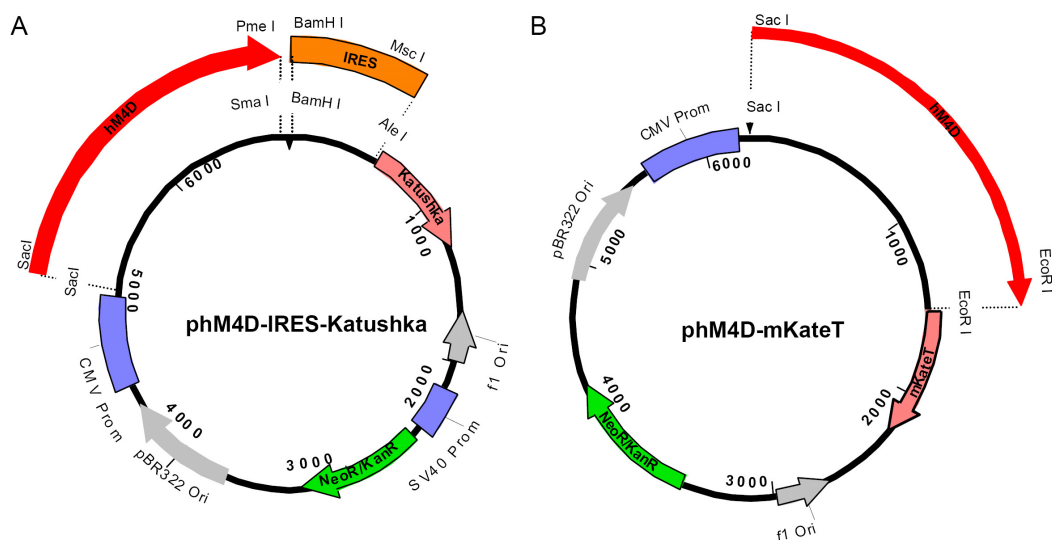


**Figure 3-25: Generation of hM4D expression vectors with two versions of genetically encoded red fluorescent markers.**

(A) hM4D was placed either in front of an IRES-Katushka cassette followed by the coding sequence for Katushka, or (B) was C-terminally fused to mKateT.

For the hM4D-IRES-Katushka construct, the IRES2-cassette was transferred from pIRES2-EGFP using BamH I and Msc I into the plasmid containing Katushka (purchased from Biocat, Heidelberg, Germany), which was opened with BamH I and Ale I. hM4D-V5-His was cut out with Sac I and Pme I and ligated into pIRES2-Katushka digested beforehand with Sac I and Sma I (Figure 3-25 A). Before directly tagging hM4D with mKate, a guanine at position 484 of the mKate coding sequence was point mutated to cytosine, resulting in a serine to threonine

amino acid substitution (mKateT), which was shown to increase photostability (Shaner, *et al.*, 2008). hM4D-V5-His was then PCR amplified with primers containing Sac I and EcoR I restriction sites and, using the same enzymes, subcloned in front of mKateT to generate phM4D-mKateT (Figure 3-25 B).

### 3.3.3 Functional tests of hm4D in neuronal cell cultures

For functional tests of the receptor constructs in neurons, Ralf Nehring (by this time in the group of Christian Rosenmund, Baylor College, Houston, Tx, USA) transferred hM4D-IRES2-Katuhska and hM4D-mKateT into lentiviral vectors with the neuron-specific synapsin-promoter. The lentiviral particles were then used for overexpression of hM4D in neuronal cell cultures and whole-cell patch clamp investigations. Hippocampal neurons prepared at P0 were grown in Neurobasal A media on 10 mm coverslips coated with stamp-solution, which results in essentially pure neuronal cultures with high inter-cell connectivity (“continental” cultures). After DIV 5, cells were infected with virus expressing hM4D. Whole cell patch clamp recordings were performed between DIV 8 and 12. As described by Armbruster *et al.*, brief application of 10  $\mu$ M CNO activated GIRK currents of  $23.7 \pm 6.9$  pA (Figure 3-26 A), resulting in hyperpolarization of the neuron by  $-5.1 \pm 1.7$  mV in current clamp recordings (Figure 3-26 B). Both constructs showed similar hyperpolarizing effects, and the data of these experiments were pooled.

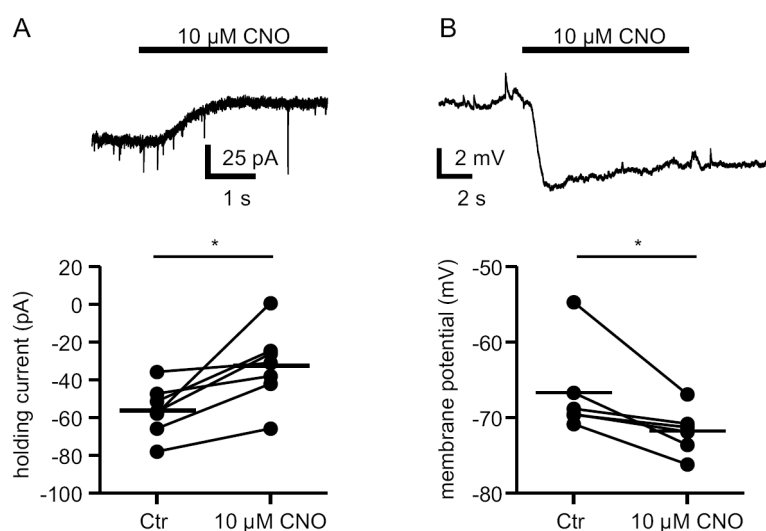


**Figure 3-26: CNO causes hyperpolarization of neurons expressing hM4D.**

(A) GIRK channel activation induces changes in holding currents after application of 10  $\mu$ M CNO. Example trace filtered at 500 Hz. (B) GIRK currents cause a hyperpolarization of the resting membrane potential. For both graphs  $n=6$ ,  $p<0.05$ . Horizontal bars indicate average of each group.

To investigate whether hM4D would also traffic into presynaptic terminals, where it then might inhibit transmitter release, autaptic cultures were prepared as described (2.1.2) and infected between DIV 5 and 8 with lentiviral particles. Whole cell patch clamp recordings were performed beginning 4 days post infection using a KCl-based intracellular solution that allowed the recording of both EPSCs and IPSCs (type II intracellular solution for cell cultures in 2.2). Indeed we found that application of low doses of CNO significantly reduced the autaptic response in both glutamatergic and GABAergic neurons (Figure 3-27), but not in uninfected control cells. In hM4D-mKateT expressing neurons, CNO exhibited a stronger effect on the EPSCs than in the neurons expressing hM4D-IRES-Katushka ( $IC_{50}$  values 8.6 nM vs. 17.1 nM). The remaining EPSC amplitude normalized to control at 1  $\mu$ M CNO was  $12.4 \pm 1.5\%$  for hM4D-mKateT vs.  $22.6 \pm 6.5\%$  EPSC for hM4D-IRES-Katushka (Figure 3-27 A). We therefore concluded that direct tagging of hM4D with a fluorescent marker does not significantly interfere with the ligand binding, but that the bicistronic vector for hM4D-IRES-Katushka might give lower expression rates compared to hM4D-mKateT (compare also Figure 3-31).

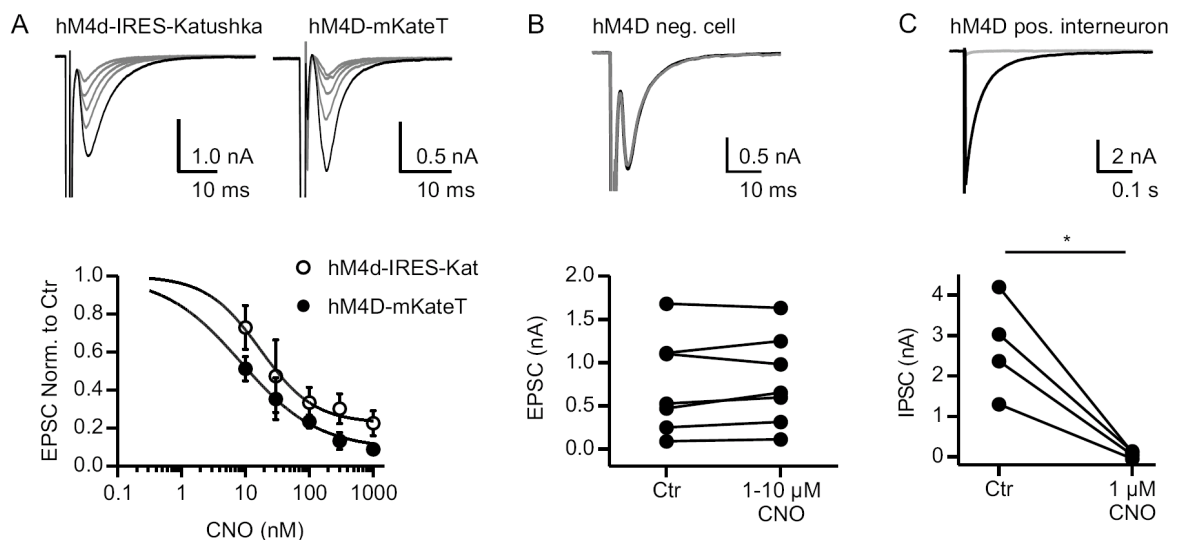


**Figure 3-27: Strong presynaptic inhibition of transmitter release by hM4D receptors expressed in autaptic cultures of hippocampal neurons.**

(A) Application of increasing concentrations of CNO (30, 100, 300, 1000 nM, grey traces) leads to pronounced reduction of EPSCs in glutamatergic neurons infected with expression constructs for hM4D-IRES-Katushka or hM4D-mKateT.  $n=3$  to 12. (B) CNO at concentrations of 1 or 10  $\mu$ M (grey trace) shows no effect in hM4D negative control neurons ( $n=7$ ,  $p=0.31$ ). (C) CNO also suppresses IPSCs when hM4D is expressed in interneurons.  $n=4$ ,  $p=0.018$ , paired two-tailed  $t$ -test.

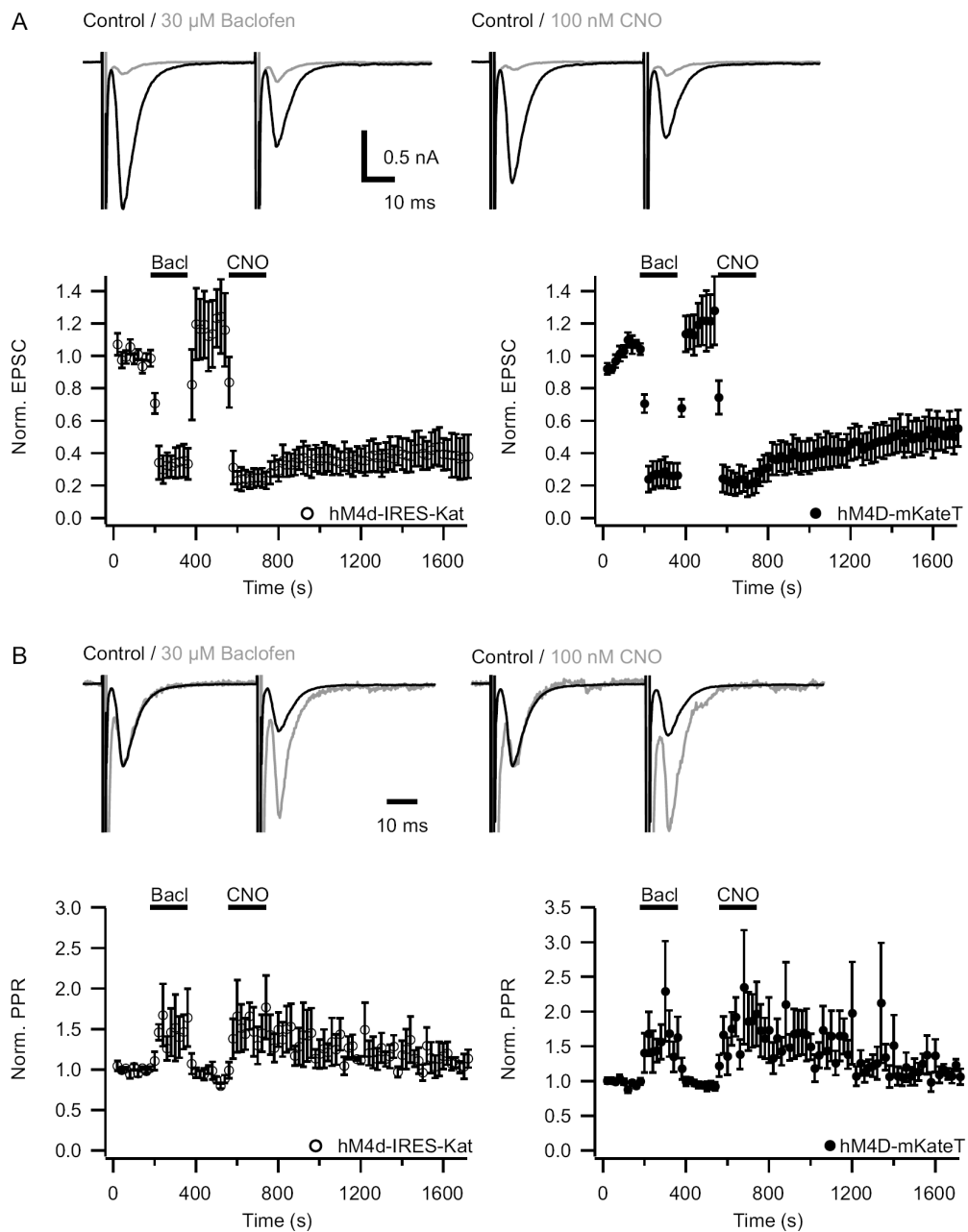


**Figure 3-28 Comparison of presynaptic inhibition by GABA<sub>B</sub> and hM4D receptors.**

(A) Subsequent application of 30  $\mu$ M baclofen and 100 nM CNO in the same cell after washout of baclofen. Example traces are taken from an hM4D-mKateT expressing autaptic neuron. Both types of metabotropic receptor suppress EPSCs to a similar extent, but washout kinetics of CNO are dramatically slower than of baclofen. No obvious difference was observed between the hM4D-mKateT and hM4D-IRES-Katushka constructs. (B) Increased paired-pulse ratio for both GABA<sub>B</sub> and hM4D receptor activation. The example traces from A were scaled to the peak of the first EPSC under control conditions for both baclofen and CNO application to illustrate the increase of the second pulse compared to the first pulse in presence of the drugs. Data plots binned by factor 2;  $n=5, 6$ .

We further wanted to compare hM4D-mediated presynaptic inhibition with inhibition by endogenous receptors, as we were concerned whether the overexpression of hM4D might

---

interfere with the function of other presynaptic receptors. To test this, we assessed the ability of GABA<sub>B</sub>Rs to inhibit transmitter release in hM4D expressing neurons. The protocol included application of 30 μM baclofen for 90 sec, washout and subsequent application of 100 nM CNO for 90 s as well (Figure 3-28). Baclofen showed similar effects on transmitter release for both hM4D vectors tested (hM4D-IRES-Katushka: 27.9±8.1% EPSC normalized to control, *n*=5; hM4D-mKateT: 26.9±7.7%, *n*=6). Interestingly, the washout of CNO was dramatically slower compared to baclofen. The reason for this is unclear at present, but one possibility might be that CNO shows a nearly irreversible binding towards hM4D receptors. Baclofen and CNO caused a similar increase of the paired-pulse ratio indicating presynaptic receptor actions (Figure 3-28 B).

### 3.3.4 Vector design for a conditional Rosa26 hM4D transgenic mouse

Based on the functional tests described above, we were encouraged to set up a transgenic mouse model that would allow conditional expression of hM4D. We decided to use the “Rosa26” locus as site for the genomic integration of the transgene, because it allows ubiquitous expression of transgenes without interfering with endogenous expression patterns. The term Rosa26 refers to the number of the mouse line in which this genomic locus was first characterized by retrovirus-mediated integration of a reverse orientation splice acceptor (Rosa) combined with β-galactosidase (Friedrich and Soriano, 1991). Furthermore we chose the CAG-promoter (CMV (cytomegalovirus) immediate early enhancer/modified chicken β-actin promoter) to drive expression of hM4D, as this promoter enables strong expression in various cell types, including the CNS (Niwa, *et al.*, 1991).

Conditional expression of a protein of interest is usually achieved by regulatory elements that confer cell type and/or onset-specificity of mRNA transcription and subsequent translation into protein. A classical trick of molecular biologists to block unwanted transcription is to place a *loxP* flanked “Stop” cassette (a “floxed” Stop) between promoter and coding DNA sequence of the protein of interest. *LoxP* sequences (locus of crossing (x) over P1) from the bacteriophage P1 are short stretches of DNA that consist of two palindromic 13 base pairs (bp) flanking an asymmetric 8 bp sequence that defines the orientation of the *loxP* sites (Figure 3-29 A). They are recognised by Cre enzymes (causes recombination) that catalyse recombination of the DNA between the sites (Sauer, 1987; Sauer and Henderson, 1988). If two *loxP* sites are placed in one stretch of DNA, Cre will either remove or invert the

intermediate DNA sequence, depending on whether the loxP sites are placed in the same or opposite orientation to each other (Figure 3-29 B). Additional variants of *loxP* (*lox2272*) and similar systems have been developed in recent years, and greatly expanded the combinatorial options for molecular tinkering (*e.g.* *Frt* sites with Flp; attP and attB sites with  $\lambda$  integrase; for review see Branda and Dymecki, 2004). In many conditional mouse models, a floxed Stop cassette is placed in front of the gene of interest. Only when the mouse is crossed with a Cre expressing mouse, the Stop cassette is removed in Cre expressing cells of the offspring, and expression of the protein is initiated. A potential problem arises in cases when a strong promoter drives translation of the mRNA before removal of the Stop cassette, which is referred to a “leakiness” of the Stop cassette (Buschow, *et al.*, ; Miyoshi and Fishell, 2006). To circumvent this potential pitfall, we chose the so-called FLEX (flip-excision) approach for Cre conditional expression of hM4D (Schnutgen, *et al.*, 2003). The coding sequence of hM4D plus fluorescent marker was flanked by two opposing *loxP* and *lox2272* sites and placed in reverse orientation to the CAG- promoter (see Figure 3-29 and Figure 3-30). This configuration prevents expression of the transgene in the absence of Cre. Cre, recognizing either the *loxP* or *lox2272* sites, causes a reversible inversion of hM4D, and subsequently removes two of the recombination sites by excision, which is an irreversible step that leaves hM4D in the same orientation as the CAG promoter (Figure 3-29 B).

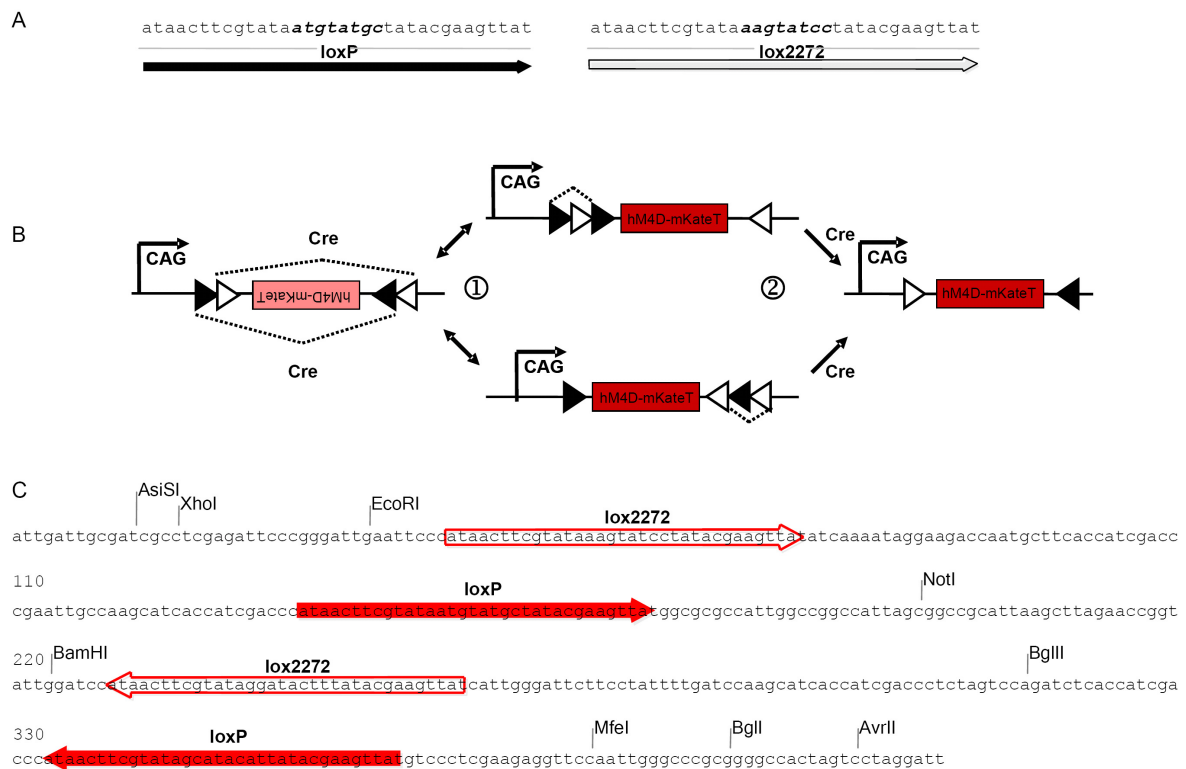


**Figure 3-29: Conditional expression of hM4D-mKateT using the FLEX cassette.**

(A) Sequence of loxP and lox2272 sites. The flanking palindromic 13 bp are identical in both variants, allowing recognition by Cre enzyme in both cases, while the central 8 bp stretch differs, preventing recombination between loxP and lox2272 sites. (B) Activation of transcription of hM4D-mKateT by a sequential flip and excision event. Expression of Cre causes the inversion of the FLEX cassette by recognition of the opposing loxP or lox2272 sites (1). The inversion event leads to a reordering of the lox sites into the same direction, which allows subsequent removal of two sites (2). As different types of lox sites cannot recombine, the coding sequence for hM4D-mKateT finally remains in the orientation that allows expression of the transgene by the CAG promoter. (C) Sequence of the FLEX cassette that was *de novo* synthesized. Restriction enzyme recognition sites and lox sites are indicated.

To target the Rosa26 locus with the conditional transgene construct, we used the RMCE technique (recombination-mediated cassette exchange) developed by the laboratory of Ralf Kühn (Hitz, *et al.*, 2007). RMCE allows insertion of transgenes into the Rosa26 locus with high success rates (~40%) instead of laborious homologous recombination. This approach relies on the integrase of phage phiC31 (C31int), which mediates recombination events between the attB and attP recognition sites of the RMCE plasmid (pRMCE) and the genetically modified acceptor embryonic stem cells (ES cells). The RMCE construct is thereby shuttled into the Rosa26 locus of the ES cells (Figure 3-30 B). In the course of the recombination event, the hygromycin resistance of the ES cells is replaced by a neomycin

resistance, which allows for selection of ES cells with positive recombination events using G418 (Figure 3-30 C). In the final mouse line, the neomycin resistance cassette can be removed by Flp-mediated recombination of the Frt sites flanking the sequence of the phosphoglycerate kinase (PGK) promoter and neomycin resistance.

The FLEX cassette was *de novo* synthesized (Eurofins MWG Operon, Ebersberg, Germany; for sequence see Figure 3-29 C), digested with AsiS I and Avr II and subcloned into pRMCE opened with AsiS I and Spe I. The CAG promoter was released from pCAG-Flpe (Addgene, Cambridge, MA, USA) with Sal I and EcoR I, and ligated in front of the FLEX-cassette using Xho I and EcoR I sites to create pRMCE-CAG-Flex (Figure 3-30 A). hM4D-IRES-Katushka and hM4D-mKateT were cut out from the respective plasmids with Not I and Bgl II and ligated in reverse orientation into the FLEX cassette opened with Not I and BamH I (Figure 3-30 A). Finally, a rabbit globulin polyA cassette including stop codons in every reading frame was placed downstream of hM4D in the same direction to prevent unintended transcriptional read-through from endogenous promoters. The cassette was PCR amplified with primers containing the stop codons, and inserted using an Mfe I site 3'-prime of the Flex cassette (Figure 3-30 B), resulting in the final donor vector for RMCE. The final construct was completely sequenced before it was used for ES cell electroporation.

### **3.3.5 Testing conditional expression of the FLEX construct in HEK293 cells**

We transfected HEK293 cells with the conditional hM4D constructs together with plasmids encoding Cre-EGFP or EGFP alone. Recombination occurred only in cells that were cotransfected with Cre-EGFP (Figure 3-31). Red fluorescence was difficult to detect in case of the hM4D-IRES-Katushka construct, presumably because the IRES sequence lowers the expression levels of the recombinant proteins. Taken into account that both constructs showed similar effects in the pharmacological characterization, we finally decided to use the hM4D-mKate construct for the transgenic mouse model.

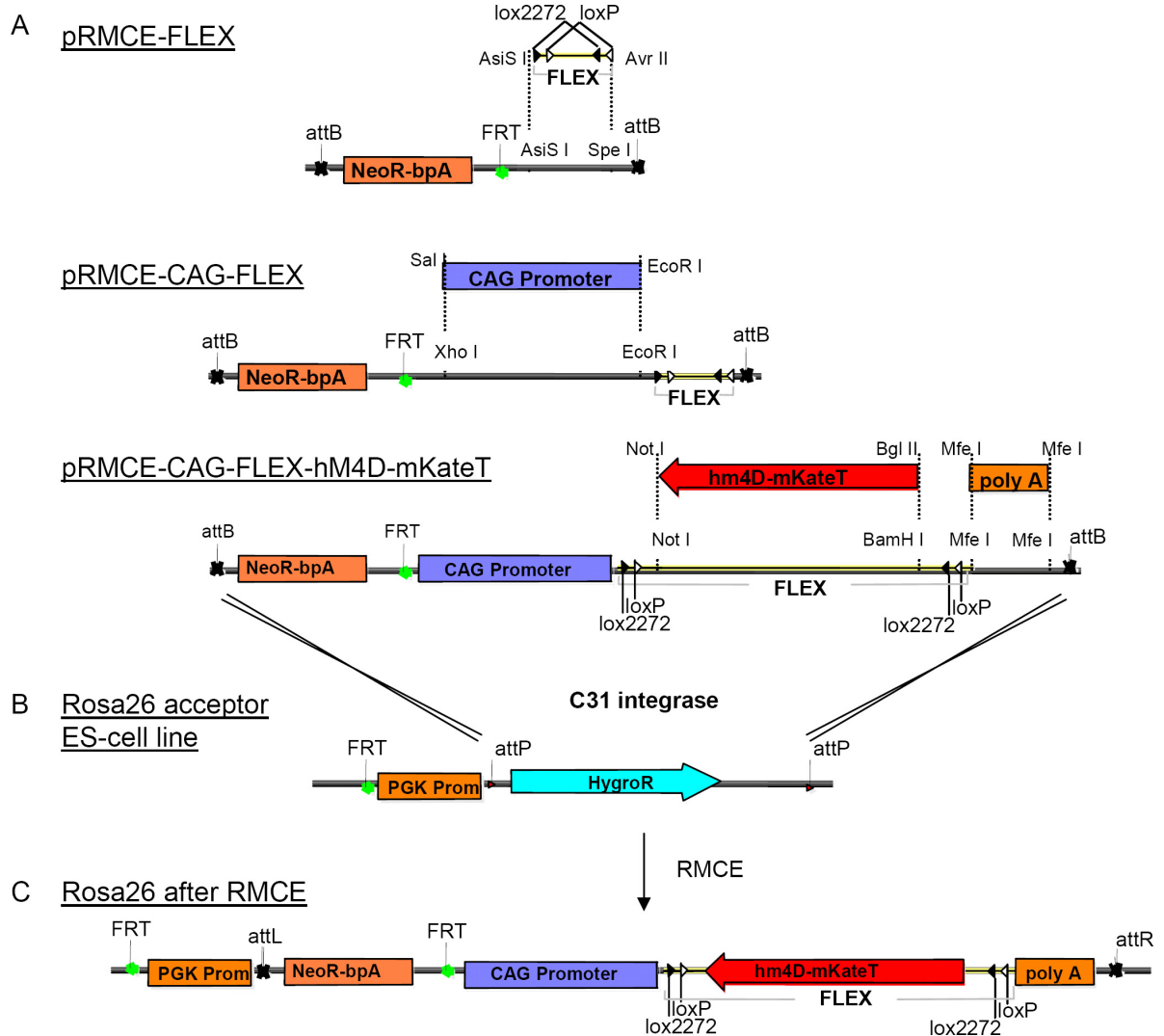


**Figure 3-30 Vector construction and RMCE for the generation of CAG-Flex-hM4D-mKateT.**

(A) Sequential assembly of the conditional expression construct in pRMCE, with hM4D-mKateT shown as example. (B) In the acceptor ES cells the ROSA26 allele harbours a PGK promoter driving the hygromycin selection marker. The hygromycin resistance is flanked by two attP sites. (C) RMCE by C31int leads to an exchange of the hygromycin resistance in the acceptor allele by the neomycin resistance of the donor vector, and a change of the attP sites into attL and attR sites.

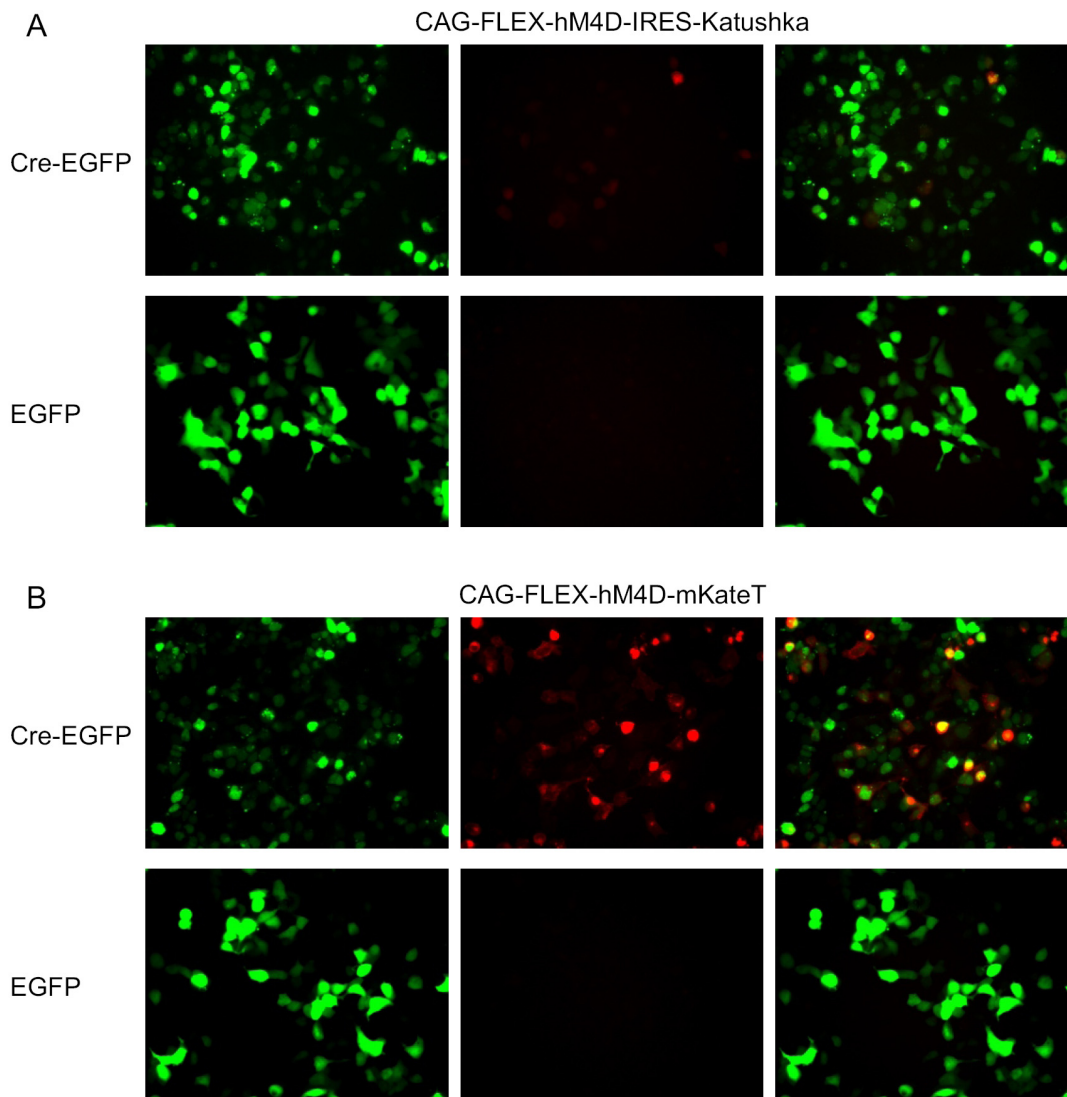


**Figure 3-31: Co-expression of Cre activates hM4D expression by recombination of the FLEX cassette in transiently transfected HEK293 cells.**

(A) HEK293 cells transfected with plasmids for hM4D-IRES-Katushka together with Cre-EGFP (upper panel) or EGFP as control (lower panel). In cells expressing Cre-EGFP, recombination of the FLEX-cassette is indicated by red fluorescence. (B) Cotransfection of plasmids for hM4D-mKateT and Cre-EGFP or EGFP. The fusion protein of hM4D and mKateT gives a much stronger fluorescence signal than the co-expression of hM4D and Katushka by the IRES cassette.

### 3.3.6 PCR analysis of embryonic stem cells for successful recombination into the Rosa26 locus

The acceptor cell line IDG3.2-R26.10-3 (I3) was kindly provided by Ralf Kühn (GSF National Research Centre for Environment and Health, Institute of Developmental Genetics, Neuherberg, Germany), and maintained by Geert Michel from the Transgene Facility of the “Research Institute for Experimental Medicine” (FEM, Charité Berlin). Electroporation of the

RMCE construct together with a plasmid encoding C31int was performed by Geert Michel according to published protocols (Hitz, *et al.*, 2007; Hitz, *et al.*, 2009). Recombinant clones were selected by incubation with 140 µg/ml G418 for at least 7 days. To activate hM4D expression by recombination of the FLEX switch, selected clones were further transfected transiently with pCAG-Cre-EGFP using Roti-Fect (Carl Roth, Karlsruhe, Germany). Three clones were resistant to G418 selection and were analysed by PCR for successful integration and recombination of the construct, as illustrated in Figure 3-32 (for primer sequences see Table 4 on page 36 in the Methods section). Clone #1 showed positive PCR results for 5' and 3' integration sites (PCR 1 and 2), and a successful FLEX-switch in cells transfected with Cre (PCR 3). This clone is now being used for injection into blastocyte stage embryos.

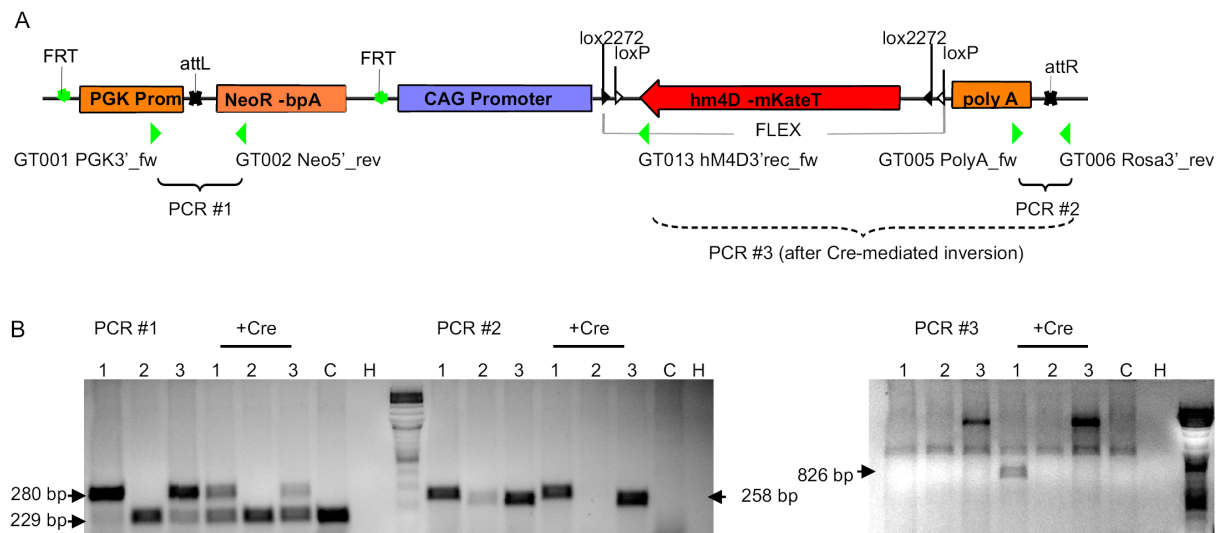


**Figure 3-32: Identification of successful genomic integration events and Cre-mediated inversion of the hM4D coding sequence by PCRs.**

(A) Localization of primers (green triangles) in the Rosa26-hM4D locus after RMCE of the conditional hM4D-mKateT construct. PCR 1 tests the correct 5' integration and PCR 2 correct 3' integration of the construct into the ROSA26 locus. PCR 3 tests for successful recombination of the FLEX site by Cre. (B) PCR 1 and 2 show successful integration for clone 1 and 3. The lower band in PCR 1 results from the Neomycin resistance cassette of the feeder cells in the ES cell culture. A successful Cre-mediated recombination of the FLEX cassette was observed for clone 1, resulting in an 826 bp product in PCR 3. C: control cells (not electroporated), H: H<sub>2</sub>O input.



---

## 4 Discussion

In the work presented, we studied the mechanisms of presynaptic GABAergic inhibition of evoked and spontaneous glutamate release. As summarised in the first part of the Results section, we could demonstrate that, in addition to the inhibition of  $\text{Ca}^{2+}$  influx through VDCCs, activation of presynaptic  $\text{GABA}_B$ Rs substantially increases the energy barrier for vesicle fusion at hippocampal pyramidal cell synapses – an effect that occurs downstream of VDCCs. Both inhibitory mechanisms ultimately decrease transmitter release, and are strictly dependent on pertussis toxin-sensitive G-protein signalling. Our experimental evidence suggests a protein of the core release machinery acting as the molecular target of the VDCC-independent pathway. In contrast to studies on other synapses and modulators, the data from our experiments with botulinum neurotoxin A tends to exclude the C-terminus of SNAP-25 as molecular target of VDCC-independent heterosynaptic inhibition by  $\text{GABA}_B$ Rs in hippocampal neurons. We also found evidence for direct inhibition of glutamate release by  $\text{GABA}_B$ Rs at synapses from hippocampal granule cells, as summarized in the second part of the Results section. The third part of the Results describes our finding of presynaptic inhibition by the artificial receptor hM4D, and the current development of a transgenic mouse line expressing hM4D receptors in a Cre-conditional manner.

The following paragraphs will address a number of questions regarding the mechanisms and consequences of presynaptic inhibition, focussing on inhibition by  $\text{GABA}_B$ Rs in the hippocampus: (1) What is the role of presynaptic inhibition in neuronal network activity? (2) What are the potential functional implications of two inhibitory presynaptic pathways on a cell-physiological level? (3) How much does direct inhibition of release contribute to overall inhibition? (4) What are the potential molecular targets of  $\text{Ca}^{2+}$ -independent presynaptic inhibition? (5) Finally, I discuss presynaptic inhibition using the artificial hM4D receptor as a tool for experimental neuroscience studies.

#### 4.1 The role of presynaptic inhibition in neuronal networks

Presynaptic inhibition by metabotropic receptors is a powerful means of reducing neuronal output from both excitatory and inhibitory synapses. In various aspects it plays an important role in the neuronal information processing and occurs at several levels of synaptic communication. Firstly, as an intrasynaptic feedback signal, presynaptic inhibition can reduce transmitter release during high-frequency activity and can thereby adjust the gain of synaptic signalling, which is a very simple yet effective means of adaptation (Abbott and Regehr, 2004). Decreasing release probability can actually help to maintain reliable signal propagation during high-frequency trains of APs by two mechanisms: it can prevent rapid depletion of the RRP in the presynaptic terminal or reduce receptor desensitisation due to transmitter overload on the postsynaptic side (Brenowitz and Trussell, 2001; Zucker and Regehr, 2002). Secondly, presynaptic inhibition between different synapses of a network can increase the signal-to-noise ratio of neuronal communication and shape the strength of synaptic transmission of neighbouring terminals in a competitive manner, providing sparse but precise inputs (Vogt and Nicoll, 1999; Guetg, *et al.*, 2009). Thirdly, a constant inhibitory tone, as observed for adenosine at some synapses (Oliet and Poulain, 1999; Moore, *et al.*, 2003; Gundlfinger, *et al.*, 2007), attenuates network activity in general and can reduce overall metabolic demand. Finally, activation of presynaptic metabotropic receptors can also cause long-lasting changes in transmitter release at some synapses: At hippocampal mossy fibre synapses, long-term depression (LTD) is induced by low-frequency stimulation (1 Hz stimulation for 15 min) and activation of group II metabotropic glutamate receptors (Yokoi, *et al.*, 1996), which leads to decreased adenylyl cyclase activity. However, the complete molecular signalling cascade underlying this long-lasting presynaptic modulatory phenomenon is not entirely understood at present (for review see Nicoll and Schmitz, 2005). Interestingly, no evidence has been found for LTD induction by activation of GABA<sub>B</sub>Rs, although they are expressed in the same synapses and couple to the same signalling cascades as mGluR group II receptors and other Gα<sub>i</sub>/Gα<sub>o</sub>-coupled receptors that can induce LTD (for review see Malenka and Bear, 2004). How the signalling of presynaptic metabotropic receptors differs with respect to plasticity induction remains unclear, but expression levels and subcellular localization of receptors and different protein interaction partners might play a role.

---

Identifying the conditions under which presynaptic GABA<sub>B</sub>Rs are activated is central to understanding the physiological role of these receptors in the hippocampus. As most presynaptic GABA<sub>B</sub>Rs are located distally to release sites (Kulik, *et al.*, 2003), their activation requires abundant release of GABA and diffusion over considerable distances, a process referred to as volume transmission. Activation of presynaptic GABA<sub>B</sub>Rs by endogenously released GABA has been demonstrated for a number of hippocampal synapses. In the CA1 region, extracellular fibre tract stimulation in *stratum radiatum* with 5 pulses at 50 Hz led to a pronounced reduction in EPSC amplitudes of other synapses in close proximity (Isaacson, *et al.*, 1993). At hippocampal mossy fibre synapses, specifically the high affinity GABA<sub>B</sub>1aR isoform was demonstrated to mediate heterosynaptic depression in response to synaptically released GABA (Guetg, *et al.*, 2009). Further, interneurons in CA1 were shown to self-regulate GABA release via GABA<sub>B</sub> autoreceptors during 5 Hz stimulation, which consequently reduced the GABAergic tone at glutamatergic synapses and allowed sufficient glutamate release for induction of postsynaptic, NMDA receptor-dependent LTP (Mott and Lewis, 1991). When GABA<sub>B</sub>Rs were pharmacologically blocked, the same protocols failed to induce LTP. At all glutamatergic synapses investigated in the hippocampus, presynaptic GABA<sub>B</sub>Rs were only activated after repetitive network stimulation and, in contrast to adenosine receptors, tonic inhibition was not found for heterosynaptic GABA<sub>B</sub>Rs (Guetg, *et al.*, 2009). Conversely, a tonic level of presynaptic inhibition by GABA<sub>B</sub>Rs was found at the GABAergic synapses of neurogliaform cells, which might be due to the large amount of GABA they release after only a single AP. Strikingly, in the axonal terminals of neurogliaform cells, presynaptic GABA<sub>B</sub>R activation was not found to affect presynaptic Ca<sup>2+</sup> transients at all, indicating that at these synapses, GABA<sub>B</sub>Rs might regulate transmitter release solely by a VDCC-independent mechanism (Price, *et al.*, 2008).

The role of GABA<sub>B</sub>Rs *in vivo* was investigated by studies on GABA<sub>B</sub>R1- and 2-deficient animals (Schuler, *et al.*, 2001; Gassmann, *et al.*, 2004): GABA<sub>B</sub>R-null mice were viable, but exhibited hyperalgesia and hyperlocomotor activity. Both knockout (KO) mouse strains suffered from tonic-clonic seizures, which were easily triggered by intense noise. They were also severely impaired in a hippocampus-dependent memory task of passive avoidance learning. In slice preparations of these mice, all GABA<sub>B</sub>R-mediated responses, both pre- and postsynaptic, were absent, supporting the notion that both GABA<sub>B</sub>R subtypes are required to form functional receptors (Kaupmann, *et al.*, 1998). Taken together, these studies revealed

that, in GABA<sub>B</sub>R KO mice, hippocampal and other neuronal circuits are hyperexcitable. This suggests that, *in vivo*, GABA<sub>B</sub>Rs prevent overactivation of neuronal networks and are therefore an important factor in balancing network activity.

The specific role of presynaptic inhibition by GABA<sub>B</sub>Rs was investigated using a selective GABA<sub>B</sub>R1a KO mouse, which still postsynaptically expressed the GABA<sub>B</sub>R1b isoform (Vigot, *et al.*, 2006). In these mice, inhibition of CA3-CA1 EPSCs by baclofen was almost completely abolished, while presynaptic inhibition by adenosine and postsynaptic GABA<sub>B</sub>R-mediated GIRK currents remained at normal levels. GABA<sub>B</sub>R1a-deficient mice were not affected by seizures, but did not perform as well in a hippocampus-dependent object recognition task. Interestingly, a GABA<sub>B</sub>R1b KO mouse strain was not impaired in the same object recognition task, indicating that presynaptic inhibition by GABA<sub>B</sub>Rs plays a fundamental role in hippocampal memory formation.

#### **4.2 Functional implications of calcium-independent inhibition**

Speculation about a potential presynaptic inhibitory signalling cascade that reduces transmitter release downstream of VDCCs initially arose from the observation that activation of presynaptic GABA<sub>B</sub> and adenosine receptors reduces mEPSC frequencies (Scanziani, *et al.*, 1992; Scholz and Miller, 1992). At that time, spontaneous miniature events were thought to be independent of extracellular Ca<sup>2+</sup> concentrations, however recent findings that mEPSC frequencies change depending on extracellular Ca<sup>2+</sup> levels suggest otherwise (Xu, *et al.*, 2009; Groffen, *et al.*, 2010). We therefore wanted to study the modulation of mEPSCs by presynaptic GABA<sub>B</sub>Rs in Ca<sup>2+</sup>-containing and Ca<sup>2+</sup>-free extracellular solutions. In recordings from acute slices and autaptic cultures, we found that the GABA<sub>B</sub>R-triggered reduction of mEPSC frequencies was very similar in the presence or absence of extracellular Ca<sup>2+</sup>. Although basal mEPSC frequencies were significantly lower in Ca<sup>2+</sup>-free solution compared to standard extracellular Ca<sup>2+</sup> concentrations, the extent of the mEPSC frequency reduction was independent of extracellular Ca<sup>2+</sup> levels. In line with the above cited publications, one plausible explanation of this could be that the reduction of mEPSC frequencies by presynaptic GABA<sub>B</sub>Rs is indeed only mediated by the inhibitory mechanism acting downstream of VDCCs. In this scenario, G-protein-mediated inhibition of VDCCs in the absence of APs does not significantly alter the presynaptic Ca<sup>2+</sup> concentration under resting conditions, which

---

could otherwise influence the mEPSC frequency. In experiments where we monitored mEPSCs during short intervals of baclofen application we observed a very fast onset of the baclofen effect on the mEPSC frequency, with latencies comparable to the G $\beta\gamma$  subunit-mediated postsynaptic activation of GIRKs, which renders phosphorylation-dependent processes rather unlikely.

We found that GABA<sub>B</sub>R activation increases the power of the exponential function describing the relation of presynaptic Ca<sup>2+</sup> influx and postsynaptic EPSP. This observation provides further evidence for an inhibitory signalling cascade that reduces transmitter release at a level downstream of VDCCs, as presynaptic inhibition by adenosine receptors, which only reduces the Ca<sup>2+</sup> influx, does not change the power (Gundlfinger, *et al.*, 2007). How can one interpret the exponent of 6.1 calculated for release in the presence of GABA<sub>B</sub>R activation at Schaffer collaterals and the even higher value of 9.7 estimated for mossy fibre synapses? These high power values indicate that more Ca<sup>2+</sup> ions have to cooperate at the Ca<sup>2+</sup> sensor to trigger transmitter release. Direct inhibition by inhibitory G-protein signalling causes vesicles to fuse more reluctantly, and shifts the activation curve for synaptotagmin-mediated fusion to increased Ca<sup>2+</sup> concentrations.

We were able to directly demonstrate the proposed increase of the fusion barrier by assessing how GABA<sub>B</sub>R activation modulates transmitter release evoked by hypertonic sucrose solutions. While hypertonicity clearly provides a trigger to primed vesicles that drives them into Ca<sup>2+</sup>-independent fusion, the exact mechanism by which this occurs is currently unknown. When the tonicity at synapses is increased, more primed vesicles reach the energy threshold for fusion. This energy threshold is not fixed, but can be altered by both physiological and experimental changes in the molecular fusion machinery. For example, the energy barrier for vesicle fusion is lowered by a gain of function mutation in the vesicle priming factor Munc13, which results in an increased sensitivity to sucrose challenges and increased spontaneous vesicle release (Basu, *et al.*, 2007). Conversely, complexin-deficient synapses display a higher energy barrier and reduction of spontaneous release rates compared to wild-type synapses (Xue, *et al.*, 2010). When the energy threshold for fusion of primed vesicles is increased, the onset of hypertonically-induced transmitter release is delayed and the maximal release rate decreases. Additionally, responses to subsaturating tonicities such as 250 mM sucrose decrease in size relative to the maximal response induced by 500 mM sucrose. This is exactly the scenario we observed for GABA<sub>B</sub>R activation in the current work:

GABA<sub>B</sub>R activation substantially slowed the kinetics of sucrose-evoked fusion and reduced the total number of vesicles released by intermediate hypertonic stimuli. Our results therefore demonstrate a direct modulatory influence of GABA<sub>B</sub>Rs on the vesicular release machinery of mammalian synapses.

What are the functional implications of this additional inhibitory mechanism in terms of presynaptic physiology? One answer to this question may lie in considering the consequences of a direct inhibition of release at the fusion machinery that leaves Ca<sup>2+</sup> influx unaffected. Apart from triggering exocytosis, intracellular Ca<sup>2+</sup> facilitates replenishment of the RRP during periods of high-frequency activity by increasing the rate of vesicle docking and priming (for review see Neher and Sakaba, 2008). Evidence also exists that increased Ca<sup>2+</sup> levels boost endocytosis rates (Kavalali, *et al.*, 1999). During periods of sustained network activity, it might therefore be advantageous for neurons to decrease transmitter release by presynaptic inhibitors that do not affect presynaptic Ca<sup>2+</sup> influx too much, and thereby maintaining other Ca<sup>2+</sup>-dependent processes in the vesicle cycle at a high level. Interestingly, it was demonstrated that adenosine 1 receptors at mossy fibre terminals suppress transmitter release by only reducing Ca<sup>2+</sup> influx (Gundlfinger, *et al.*, 2007), while we found that GABA<sub>B</sub>Rs also have a strong component of VDCC-independent inhibition at mossy fibre synapses. Adenosine signalling tonically inhibits release from mossy fibres, which shapes short-term plasticity and also maintains the dynamic range for long-term plasticity (Moore, *et al.*, 2003; Gundlfinger, *et al.*, 2007; but see Kukley, *et al.*, 2005). Conversely, presynaptic GABA<sub>B</sub>Rs are only activated after bursts of APs, when rapid endocytosis of emptied vesicles is required (Vogt and Nicoll, 1999; Guetg, *et al.*, 2009). A massive influx of Ca<sup>2+</sup> ions into mossy fibre boutons during these AP bursts activates soluble adenylyl cyclase, which increases cAMP levels and PKA activity, ultimately leading to a presynaptically expressed form of LTP (Nicoll and Schmitz, 2005). In this particular setting, an inhibitory presynaptic mechanism that excludes Ca<sup>2+</sup> channel activation could still allow the induction of presynaptic LTP and thereby enable a higher range of computational variation at the level of transmitter release.

At present, it is unclear how different metabotropic receptors coupling to the same class of signalling molecules cause different forms of presynaptic inhibition within a synaptic terminal. One possible explanation might be that the receptors couple to different Gα<sub>i</sub>/Gα<sub>o</sub>-protein subunit isoforms, which in turn could have different preferences to trigger one or

---

another pathway. For instance, G-protein  $\beta_1\gamma_2$ -dimers infused into PC12 cells were shown to inhibit  $\text{Ca}^{2+}$ -triggered noradrenalin release with a 20-fold higher efficacy than  $\beta_1\gamma_1$ , which is in line with the finding that the  $\beta_1\gamma_2$ -dimers have a much higher affinity to SNARE-complexes than  $\beta_1\gamma_1$  (Blackmer, *et al.*, 2005). However, to date little evidence was been found for a role of specific  $\text{G}\beta\gamma$  subunit combinations in receptor coupling and effector activation (Jones, *et al.*, 2004). Additionally, it is yet not clear how a given type of receptor, such as the  $\text{GABA}_{\text{B}}\text{R}$ , can trigger VDCC-dependent and -independent inhibition to various extents at different synapses. The synaptic localisation of the receptor and the molecular composition of the presynaptic terminal may play a role, but this remains to be investigated.

### 4.3 Estimated contribution of calcium-independent mechanisms on overall presynaptic inhibition

How does the combination of  $\text{Ca}^{2+}$ -dependent and -independent inhibition shape synaptic release probability? The reported extent of VDCC-independent presynaptic inhibition by  $\text{GABA}_{\text{B}}\text{Rs}$  varies considerably in the literature, probably due to the variety of synapses investigated. The most drastic example are the terminals of neurogliaform cells, where  $\text{GABA}_{\text{B}}\text{R}$  activation causes no change in  $\text{Ca}^{2+}$  influx, despite strong and sustained presynaptic inhibition (Price, *et al.*, 2008). In a theoretical paper, Trommershauser *et al.* proposed that the relationship of vesicular release probability ( $P_{\text{vr}}$ ) to intracellular  $\text{Ca}^{2+}$  concentration  $[\text{Ca}^{2+}]_{\text{i}}$  could be expressed as a fourth-order Hill equation. Here, the intracellular  $\text{Ca}^{2+}$  concentration  $[\text{Ca}^{2+}]_{\text{i}}$  that elicits half-maximal release was taken as  $42.5 \mu\text{M}$   $\text{Ca}^{2+}$ , based on experimental evidence (Trommershauser, *et al.*, 2003):

$$(6) P_{\text{vr}}(\Delta\text{Ca}^{2+}) = \frac{[\text{Ca}^{2+}]_{\text{i}}^4}{[\text{Ca}^{2+}]_{\text{i}}^4 + K_{1/2}^4}$$

The fourth-order dependency of the model takes into account that on average four  $\text{Ca}^{2+}$  ions have to bind to the  $\text{Ca}^{2+}$  sensor to initiate transmitter release (Schneppenburger and Neher, 2000). This value is very close to the exponent of 4.1 that we calculated for the power-function of transmitter release in CA1, based on macroscopic observations (3.1.1.). In contrast, a nonlinear fit of our data acquired in baclofen revealed a power of 6.1 for the  $\text{Ca}^{2+}$ -fEPSP relationship. By plotting Equation (6) for a physiological range of intracellular  $\text{Ca}^{2+}$  concentrations, it becomes evident that for lower  $\text{Ca}^{2+}$  concentrations, the  $P_{\text{vr}}$  decreases more

strongly if a higher exponent function is applied (Figure 4-1 A). Based on this calculation, we can determine changes in the  $P_{vr}$  as a result of presynaptic inhibition that reduces only the  $Ca^{2+}$ -influx, compared to  $P_{vr}$  changes due to presynaptic inhibition that employs an additional inhibitory mechanism at the release machinery. For both scenarios, we estimate that the effective intracellular  $Ca^{2+}$  concentration is reduced by 25%, as measured by  $Ca^{2+}$  imaging in CA1 (see 3.1.1). Based on the sucrose application experiments in autaptic cultures (see 3.2.4.2), we assume a  $P_{vr}$  of 10% in control conditions as a starting value for the release probability. If only the intracellular  $Ca^{2+}$  is reduced, the  $P_{vr}$  decreases to 3.4%. If an additional inhibitory mechanism is included that increases the exponent of the release function to 6, the  $P_{vr}$  decreases to 0.6% (green curve in Figure 4-1 B).

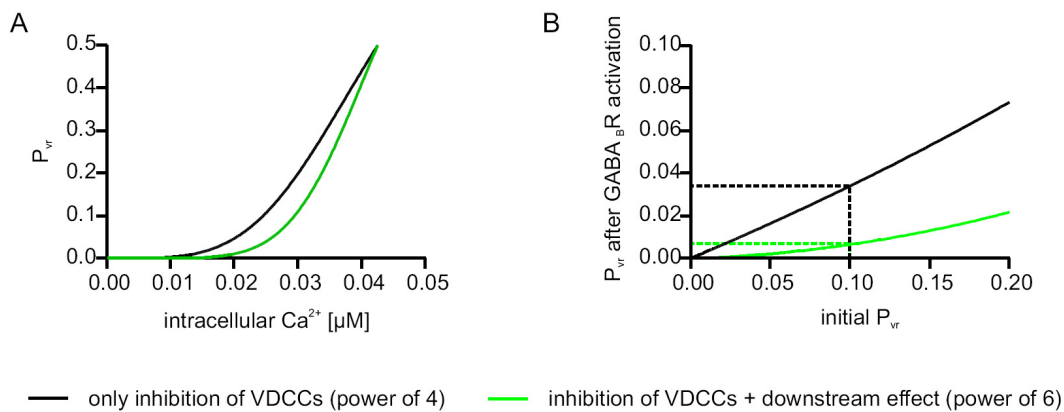


**Figure 4-1: The relation of the intracellular  $Ca^{2+}$  concentration to the vesicular release probability is strongly influenced by the power of the release function.**

(A) Plot of two Hill equations describing the dependency of the release probability on the intracellular  $Ca^{2+}$  concentration. The fourth-order curve (black) has an exponent of 4, as found in control conditions, while the sixth-order curve (green) represents a scenario with inhibition on the level of VDCCs and an additional inhibition mechanism reducing the fusion willingness. (B) Compared to the  $P_{vr}$  in control conditions, the  $P_{vr}$  after  $GABA_B R$  activation is greatly reduced when a change in the power is assumed. Dashed lines indicate the  $P_{vr}$  in the two different scenarios of inhibition, with a  $P_{vr}$  of 10% in control conditions as starting value. For both scenarios, the reduction of intracellular  $Ca^{2+}$  concentration was assumed as 25%.

This means that, in our model, presynaptic inhibition of transmitter release that only decreases the  $Ca^{2+}$  influx reduces the  $P_{vr}$  to approximately one third of the control value, compared to combined inhibition by both VDCCs and the release machinery, which reduces the  $P_{vr}$  to less than one tenth of the control value. In this example, inhibition downstream of VDCCs that directly increases the energy barrier of transmitter release contributes ~30% to the overall inhibition. Although based on a number of assumptions, the model illustrates that inhibition

---

acting on VDCCs alone is much less efficient than inhibition that employs additional downstream mechanisms.

The above considerations are supported by a review on presynaptic inhibition published by Wu and Saggau in 1997. The authors estimated the relative contribution of  $\text{Ca}^{2+}$ -independent mechanisms to total inhibition based on a multiplicative model of probabilities for  $\text{Ca}^{2+}$  influx and vesicle fusion. Interestingly, their calculations yielded a ~30% fraction of inhibition that was not due to inhibition of VDCCs, which is very similar to the fraction of direct inhibition calculated above using the Hill equation for the release probability.

#### **4.4 What is the target of presynaptic inhibition acting at the release machinery?**

We found that heterosynaptic  $\text{GABA}_B$ Rs directly inhibit transmitter release in addition to inhibition of VDCC opening at two different types of glutamatergic synapses in the hippocampus. The higher exponent of the function describing the relation of intracellular  $\text{Ca}^{2+}$  concentration to the postsynaptic signal argues for an increased need of  $\text{Ca}^{2+}$  binding to the  $\text{Ca}^{2+}$  sensor synaptotagmin to overcome the energy barrier for vesicle fusion and to trigger neurotransmitter release. Our experiments using hypertonic stimuli also imply that metabotropic signalling interferes directly with synaptic vesicle fusion. The next logical step was investigating the potential molecular target of this signalling cascade.

Serotonergic inhibition of transmitter release at the lamprey reticulospinal synapse is supposedly completely independent of VDCCs (Blackmer, *et al.*, 2001; but see from the same group Takahashi, *et al.*, 2001). Evidence has been presented for this synapse that G-protein  $\text{G}\beta\gamma$  subunits can bind to the C-terminus of SNAP-25, and thereby inhibit binding of synaptotagmin I to the SNARE complex (Gerachshenko, *et al.*, 2005). This interaction is thought to reduce and alter the mode of  $\text{Ca}^{2+}$ -dependent vesicle fusion (Photowala, *et al.*, 2006). Furthermore, investigations of noradrenalin release from PC12 cells and *in vitro* binding studies indicated that treatment with BoNT-A interferes with the binding of  $\text{G}\beta\gamma$  subunits to the SNARE complex (Blackmer, *et al.*, 2005).

These results were taken as reference for a study on adrenergic,  $\alpha_2$ -receptor-mediated inhibition in the amygdala of rats. Acute slice preparations were incubated with BoNT-A for up to 6 hours, which reduced evoked transmission to ~40%, and surprisingly resulted in a

complete loss of presynaptic inhibition. The results were interpreted as evidence that SNAP-25 is the target of G $\beta\gamma$  subunit-mediated direct interference with transmitter release (Delaney, *et al.*, 2007). However, the latter experiment did not explain why partial cleavage of SNAP-25 spared a certain fraction of vesicles, which remained competent for SNARE-mediated fusion, but were, on the other hand, subsequently largely insensitive to noradrenergic inhibition.

In light of these studies, we wanted to test whether SNAP-25 is the molecular target of G-protein-mediated inhibition at the release machinery of mammalian neurons by using hippocampal autaptic cell cultures. In these cultures, we studied Ca<sup>2+</sup>-independent presynaptic inhibition by GABA<sub>B</sub>Rs using three different experimental approaches. The results of all three approaches indicated that the interaction of SNAP-25 with synaptotagmin is not the target of G $\beta\gamma$  subunit-mediated direct inhibition. Firstly, we found a reduction of mEPSC frequencies by GABA<sub>B</sub>R activation in Ca<sup>2+</sup>-free extracellular solution, arguing against the involvement of the Ca<sup>2+</sup> sensor. Secondly, we observed that GABA<sub>B</sub>Rs cause a reduction of sucrose-evoked vesicle fusion, a form of transmitter release that is independent of Ca<sup>2+</sup> (Rosenmund and Stevens, 1996) and synaptotagmin 1 (Xu, *et al.*, 2009). Thirdly, we showed that cleavage of SNAP-25 by BoNT-A does not abolish the inhibitory effect of GABA<sub>B</sub>Rs on ionomycin-evoked release. In order to optimize the toxin concentration and incubation time of neuronal cultures for this experiment, we performed Western blots to verify full cleavage of SNAP-25 with BoNT-A. We additionally ensured complete loss of AP-evoked transmission in every recorded cell. In contrast to the earlier studies, in which BoNT-A was acutely applied to the terminals and evoked transmission persisted, we could thereby ensure that only cleaved SNAP-25, which lacks the putative interaction site for G $\beta\gamma$  subunits, was present in the neurons investigated. Taken together, our observations on GABA<sub>B</sub>R-mediated inhibition of mEPSCs in Ca<sup>2+</sup>-free conditions, inhibition of sucrose-evoked release, and inhibition of ionomycin-evoked release in BoNT-A treated neurons exclude the possibility that GABA<sub>B</sub>R signalling targets the C-terminus of SNAP-25 to inhibit transmitter release.

Metabotropic receptors might utilise different pathways at distinct synapses (Jones, *et al.*, 2004), and thereby possess diverse targets for modulation, which might explain the discrepancy of our work to other studies that did find SNAP-25 to be the target of direct inhibition. In fact, other molecules in the release machinery might be the target of G-protein-mediated inhibition by GABA<sub>B</sub>Rs. Interestingly, the affinity of G $\beta_1\gamma_2$  to individual SNARE-

---

proteins was determined in the following order (EC<sub>50</sub> in parenthesis): syntaxin (0.33 μM) > synaptobrevin (0.94 μM) > SNAP25 (1.07 μM) (Yoon, *et al.*, 2007). Alternatively, Gβγ subunits might preferentially interact with the fully assembled SNARE complex, without the existence of a specific protein target. Evidence for this hypothesis was provided by biochemical assays demonstrating that the affinity of Gβγ subunits to the assembled SNARE-complex is much higher than to isolated SNAP-25 (Blackmer, *et al.*, 2005). In future studies, we plan to test the involvement of other members of the release machinery using ablation experiments. We will continue with experiments using different clostridial toxins, and also intend establishing neuronal cultures of mice deficient for proteins of the synaptic release machinery, e.g. synaptobrevin. These experiments should clarify whether a single molecule can be identified as the target of direct inhibition of vesicular fusion or whether other mechanisms that do not require a specific protein-protein interaction account for the observed effect, e.g. a sterical interference of Gβγ subunits with the release process.

#### **4.5 Potential experimental use of the Cre-conditional hM4D transgenic mouse**

The third part of the Results summarizes our findings of strong presynaptic inhibition by the artificial receptor hM4D, and our development of a transgenic mouse line expressing hM4D receptors in a Cre-conditional manner. This mouse model would allow time-controlled, experimentally induced presynaptic inhibition by the artificial hM4D receptor in a cell type-specific manner. In the future, the hM4D-transgenic mice may facilitate studies on the influence of specific neuronal subtypes on network activity, as I will discuss below.

The human muscarinic type 4 like designer (hM4D) receptor was engineered as part of an attempt to design a family of GPCRs that are activated specifically by an inert drug, clozapine-N-oxide (CNO), but are insensitive to the natural ligand acetylcholine (Armbruster, *et al.*, 2007). We expressed hM4D in autaptic neurons and found that it induces strong presynaptic inhibition when activated with CNO at nanomolar concentrations. This result was unexpected in light of the original publication, which only reported a postsynaptic, GIRK-channel dependent inhibitory effect. However, wildtype muscarinic M4 receptors, from which hM4D was derived, were also described as mediating presynaptic inhibition in the central nervous system (Levey, *et al.*, 1995). Thus, apart from the altered affinity for its ligands, the mutant hM4D seems to traffic and signal similarly to the wildtype receptor.

We expect that the hM4D-receptor/CNO system will also be a useful tool to suppress transmitter release from cells expressing the artificial receptor *in vivo*. Rapid pharmacological silencing of neuronal output by a specific receptor/drug system circumvents some of the difficulties encountered when neurons are inactivated with chronic ablation methods or other invasive techniques (compare also Table 1, page 26): Firstly, CNO is a blood-brain barrier-permeable molecule, and can be administered by intraperitoneal injection or via drinking water, and consequently does not require permanent implantation of local perfusion systems or light cannulae in the brain. Secondly, it also activates hM4D receptors that are expressed by scattered populations of neurons. Thirdly, the action of the system is reversible and considerably fast, with an approximate delay of 20 min *in vivo* (Alexander, *et al.*, 2009), which ensures that compensatory mechanisms of local networks are unlikely to counterbalance the effect of the sudden loss of neurotransmission from the group of neurons expressing hM4D. We therefore believe that the combination of a genetically encoded hM4D receptor and its pharmacological activation by CNO presents a novel, promising method to study the role of neurons in network activity, computation and behaviour.

We have begun developing a transgenic mouse model, in which expression of hM4D receptors will depend on a Cre-mediated recombination event. When crossed with Cre-transgenic mice, the Cre-hM4D double-transgenic offspring will express hM4D in all Cre-expressing cells. To demonstrate the *in vivo* applicability of presynaptic inhibition by means of the hM4D/CNO system to specifically silence a defined neuronal population, a possible first experiment would be to target hM4D expression to Purkinje cells of the cerebellum. Purkinje cells are GABAergic and the only output of the cerebellum cortex to the deep cerebellar nuclei. Selective hM4D expression in Purkinje cells can be achieved by crossing the hM4D-transgenic mouse line with a mouse line that expresses Cre under the Purkinje cell-specific L7 promoter (Barski, *et al.*, 2000). A similar approach was described using a mouse line generated by Wulff *et al.*, in which application of Zolpidem resulted in an increased activation of GABA<sub>A</sub>Rs selectively in Purkinje cells (Wulff, *et al.*, 2007). When the mice were injected with the drug, they showed a drastically reduced motor performance on a rotarod test, indicating reduced cerebellar performance. Motor performance tests on a rotarod are relatively easy to perform, and the observations by Wulff *et al.* might serve as reference for us when testing the conditional hM4D/CNO system.

---

In a second experiment, we would like to breed conditional hM4D transgenic mice with mice expressing Cre under the parvalbumin promoter. In the hippocampus, this would restrict hM4D expression to parvalbumin-positive interneurons (Fuchs, *et al.*, 2007), which comprise interneurons targeting the dendrites of pyramidal neurons (bistratified, and possibly Oriens-Lacunosum moleculare cells), and interneurons providing perisomatic inhibition (basket cells and axo-axonic cells). These neurons have been implicated in hippocampal rhythm generation in the theta (5–10 Hz) and gamma (35–85 Hz) frequency, and in fast (100 to 200 Hz), sharp wave-associated ripple complexes (Klausberger and Somogyi, 2008). However, to date acutely silencing parvalbuminergic neurons and investigating the effect on hippocampal oscillations has not been possible. Our lab has acquired considerable technical experience in recording hippocampal ripple oscillations from acute slices (Maier, *et al.*, 2009). Recording gamma oscillations *in vitro* is also possible using the same methods (Fisahn, *et al.*, 1998). We could therefore record network oscillations in slices from transgenic animals expressing hM4D only in parvalbumin-positive interneurons, and compare baseline network oscillations with oscillation patterns after CNO application. This kind of experiment may advance our current understanding of how local interneurons shape oscillation patterns in the hippocampal network.

Clearly, due to its Cre-dependency, our conditional hM4D transgenic mouse model might have limited cell-specificity. In transgenic Cre lines, the cellular expression pattern of Cre depends on the promoter used to drive Cre-expression, and on the genomic insertion site of the transgene, which is often unknown. Cre expression can therefore vary in strength, and occur in unexpected locations due to “offsite” activity of the promoter. Further, transgene expression might also occur outside of the CNS, as is obvious for the use of the parvalbumin promoter-Cre mouse, because parvalbumin is also expressed in muscles (Heizmann, *et al.*, 1982). In parvalbumin promoter-Cre/ hM4D mice, systemic application of CNO would most likely result in muscle paralysis, which is the reason why I proposed slice recordings to investigate the role of parvalbumin-positive cells in hippocampal oscillations. Furthermore, some of the genes that serve as specific neuronal markers in the adult CNS might be activated during development in a much more widespread manner. Even a short, transient expression of Cre will cause recombination of the FLEX switch and irreversibly initiate hM4D expression, so careful examination of the Cre-driver line is required. An alternative strategy to circumvent these obstacles is the use of a conditional, virus-based expression system of hM4D. A future

project will therefore aim to develop a system that allows conditional expression of hM4D in Cre-transgenic cells using viral infections. When used for *in vivo* injections, this viral system would enable us to specifically target the expression site and onset of hM4D in neurons.

In conclusion, we have demonstrated that inhibitory GPCR signalling can directly interfere with the fusion process of neurotransmitter vesicles. This metabotropic action occurs downstream of and in addition to classical VDCC-dependent inhibition. Our research thereby contributes to the emerging understanding of metabotropic signalling in presynaptic terminals. As presynaptic inhibition is a powerful tool for shaping information propagation in neuronal networks and can actually exclude neurons from neuronal communication, we propose using the artificial, genetically encoded presynaptic GPCR hM4D in future studies to investigate the role of individual types of neurons in networks.

---



---

## 5 Appendix

### 5.1 References

- Abbott, L. F. and Regehr, W. G. (2004) Synaptic computation. *Nature*, 431, 796-803.
- Ahuja, S. and Smith, S. O. (2009) Multiple switches in G protein-coupled receptor activation. *Trends Pharmacol Sci*, 30, 494-502.
- Alexander, G. M., Rogan, S. C., Abbas, A. I., *et al.* (2009) Remote control of neuronal activity in transgenic mice expressing evolved G protein-coupled receptors. *Neuron*, 63, 27-39.
- Andersen, P., Morris, R., Amaral, D., Bliss, T. and O'Keefe, J. (2006) *The Hippocampus Book*. Oxford University Press, New York.
- Armbruster, B. N., Li, X., Pausch, M. H., Herlitze, S. and Roth, B. L. (2007) Evolving the lock to fit the key to create a family of G protein-coupled receptors potently activated by an inert ligand. *Proc Natl Acad Sci U S A*, 104, 5163-8.
- Auger, C. and Marty, A. (2000) Quantal currents at single-site central synapses. *J Physiol*, 526 Pt 1, 3-11.
- Barski, J. J., Dethleffsen, K. and Meyer, M. (2000) Cre recombinase expression in cerebellar Purkinje cells. *Genesis*, 28, 93-8.
- Basarsky, T. A., Parpura, V. and Haydon, P. G. (1994) Hippocampal synaptogenesis in cell culture: developmental time course of synapse formation, calcium influx, and synaptic protein distribution. *J Neurosci*, 14, 6402-11.
- Basu, J., Betz, A., Brose, N. and Rosenmund, C. (2007) Munc13-1 C1 domain activation lowers the energy barrier for synaptic vesicle fusion. *J Neurosci*, 27, 1200-10.
- Bekkers, J. M. and Clements, J. D. (1999) Quantal amplitude and quantal variance of strontium-induced asynchronous EPSCs in rat dentate granule neurons. *J Physiol*, 516 ( Pt 1), 227-48.
- Bekkers, J. M. and Stevens, C. F. (1991) Excitatory and inhibitory autaptic currents in isolated hippocampal neurons maintained in cell culture. *Proc Natl Acad Sci U S A*, 88, 7834-8.
- Biermann, B., Ivankova-Susankova, K., Bradaia, A., *et al.* (2010) The Sushi domains of GABAB receptors function as axonal targeting signals. *J Neurosci*, 30, 1385-94.
- Blackmer, T., Larsen, E. C., Bartleson, C., *et al.* (2005) G protein betagamma directly regulates SNARE protein fusion machinery for secretory granule exocytosis. *Nat Neurosci*, 8, 421-5.
- Blackmer, T., Larsen, E. C., Takahashi, M., *et al.* (2001) G protein betagamma subunit-mediated presynaptic inhibition: regulation of exocytotic fusion downstream of Ca<sup>2+</sup> entry. *Science*, 292, 293-7.
- Branda, C. S. and Dymecki, S. M. (2004) Talking about a revolution: The impact of site-specific recombinases on genetic analyses in mice. *Dev Cell*, 6, 7-28.
- Breidenbach, M. A. and Brunger, A. T. (2005) New insights into clostridial neurotoxin-SNARE interactions. *Trends Mol Med*, 11, 377-81.

- Brenowitz, S. and Trussell, L. O. (2001) Minimizing synaptic depression by control of release probability. *J Neurosci*, 21, 1857-67.
- Breustedt, J., Gundlfinger, A., Varoqueaux, F., *et al.* (2009) Munc13-2 differentially affects hippocampal synaptic transmission and plasticity. *Cereb Cortex*, 20, 1109-20.
- Buschow, C., Charo, J., Anders, K., *et al.* In Vivo Imaging of an Inducible Oncogenic Tumor Antigen Visualizes Tumor Progression and Predicts CTL Tolerance. *J Immunol*.
- Capogna, M., Gähwiler, B. H. and Thompson, S. M. (1996) Presynaptic inhibition of calcium-dependent and -independent release elicited with ionomycin, gadolinium, and alpha-latrotoxin in the hippocampus. *J Neurophysiol*, 75, 2017-28.
- Capogna, M., McKinney, R. A., O'Connor, V., Gähwiler, B. H. and Thompson, S. M. (1997) Ca<sup>2+</sup> or Sr<sup>2+</sup> partially rescues synaptic transmission in hippocampal cultures treated with botulinum toxin A and C, but not tetanus toxin. *J Neurosci*, 17, 7190-202.
- Chalifoux, J. R. and Carter, A. G. (2010) GABAB receptors modulate NMDA receptor calcium signals in dendritic spines. *Neuron*, 66, 101-13.
- Conklin, B. R. (2007) New tools to build synthetic hormonal pathways. *Proc Natl Acad Sci U S A*, 104, 4777-8.
- Conklin, B. R., Farfel, Z., Lustig, K. D., Julius, D. and Bourne, H. R. (1993) Substitution of three amino acids switches receptor specificity of Gq alpha to that of Gi alpha. *Nature*, 363, 274-6.
- Conklin, B. R., Hsiao, E. C., Claeysen, S., *et al.* (2008) Engineering GPCR signaling pathways with RASSLs. *Nat Methods*, 5, 673-8.
- Cossart, R., Epsztein, J., Tyzio, R., *et al.* (2002) Quantal release of glutamate generates pure kainate and mixed AMPA/kainate EPSCs in hippocampal neurons. *Neuron*, 35, 147-59.
- Del Castillo, J. and Katz, B. (1954) Quantal components of the end-plate potential. *J Physiol*, 124, 560-73.
- Delaney, A. J., Crane, J. W. and Sah, P. (2007) Noradrenaline modulates transmission at a central synapse by a presynaptic mechanism. *Neuron*, 56, 880-92.
- Dittman, J. S. and Regehr, W. G. (1996) Contributions of calcium-dependent and calcium-independent mechanisms to presynaptic inhibition at a cerebellar synapse. *J Neurosci*, 16, 1623-33.
- Dodge, F. A., Jr. and Rahamimoff, R. (1967) Co-operative action a calcium ions in transmitter release at the neuromuscular junction. *J Physiol*, 193, 419-32.
- Dutar, P. and Nicoll, R. A. (1988) Pre- and postsynaptic GABAB receptors in the hippocampus have different pharmacological properties. *Neuron*, 1, 585-91.
- Epsztein, J., Represa, A., Jorquera, I., Ben-Ari, Y. and Crepel, V. (2005) Recurrent mossy fibers establish aberrant kainate receptor-operated synapses on granule cells from epileptic rats. *J Neurosci*, 25, 8229-39.
- Fatt, P. and Katz, B. (1952) Spontaneous subthreshold activity at motor nerve endings. *J Physiol*, 117, 109-28.
- Fisahn, A., Pike, F. G., Buhl, E. H. and Paulsen, O. (1998) Cholinergic induction of network oscillations at 40 Hz in the hippocampus in vitro. *Nature*, 394, 186-9.
- Friedrich, G. and Soriano, P. (1991) Promoter traps in embryonic stem cells: a genetic screen to identify and mutate developmental genes in mice. *Genes Dev*, 5, 1513-23.
- Fuchs, E. C., Zivkovic, A. R., Cunningham, M. O., *et al.* (2007) Recruitment of parvalbumin-positive interneurons determines hippocampal function and associated behavior. *Neuron*, 53, 591-604.

- 
- Furshpan, E. J., MacLeish, P. R., O'Lague, P. H. and Potter, D. D. (1976) Chemical transmission between rat sympathetic neurons and cardiac myocytes developing in microcultures: evidence for cholinergic, adrenergic, and dual-function neurons. *Proc Natl Acad Sci U S A*, 73, 4225-9.
- Gassmann, M., Shaban, H., Vigot, R., *et al.* (2004) Redistribution of GABAB(1) protein and atypical GABAB responses in GABAB(2)-deficient mice. *J Neurosci*, 24, 6086-97.
- Geppert, M., Goda, Y., Hammer, R. E., *et al.* (1994) Synaptotagmin I: a major Ca<sup>2+</sup> sensor for transmitter release at a central synapse. *Cell*, 79, 717-27.
- Gerachshenko, T., Blackmer, T., Yoon, E. J., *et al.* (2005) Gbetagamma acts at the C terminus of SNAP-25 to mediate presynaptic inhibition. *Nat Neurosci*, 8, 597-605.
- Gerber, S. H., Rah, J. C., Min, S. W., *et al.* (2008) Conformational switch of syntaxin-1 controls synaptic vesicle fusion. *Science*, 321, 1507-10.
- Golgi, C., Bentivoglio, M. and Swanson, L. (2001) On the fine structure of the pes Hippocampi major (with plates XIII-XXIII). 1886. *Brain Res Bull*, 54, 461-83.
- Gomperts, S. N., Carroll, R., Malenka, R. C. and Nicoll, R. A. (2000) Distinct roles for ionotropic and metabotropic glutamate receptors in the maturation of excitatory synapses. *J Neurosci*, 20, 2229-37.
- Grabs, D., Bergmann, M., Schuster, T., *et al.* (1994) Differential expression of synaptophysin and synaptoporin during pre- and postnatal development of the rat hippocampal network. *Eur J Neurosci*, 6, 1765-71.
- Graham, M. E., Handley, M. T., Barclay, J. W., *et al.* (2008) A gain-of-function mutant of Munc18-1 stimulates secretory granule recruitment and exocytosis and reveals a direct interaction of Munc18-1 with Rab3. *Biochem J*, 409, 407-16.
- Groemer, T. W. and Klingauf, J. (2007) Synaptic vesicles recycling spontaneously and during activity belong to the same vesicle pool. *Nat Neurosci*, 10, 145-7.
- Groffen, A. J., Martens, S., Diez Arazola, R., *et al.* (2010) Doc2b is a high-affinity Ca<sup>2+</sup> sensor for spontaneous neurotransmitter release. *Science*, 327, 1614-8.
- Grosse, G., Eulitz, D., Thiele, T., *et al.* (2003) Axonal sorting of Kir3.3 defines a GABA-containing neuron in the CA3 region of rodent hippocampus. *Mol Cell Neurosci*, 24, 709-24.
- Guetg, N., Seddik, R., Vigot, R., *et al.* (2009) The GABAB1a isoform mediates heterosynaptic depression at hippocampal mossy fiber synapses. *J Neurosci*, 29, 1414-23.
- Gundlfinger, A., Bischofberger, J., Jochenning, F. W., *et al.* (2007) Adenosine modulates transmission at the hippocampal mossy fibre synapse via direct inhibition of presynaptic calcium channels. *J Physiol*, 582, 263-77.
- Han, X. and Boyden, E. S. (2007) Multiple-Color Optical Activation, Silencing, and Desynchronization of Neural Activity, with Single-Spike Temporal Resolution. *PLoS ONE*, 2, e299.
- Heizmann, C. W., Berchtold, M. W. and Rowlerson, A. M. (1982) Correlation of parvalbumin concentration with relaxation speed in mammalian muscles. *Proc Natl Acad Sci U S A*, 79, 7243-7.
- Henze, D. A., Urban, N. N. and Barrionuevo, G. (2000) The multifarious hippocampal mossy fiber pathway: a review. *Neuroscience*, 98, 407-27.
- Hitz, C., Steuber-Buchberger, P., Delic, S., Wurst, W. and Kuhn, R. (2009) Generation of shRNA transgenic mice. *Methods Mol Biol*, 530, 101-29.
- Hitz, C., Wurst, W. and Kuhn, R. (2007) Conditional brain-specific knockdown of MAPK using Cre/loxP regulated RNA interference. *Nucleic Acids Res*, 35, e90.

- Huang, Z. J. (2006) GABAB receptor isoforms caught in action at the scene. *Neuron*, 50, 521-4.
- Ibanez-Tallon, I., Wen, H., Miwa, J. M., *et al.* (2004) Tethering naturally occurring peptide toxins for cell-autonomous modulation of ion channels and receptors in vivo. *Neuron*, 43, 305-11.
- Isaacson, J. S., Solis, J. M. and Nicoll, R. A. (1993) Local and diffuse synaptic actions of GABA in the hippocampus. *Neuron*, 10, 165-75.
- Isaacson, J. S. (1998) GABAB receptor-mediated modulation of presynaptic currents and excitatory transmission at a fast central synapse. *J Neurophysiol*, 80, 1571-6.
- Jahn, R. and Sudhof, T. C. (1999) Membrane fusion and exocytosis. *Annu Rev Biochem*, 68, 863-911.
- Jones, M. B., Siderovski, D. P. and Hooks, S. B. (2004) The G betagamma dimer as a novel source of selectivity in G-protein signaling: GGL-ing at convention. *Mol Interv*, 4, 200-14.
- Junge, H. J., Rhee, J. S., Jahn, O., *et al.* (2004) Calmodulin and Munc13 form a Ca<sup>2+</sup> sensor/effector complex that controls short-term synaptic plasticity. *Cell*, 118, 389-401.
- Kajikawa, Y., Saitoh, N. and Takahashi, T. (2001) GTP-binding protein beta gamma subunits mediate presynaptic calcium current inhibition by GABA(B) receptor. *Proc Natl Acad Sci U S A*, 98, 8054-8.
- Kamiya, H. and Ozawa, S. (1998) Kainate receptor-mediated inhibition of presynaptic Ca<sup>2+</sup> influx and EPSP in area CA1 of the rat hippocampus. *J Physiol*, 509 ( Pt 3), 833-45.
- Karpova, A. Y., Tervo, D. G., Gray, N. W. and Svoboda, K. (2005) Rapid and reversible chemical inactivation of synaptic transmission in genetically targeted neurons. *Neuron*, 48, 727-35.
- Kaupmann, K., Malitschek, B., Schuler, V., *et al.* (1998) GABA(B)-receptor subtypes assemble into functional heteromeric complexes. *Nature*, 396, 683-7.
- Kavalali, E. T., Klingauf, J. and Tsien, R. W. (1999) Properties of fast endocytosis at hippocampal synapses. *Philos Trans R Soc Lond B Biol Sci*, 354, 337-46.
- Kirschstein, T., von der Brélie, C., Steinhäuser, M., *et al.* (2004) L-CCG-I activates group III metabotropic glutamate receptors in the hippocampal CA3 region. *Neuropharmacology*, 47, 157-62.
- Klausberger, T. and Somogyi, P. (2008) Neuronal diversity and temporal dynamics: the unity of hippocampal circuit operations. *Science*, 321, 53-7.
- Koh, T. W. and Bellen, H. J. (2003) Synaptotagmin I, a Ca<sup>2+</sup> sensor for neurotransmitter release. *Trends Neurosci*, 26, 413-22.
- Kukley, M., Schwan, M., Fredholm, B. B. and Dietrich, D. (2005) The role of extracellular adenosine in regulating mossy fiber synaptic plasticity. *J Neurosci*, 25, 2832-7.
- Kulik, A., Vida, I., Lujan, R., *et al.* (2003) Subcellular localization of metabotropic GABA(B) receptor subunits GABA(B1a/b) and GABA(B2) in the rat hippocampus. *J Neurosci*, 23, 11026-35.
- Lechner, H. A., Lein, E. S. and Callaway, E. M. (2002) A genetic method for selective and quickly reversible silencing of Mammalian neurons. *J Neurosci*, 22, 5287-90.
- Levey, A. I., Edmunds, S. M., Koliatsos, V., Wiley, R. G. and Heilman, C. J. (1995) Expression of m1-m4 muscarinic acetylcholine receptor proteins in rat hippocampus and regulation by cholinergic innervation. *J Neurosci*, 15, 4077-92.
- Linial, M. (1997) SNARE proteins--why so many, why so few? *J Neurochem*, 69, 1781-92.
- Liu, C. and Hermann, T. E. (1978) Characterization of ionomycin as a calcium ionophore. *J Biol Chem*, 253, 5892-4.

- 
- Lois, C., Hong, E. J., Pease, S., Brown, E. J. and Baltimore, D. (2002) Germline transmission and tissue-specific expression of transgenes delivered by lentiviral vectors. *Science*, 295, 868-72.
- Lomber, S. G. (1999) The advantages and limitations of permanent or reversible deactivation techniques in the assessment of neural function. *Journal of Neuroscience Methods*, 86, 109-17.
- Lou, X., Scheuss, V. and Schneggenburger, R. (2005) Allosteric modulation of the presynaptic Ca<sup>2+</sup> sensor for vesicle fusion. *Nature*, 435, 497-501.
- Luo, L., Callaway, E. M. and Svoboda, K. (2008) Genetic dissection of neural circuits. *Neuron*, 57, 634-60.
- Luquet, S., Perez, F. A., Hnasko, T. S. and Palmiter, R. D. (2005) NPY/AgRP Neurons Are Essential for Feeding in Adult Mice but Can Be Ablated in Neonates. *Science*, 310, 683-5.
- Luscher, C., Jan, L. Y., Stoffel, M., Malenka, R. C. and Nicoll, R. A. (1997) G protein-coupled inwardly rectifying K<sup>+</sup> channels (GIRKs) mediate postsynaptic but not presynaptic transmitter actions in hippocampal neurons. *Neuron*, 19, 687-95.
- Madziva, M. T. and Edwardson, J. M. (2001) Trafficking of green fluorescent protein-tagged muscarinic M4 receptors in NG108-15 cells. *Eur J Pharmacol*, 428, 9-18.
- Maier, N., Morris, G., Jenkinson, F. W. and Schmitz, D. (2009) An approach for reliably investigating hippocampal sharp wave-ripples in vitro. *PLoS One*, 4, e6925.
- Malenka, R. C. and Bear, M. F. (2004) LTP and LTD: an embarrassment of riches. *Neuron*, 44, 5-21.
- Marchal, C. and Mulle, C. (2004) Postnatal maturation of mossy fibre excitatory transmission in mouse CA3 pyramidal cells: a potential role for kainate receptors. *J Physiol*, 561, 27-37.
- Matveev, V., Bertram, R. and Sherman, A. (2009) Ca<sup>2+</sup> current versus Ca<sup>2+</sup> channel cooperativity of exocytosis. *J Neurosci*, 29, 12196-209.
- Maximov, A., Shin, O. H., Liu, X. and Sudhof, T. C. (2007) Synaptotagmin-12, a synaptic vesicle phosphoprotein that modulates spontaneous neurotransmitter release. *J Cell Biol*, 176, 113-24.
- Miyoshi, G. and Fishell, G. (2006) Directing neuron-specific transgene expression in the mouse CNS. *Curr Opin Neurobiol*, 16, 577-84.
- Mongillo, G., Barak, O. and Tsodyks, M. (2008) Synaptic theory of working memory. *Science*, 319, 1543-6.
- Montecucco, C., Schiavo, G. and Pantano, S. (2005) SNARE complexes and neuroexocytosis: how many, how close? *Trends Biochem Sci*, 30, 367-72.
- Moore, K. A., Nicoll, R. A. and Schmitz, D. (2003) Adenosine gates synaptic plasticity at hippocampal mossy fiber synapses. *Proc Natl Acad Sci U S A*, 100, 14397-402.
- Mott, D. D. and Lewis, D. V. (1991) Facilitation of the induction of long-term potentiation by GABAB receptors. *Science*, 252, 1718-20.
- Neher, E. and Sakaba, T. (2008) Multiple roles of calcium ions in the regulation of neurotransmitter release. *Neuron*, 59, 861-72.
- Newberry, N. R. and Nicoll, R. A. (1984) Direct hyperpolarizing action of baclofen on hippocampal pyramidal cells. *Nature*, 308, 450-2.
- Nicoll, R. A. and Schmitz, D. (2005) Synaptic plasticity at hippocampal mossy fibre synapses. *Nat Rev Neurosci*, 6, 863-76.
- Niwa, H., Yamamura, K. and Miyazaki, J. (1991) Efficient selection for high-expression transfectants with a novel eukaryotic vector. *Gene*, 108, 193-9.

- Oliet, S. H. and Poulain, D. A. (1999) Adenosine-induced presynaptic inhibition of IPSCs and EPSCs in rat hypothalamic supraoptic nucleus neurones. *J Physiol*, 520 Pt 3, 815-25.
- Pang, Z. P., Sun, J., Rizo, J., Maximov, A. and Sudhof, T. C. (2006) Genetic analysis of synaptotagmin 2 in spontaneous and Ca<sup>2+</sup>-triggered neurotransmitter release. *Embo J*, 25, 2039-50.
- Perez-Garci, E., Gassmann, M., Bettler, B. and Larkum, M. E. (2006) The GABAB1b isoform mediates long-lasting inhibition of dendritic Ca<sup>2+</sup> spikes in layer 5 somatosensory pyramidal neurons. *Neuron*, 50, 603-16.
- Photowala, H., Blackmer, T., Schwartz, E., Hamm, H. E. and Alford, S. (2006) G protein betagamma-subunits activated by serotonin mediate presynaptic inhibition by regulating vesicle fusion properties. *Proc Natl Acad Sci U S A*, 103, 4281-6.
- Pierce, K. L., Premont, R. T. and Lefkowitz, R. J. (2002) Seven-transmembrane receptors. *Nat Rev Mol Cell Biol*, 3, 639-50.
- Price, C. J., Scott, R., Rusakov, D. A. and Capogna, M. (2008) GABA(B) receptor modulation of feedforward inhibition through hippocampal neurogliaform cells. *J Neurosci*, 28, 6974-82.
- Pyott, S. J. and Rosenmund, C. (2002) The effects of temperature on vesicular supply and release in autaptic cultures of rat and mouse hippocampal neurons. *J Physiol*, 539, 523-35.
- Redman, S. (1990) Quantal analysis of synaptic potentials in neurons of the central nervous system. *Physiol Rev*, 70, 165-98.
- Regehr, W. G. and Tank, D. W. (1991) Selective fura-2 loading of presynaptic terminals and nerve cell processes by local perfusion in mammalian brain slice. *J Neurosci Methods*, 37, 111-9.
- Rizo, J. and Rosenmund, C. (2008) Synaptic vesicle fusion. *Nat Struct Mol Biol*, 15, 665-74.
- Rizzoli, S. O. and Betz, W. J. (2005) Synaptic vesicle pools. *Nat Rev Neurosci*, 6, 57-69.
- Rizzoli, S. O. and Jahn, R. (2007) Kiss-and-run, collapse and 'readily retrievable' vesicles. *Traffic*, 8, 1137-44.
- Rosenmund, C., Feltz, A. and Westbrook, G. L. (1995) Synaptic NMDA receptor channels have a low open probability. *J Neurosci*, 15, 2788-95.
- Rosenmund, C. and Stevens, C. F. (1996) Definition of the readily releasable pool of vesicles at hippocampal synapses. *Neuron*, 16, 1197-207.
- Rost, B. R., Breustedt, J., Schoenherr, A., *et al.* (2010) Autaptic cultures of single hippocampal granule cells of mice and rats. *Eur J Neurosci*, 32, 939-47.
- Sakaba, T. and Neher, E. (2003) Direct modulation of synaptic vesicle priming by GABA(B) receptor activation at a glutamatergic synapse. *Nature*, 424, 775-8.
- Sara, Y., Virmani, T., Deak, F., Liu, X. and Kavalali, E. T. (2005) An isolated pool of vesicles recycles at rest and drives spontaneous neurotransmission. *Neuron*, 45, 563-73.
- Sauer, B. (1987) Functional expression of the cre-lox site-specific recombination system in the yeast *Saccharomyces cerevisiae*. *Mol Cell Biol*, 7, 2087-96.
- Sauer, B. and Henderson, N. (1988) Site-specific DNA recombination in mammalian cells by the Cre recombinase of bacteriophage P1. *Proc Natl Acad Sci U S A*, 85, 5166-70.
- Scanziani, M., Capogna, M., Gähwiler, B. H. and Thompson, S. M. (1992) Presynaptic inhibition of miniature excitatory synaptic currents by baclofen and adenosine in the hippocampus. *Neuron*, 9, 919-27.
- Schiavo, G., Matteoli, M. and Montecucco, C. (2000) Neurotoxins affecting neuroexocytosis. *Physiol Rev*, 80, 717-66.

- 
- Schneggenburger, R. and Neher, E. (2000) Intracellular calcium dependence of transmitter release rates at a fast central synapse. *Nature*, 406, 889-93.
- Schneggenburger, R. and Neher, E. (2005) Presynaptic calcium and control of vesicle fusion. *Curr Opin Neurobiol*, 15, 266-74.
- Schnutgen, F., Doerflinger, N., Calleja, C., *et al.* (2003) A directional strategy for monitoring Cre-mediated recombination at the cellular level in the mouse. *Nat Biotechnol*, 21, 562-5.
- Schoch, S., Deak, F., Konigstorfer, A., *et al.* (2001) SNARE function analyzed in synaptobrevin/VAMP knockout mice. *Science*, 294, 1117-22.
- Schoch, S. and Gundelfinger, E. D. (2006) Molecular organization of the presynaptic active zone. *Cell Tissue Res*, 326, 379-91.
- Scholz, K. P. and Miller, R. J. (1992) Inhibition of quantal transmitter release in the absence of calcium influx by a G protein-linked adenosine receptor at hippocampal synapses. *Neuron*, 8, 1139-50.
- Schuler, V., Luscher, C., Blanchet, C., *et al.* (2001) Epilepsy, hyperalgesia, impaired memory, and loss of pre- and postsynaptic GABA(B) responses in mice lacking GABA(B(1)). *Neuron*, 31, 47-58.
- Schwartz, E. J., Blackmer, T., Gerachshenko, T. and Alford, S. (2007) Presynaptic G-protein-coupled receptors regulate synaptic cleft glutamate via transient vesicle fusion. *J Neurosci*, 27, 5857-68.
- Scoville, W. B. and Milner, B. (1957) Loss of recent memory after bilateral hippocampal lesions. *J Neurol Neurosurg Psychiatry*, 20, 11-21.
- Shaner, N. C., Lin, M. Z., McKeown, M. R., *et al.* (2008) Improving the photostability of bright monomeric orange and red fluorescent proteins. *Nat Methods*, 5, 545-51.
- Shcherbo, D., Merzlyak, E. M., Chepurnykh, T. V., *et al.* (2007) Bright far-red fluorescent protein for whole-body imaging. *Nat Methods*, 4, 741-6.
- Shepherd, G. M. and Erulkar, S. D. (1997) Centenary of the synapse: from Sherrington to the molecular biology of the synapse and beyond. *Trends Neurosci*, 20, 385-92.
- Slimko, E. M. and Lester, H. A. (2003) Codon optimization of *Caenorhabditis elegans* GluCl ion channel genes for mammalian cells dramatically improves expression levels. *J Neurosci Methods*, 124, 75-81.
- Sollner, T., Bennett, M. K., Whiteheart, S. W., Scheller, R. H. and Rothman, J. E. (1993) A protein assembly-disassembly pathway in vitro that may correspond to sequential steps of synaptic vesicle docking, activation, and fusion. *Cell*, 75, 409-18.
- Sorensen, J. B. (2009) Conflicting views on the membrane fusion machinery and the fusion pore. *Annu Rev Cell Dev Biol*, 25, 513-37.
- Steiger, J. L., Bandyopadhyay, S., Farb, D. H. and Russek, S. J. (2004) cAMP response element-binding protein, activating transcription factor-4, and upstream stimulatory factor differentially control hippocampal GABABR1a and GABABR1b subunit gene expression through alternative promoters. *J Neurosci*, 24, 6115-26.
- Stevens, C. F. and Williams, J. H. (2000) "Kiss and run" exocytosis at hippocampal synapses. *Proc Natl Acad Sci U S A*, 97, 12828-33.
- Stosiek, C., Garaschuk, O., Holthoff, K. and Konnerth, A. (2003) In vivo two-photon calcium imaging of neuronal networks. *Proc Natl Acad Sci U S A*, 100, 7319-24.
- Südhof, T., Starke, K (2008) *Pharmacology of Neurotransmitter Release*. Springer, Heidelberg.

- Sudhof, T. C. (2001) alpha-Latrotoxin and its receptors: neurexins and CIRL/latrophilins. *Annu Rev Neurosci*, 24, 933-62.
- Takahashi, M., Freed, R., Blackmer, T. and Alford, S. (2001) Calcium influx-independent depression of transmitter release by 5-HT at lamprey spinal cord synapses. *J Physiol*, 532, 323-36.
- Takahashi, T., Kajikawa, Y. and Tsujimoto, T. (1998) G-Protein-coupled modulation of presynaptic calcium currents and transmitter release by a GABAB receptor. *J Neurosci*, 18, 3138-46.
- Thompson, S. M. and Gahwiler, B. H. (1992) Comparison of the actions of baclofen at pre- and postsynaptic receptors in the rat hippocampus in vitro. *J Physiol*, 451, 329-45.
- Tong, G., Malenka, R. C. and Nicoll, R. A. (1996) Long-term potentiation in cultures of single hippocampal granule cells: a presynaptic form of plasticity. *Neuron*, 16, 1147-57.
- Trommershauser, J., Schneggenburger, R., Zippelius, A. and Neher, E. (2003) Heterogeneous presynaptic release probabilities: functional relevance for short-term plasticity. *Biophys J*, 84, 1563-79.
- Tsetsenis, T., Ma, X. H., Lo Iacono, L., Beck, S. G. and Gross, C. (2007) Suppression of conditioning to ambiguous cues by pharmacogenetic inhibition of the dentate gyrus. *Nat Neurosci*, 10, 896-902.
- van den Bogaart, G., Holt, M. G., Bunt, G., *et al.* (2010) One SNARE complex is sufficient for membrane fusion. *Nat Struct Mol Biol*, 17, 358-64.
- Vigot, R., Barbieri, S., Brauner-Osborne, H., *et al.* (2006) Differential compartmentalization and distinct functions of GABAB receptor variants. *Neuron*, 50, 589-601.
- Vogt, K. E. and Nicoll, R. A. (1999) Glutamate and gamma-aminobutyric acid mediate a heterosynaptic depression at mossy fiber synapses in the hippocampus. *Proc Natl Acad Sci U S A*, 96, 1118-22.
- Vogt, K. E. and Regehr, W. G. (2001) Cholinergic modulation of excitatory synaptic transmission in the CA3 area of the hippocampus. *J Neurosci*, 21, 75-83.
- von Gersdorff, H. and Borst, J. G. (2002) Short-term plasticity at the calyx of held. *Nat Rev Neurosci*, 3, 53-64.
- Washbourne, P., Thompson, P. M., Carta, M., *et al.* (2002) Genetic ablation of the t-SNARE SNAP-25 distinguishes mechanisms of neuroexocytosis. *Nat Neurosci*, 5, 19-26.
- Weisskopf, M. G., Castillo, P. E., Zalutsky, R. A. and Nicoll, R. A. (1994) Mediation of hippocampal mossy fiber long-term potentiation by cyclic AMP. *Science*, 265, 1878-82.
- White, J. H., Wise, A., Main, M. J., *et al.* (1998) Heterodimerization is required for the formation of a functional GABA(B) receptor. *Nature*, 396, 679-82.
- Wu, L. G. and Saggau, P. (1995) GABAB receptor-mediated presynaptic inhibition in guinea-pig hippocampus is caused by reduction of presynaptic Ca<sup>2+</sup> influx. *J Physiol*, 485 ( Pt 3), 649-57.
- Wu, L. G. and Saggau, P. (1997) Presynaptic inhibition of elicited neurotransmitter release. *Trends Neurosci*, 20, 204-12.
- Wulff, P., Goetz, T., Leppa, E., *et al.* (2007) From synapse to behavior: rapid modulation of defined neuronal types with engineered GABAA receptors. *Nat Neurosci*, 10, 923-9.
- Wulff, P. and Wisden, W. (2005) Dissecting neural circuitry by combining genetics and pharmacology. *Trends Neurosci*, 28, 44-50.
- Xu, J., Mashimo, T. and Sudhof, T. C. (2007) Synaptotagmin-1, -2, and -9: Ca<sup>2+</sup> sensors for fast release that specify distinct presynaptic properties in subsets of neurons. *Neuron*, 54, 567-81.

- 
- Xu, J., Pang, Z. P., Shin, O. H. and Sudhof, T. C. (2009) Synaptotagmin-1 functions as a Ca<sup>2+</sup> sensor for spontaneous release. *Nat Neurosci*, 12, 759-66.
- Xue, M., Craig, T. K., Xu, J., *et al.* (2010) Binding of the complexin N terminus to the SNARE complex potentiates synaptic-vesicle fusogenicity. *Nat Struct Mol Biol*, 17, 568-75.
- Xue, M., Lin, Y. Q., Pan, H., *et al.* (2009) Tilting the balance between facilitatory and inhibitory functions of mammalian and *Drosophila* Complexins orchestrates synaptic vesicle exocytosis. *Neuron*, 64, 367-80.
- Yamamoto, M., Wada, N., Kitabatake, Y., *et al.* (2003) Reversible Suppression of Glutamatergic Neurotransmission of Cerebellar Granule Cells In Vivo by Genetically Manipulated Expression of Tetanus Neurotoxin Light Chain. *J. Neurosci.*, 23, 6759-67.
- Yokoi, M., Kobayashi, K., Manabe, T., *et al.* (1996) Impairment of hippocampal mossy fiber LTD in mice lacking mGluR2. *Science*, 273, 645-7.
- Yoon, E. J., Gerachshenko, T., Spiegelberg, B. D., Alford, S. and Hamm, H. E. (2007) Gbetagamma interferes with Ca<sup>2+</sup>-dependent binding of synaptotagmin to the soluble N-ethylmaleimide-sensitive factor attachment protein receptor (SNARE) complex. *Mol Pharmacol*, 72, 1210-9.
- Zhang, F., Wang, L.-P., Brauner, M., *et al.* (2007) Multimodal fast optical interrogation of neural circuitry. 446, 633-9.
- Zucker, R. S. and Regehr, W. G. (2002) Short-term synaptic plasticity. *Annu Rev Physiol*, 64, 355-405.

## 5.2 List of figures

Figure 1-1: The synaptic vesicle cycle and individual vesicle pools.....	11
Figure 1-2: The vesicular release machinery and clostridial toxin activity.....	13
Figure 1-3: Activation cycle of G-proteins by G-protein coupled receptors.....	18
Figure 1-4: GABA <sub>B</sub> R subunit distribution and GABA <sub>B</sub> R signalling in hippocampal neurons.....	20
Figure 1-5: Principal neurons of the hippocampal formation and their connectivity.....	23
Figure 2-1: Autaptic culture preparation.....	31
Figure 2-2: Hippocampal granule cell preparation and morphological characterization of autaptic hippocampal neurons.....	33
Figure 2-3: Ca <sup>2+</sup> imaging at mossy fibre terminals in hippocampal slices.....	39
Figure 2-4: A fast flow device enables rapid applications of hypertonic solutions and pharmacological manipulations in recordings of autaptic neuronal cultures.....	41
Figure 3-1: Evidence for Ca <sup>2+</sup> -independent inhibition of transmitter release by presynaptic GABA <sub>B</sub> Rs at hippocampal Schaffer collateral synapses.....	57
Figure 3-2: Baclofen reduces the mEPSC frequency, but does not alter the amplitude of quantal events in CA1 pyramidal neurons.....	59
Figure 3-3: Autaptic cultures of hippocampal pyramidal neurons are useful tools to study mechanisms of presynaptic inhibition by GABA <sub>B</sub> Rs.....	61
Figure 3-4: Pertussis toxin treatment of autaptic cultures abolishes presynaptic inhibition by GABA <sub>B</sub> Rs.....	63
Figure 3-5: GABA <sub>B</sub> R activation does not change the size of the RRP, but decreases the number of vesicles released by hypertonic stimuli of intermediate strength.....	64
Figure 3-6: Peak release rates of sucrose-evoked release are slowed in baclofen.....	66
Figure 3-7: GABA <sub>B</sub> R activation slows the kinetics of transmitter release evoked by hypertonic stimuli.....	67

---

Figure 3-8: Full cleavage of SNAP-25 by extensive treatment of neuronal cultures with BoNT-A.....	68
Figure 3-9: Cleavage of SNAP-25 with BoNT-A does not abolish presynaptic inhibition by GABA <sub>B</sub> Rs. ....	69
Figure 3-10: SCH23390 can be used to block GIRK-mediated currents activated by postsynaptic GABA <sub>B</sub> Rs. ....	70
Figure 3-11: Subtraction of non-AMPA receptor currents during baclofen application from the ionomycin-induced release events confirms that cleavage of SNAP-25 by BoNT-A does not occlude direct inhibition of transmitter release by GABA <sub>B</sub> Rs. ....	71
Figure 3-12: Configuration and quality standards for electrophysiological field recordings of mossy fibre synaptic transmission. ....	75
Figure 3-13: Activation of presynaptic GABA <sub>B</sub> Rs strongly inhibits transmitter release from mossy fibres and decreases presynaptic Ca <sup>2+</sup> influx. ....	76
Figure 3-14: Baclofen effect on presynaptic Ca <sup>2+</sup> transients in mossy fibre boutons recorded by high resolution confocal Nipkow spinning disc imaging.....	77
Figure 3-15: Comparison of changes in Ca <sup>2+</sup> influx and fEPSP by manipulation of extracellular Ca <sup>2+</sup> or by GABA <sub>B</sub> R activation.....	79
Figure 3-16: Synaptoporin is a marker specific for hippocampal granule cells.....	80
Figure 3-17: Inhibition of transmitter release by activation of presynaptic mGluR 2/3 can be used to identify granule cells in autaptic cultures. ....	82
Figure 3-18: Pharmacological characterization by L-CCG I application and subsequent immunocytochemistry for synaptoporin expression in the same autaptic neurons. ....	83
Figure 3-19: Comparable efficacy of 1 μM DCG IV and 10 μM L-CCG I to suppress autaptic granule cell EPSCs. ....	85
Figure 3-20: Hippocampal granule cells have a smaller readily releasable pool but similar vesicular release probability compared to pyramidal neurons.....	86
Figure 3-21: Short-term plasticity of EPSCs during 1 Hz stimulation in autaptic neurons. ...	87

Figure 3-22: Application of FSK leads to a presynaptic potentiation of transmitter release in autaptic granule cells. ....	88
Figure 3-23: Baclofen reduces frequency but not amplitude of mossy fibre mEPSCs.....	90
Figure 3-24: Development of the hM4D receptor family. ....	92
Figure 3-25: Generation of hM4D expression vectors with two versions of genetically encoded red fluorescent markers. ....	93
Figure 3-26: CNO causes hyperpolarization of neurons expressing hM4D. ....	94
Figure 3-27: Strong presynaptic inhibition of transmitter release by hM4D receptors expressed in autaptic cultures of hippocampal neurons. ....	95
Figure 3-28 Comparison of presynaptic inhibition by GABA <sub>B</sub> and hM4D receptors.....	96
Figure 3-29: Conditional expression of hM4D-mKateT using the FLEX cassette.....	99
Figure 3-30 Vector construction and RMCE for the generation of CAG-Flex-hM4D-mKateT. ....	101
Figure 3-31: Co-expression of Cre activates hM4D expression by recombination of the FLEX cassette in transiently transfected HEK293 cells.....	102
Figure 3-32: Identification of successful genomic integration events and Cre-mediated inversion of the hM4D coding sequence by PCRs. ....	103
Figure 4-1: The relation of the intracellular Ca <sup>2+</sup> concentration to the vesicular release probability is strongly influenced by the power of the release function.....	112

---

### 5.3 List of tables

Table 1: Published methods to artificially silence neurons in the mammalian brain.....	26
Table 2: Drugs used for pharmacological manipulations.....	36
Table 3: Enzymes used in the laboratory for molecular biology work. ....	45
Table 4: Primers used for DNA amplification by PCR.....	49
Table 5: Antibodies used for immunocytochemistry (ICC), Western blots (WB) and secondary antibodies (2nd): .....	52
Table 6: GABA <sub>B</sub> R-induced changes of frequency, amplitude and kinetics of mEPSCs measured in autaptic cultures in Ca <sup>2+</sup> -containing and Ca <sup>2+</sup> -free conditions. ....	62

## 5.4 Frequently used abbreviations

### A

AMPA	$\alpha$ -amino-3-hydroxyl-5-methyl-4-isoxazole-propionate (specific agonist for subgroup of ionotropic glutamate receptors)
AP	action potential
ATP	adenosine triphosphate

### B

BoNT-A	Botulinum neurotoxin-A
--------	------------------------

### C

C31int	integrase of phage phiC31
Ca <sup>2+</sup>	calcium
CAG	CMV immediate early enhancer/ modified chicken $\beta$ -actin promoter)
cAMP	cyclic adenosine monophosphate
Cd <sup>2+</sup>	cadmium
CMV	cytomegalovirus
CNO	clozapine-N-oxide
CNS	central nervous system
Cre	causes recombination

### D

DIV	days in vitro
DMSO	dimethylsulfoxide
DNA	desoxynucleic acid

### E

EBSS	Earle's balanced salt solution
EC	entorhinal cortex
EC <sub>50</sub>	half maximal effective concentration
EGFP	enhanced green fluorescent protein
EGTA	ethylene glycol-bis( $\beta$ -aminoethyl ether)-N,N,N',N'-tetraacetic acid
EPSC	excitatory postsynaptic potential
ERC	ELKS/Rab6-interacting protein/CAST

### F

FCS	fetal calf serum
FLEX	flip and excision
FSK	forskolin

### G

GABA	gamma-aminobutyric acid
GABA <sub>A</sub> R	GABA receptor (subtype A; ionotropic)
GABA <sub>B</sub> R	GABA receptor (subtype B; metabotropic)
GIRK	G-protein-activated inwardly rectifying potassium (K <sup>+</sup> ) channel
GPCR	G-protein coupled receptor
G-protein	Guanine nucleotide-binding protein
GTP	guanosine triphosphate

### H

HEK cells	human embryonic kidney cells
hM4D	human muscarinic type 4 like designer receptor

### I

IRES	internal ribosomal entry site
------	-------------------------------

### K

KO	knockout
----	----------

### L

loxP	locus of crossing (x) over of P1
LTD	long-term depression
LTP	long-term potentiation

### M

mEPSC	miniature excitatory postsynaptic potential
mIPSC	miniature inhibitory postsynaptic potential
mGluR	metabotropic glutamate receptor

<hr/>			
<b><i>N</i></b>			
NMDA	N-methyl-D-aspartic acid (specific agonist for subgroup of ionotropic glutamate receptors)	RRP	readily releasable pool
		RT	room temperature
		<b><i>S</i></b>	
		SDS	sodium dodecyl sulphate
NO	nitric oxide	SDS-PAGE	SDS polyacrylamide gel electrophoresis
n.s.	not significant		
NSF	N-ethylmaleimide-sensitive fusion protein	SNAP	soluble NSF attachment protein
		SNAP-25	synaptosomal-associated protein of 25 kDa
<b><i>P</i></b>		SNARE	soluble NSF attachment protein receptor
PBS	phosphate buffered saline		
PCR	polymerase chain reaction	<b><i>T</i></b>	
PGK	phosphoglycerate kinase (promoter)	TBS	Tris buffered saline
PTX	Pertussis toxin	TeNT	Tetanus neurotoxin
P <sub>vr</sub>	release probability	TTX	Tetrodotoxin
<b><i>R</i></b>			
RIM	Rab3-interacting molecule	<b><i>V</i></b>	
RMCE	recombination-mediated cassette exchange	VDCCs	voltage-dependent Ca <sup>2+</sup> channels
Rosa	reverse orientation splice acceptor		



---

## 5.5 Statement of contribution

The experiments described in this Thesis resulted from collaborative scientific projects. In the following I state the respective contribution to the data presented:

### Chapter 3.1: Presynaptic inhibition by GABA<sub>B</sub>Rs in hippocampus area CA1

Dr. Jörg Breustedt and Patrick Nicholson (AG Schmitz, Berlin) contributed the photodiode Ca<sup>2+</sup> imaging experiments and some of the extracellular field potential recordings in CA1. I have performed all other experiments described in this chapter.

### Chapter 3.2 - GABA<sub>B</sub>R-mediated inhibition at mossy fibre terminals and characterization of autaptic hippocampal granule cells

Dr. Jörg Breustedt and Patrick Nicholson performed all the photodiode Ca<sup>2+</sup> imaging experiments and extracellular field potential recordings in CA3. Anke Schönherr (AG Schmitz), Dr. Gisela Grosse and Prof. Gudrun Ahnert-Hilger (both from the Institute of Anatomy, Charité Berlin) helped to establish autaptic cultures of hippocampal granule cells. I have performed all other experiments described in this chapter.

### Chapter 3.3 - Presynaptic inhibition by an artificial receptor as a tool to silence neuronal output

The molecular cloning was performed by Anke Schönherr and me. Dr. Ralf Nehring (AG Rosenmund, Baylor College Houston, TX, USA) produced the lentiviral particles. Prof. Christoph Harms (Department of Experimental Neurology, Charité Berlin) helped in the design of the targeting construct for the transgenic mouse. Jeanette Lips from the group of Christoph Harms performed the PCRs for identification of the positive clones. Dr. Geert Michel (Forschungseinrichtung für experimentelle Medizin, Charité Berlin) conducted the embryonic stem cell culture work. All other experiments were performed by me.

## 5.6 Acknowledgments

My work for this thesis was supported and influenced by a number of people, without whom I would not have started, continued and completed my projects.

Foremost I want to thank Dietmar Schmitz. He strongly promoted my scientific development and enthusiastically encouraging me to start new projects, not hesitating to financing them and following new ideas. I became part of his great team in the lab, and also of the Berlin neuroscience community he founded as part of the Neurocure initiative. He was always of great help, friendly and inspiring.

I want to thank Jörg Breustedt for teaching me electrophysiology in all its facets, for his help and advice with my scientific work, his major contributions to the writing of our manuscripts, and all the discussions I enjoyed to have with him.

Anke Schönherr - I'm deeply committed to thank her for the molecular biology and cell culture work she did in the last four years. Without her support many of my experiments wouldn't have gone as smoothly as they did. Likewise, I want to thank Susanne Rieckmann for her help.

In the hM4D transgenic mouse project, I'm very grateful to Christoph Harms, who took a great deal of pushing forward the project. I want to thank Ralf Kühn (GSF National Research Centre for Environment and Health, Neuherberg, Germany) for providing the Rosa26 RMCE system, and Geert Michel (Transgene Facility of the "Forschungsinstitut für experimentelle Medizin", Charité Berlin) for performing the ES cell electroporation and injection.

I want to thank Gudrun Ahnert-Hilger for our cooperation in the autaptic granule cell project, and her help with the BoNT-A assays. Furthermore, I very much appreciated the insightful discussions with her.

Meeting Christian Rosenmund turned out to bring my work a big step forward, and I want to express my gratitude to him for inviting me to his laboratory and house in Houston, and that he gave me the opportunity to experience two intensive, highly productive weeks there.

---

I very much appreciated to work with all members of the “Schmitzlab”; it is a great lab with an outstanding spirit. In particular I want to thank Vanessa Stempel for critically reading this thesis.

A number of people from outside the lab helped me with many of the scientific challenges I experienced in the last years - most of all Denise Hübner and Björn von Eyss, who are also most valuable friends. I appreciated to work with Anja Harmeier in a very interesting and productive collaboration on A $\beta$ -induced neurotoxicity. I further want to thank Ari Liebkowsky for reading and correcting parts of this Thesis.

I am grateful to the GRK 1123 for funding my trips to a number of congresses, national and international ones, and for the soft skill courses I had the chance to take part in.

Finally, I want to thank my family - parents, brothers, and grandparents – and most of all Antje, for here support and trust, tolerating all the lab-frustrations and for making it a wonderful time in Berlin.

## **5.7 Curriculum Vitae**

Mein Lebenslauf wird aus datenschutzrechtlichen Gründen in der elektronischen Version meiner Arbeit nicht veröffentlicht.

---

## 5.8 Publications

- Rost, B.R.**, Nicholson, P., Rosenmund, C., Breustedt, J., Schmitz, D.: Activation of metabotropic GABA receptors increases the energy barrier for vesicle fusion. In revision for *Journal of Cell Science*.
- Vogt, J., Glumm, R., Schlüter, L., Khrulev, S., Schmitz, D., **Rost, B.R.**, Naumann, T., Savaskan, N.E., Brauer, A.U., Reutter, W., Heimrich, B., Nitsch, R., Horstkorte, R.: PSA-NCAM regulates axon targeting but inhibits axonal regeneration after lesion. In preparation.
- Harmeier, A., Barucker, C., Gensler, M., **Rost, B. R.**, Zhuang, W., Beyermann, M., Hildebrand, P. W., Schmitz, D., Lurz, R., Rabe, J. P., Multhaup, G.: Structural analysis of A $\beta$  aggregates influenced by the GxxxG motif. In preparation.
- Kaden, D., Harmeier, A., Bethge, T., Althoff, V., **Rost, B. R.**, Schaefer, M., Lurz, R., Schmitz, D., Skodda, S., Finckh, U., Multhaup, G.: A familial Alzheimer's disease mutation - APP695-K612N. In preparation.
- Rost, B.R.**, Breustedt, J., Schoenherr, A., Grosse, G., Ahnert-Hilger, G. & Schmitz, D. (2010) Autaptic cultures of single hippocampal granule cells of mice and rats. *Eur J Neurosci*, 32, 939-947.
- Harmeier, A., Wozny, C., **Rost, B.R.**, Munter, L.M., Hua, H., Georgiev, O., Beyermann, M., Hildebrand, P.W., Weise, C., Schaffner, W., Schmitz, D. & Multhaup, G. (2009) Role of amyloid-beta glycine 33 in oligomerization, toxicity, and neuronal plasticity. *J Neurosci*, 29, 7582-7590.
- Sel, S.\* , **Rost, B.R.\***, Yildirim, A.O., Sel, B., Kalwa, H., Fehrenbach, H., Renz, H., Gudermann, T. & Dietrich, A. (2008) Loss of classical transient receptor potential 6 channel reduces allergic airway response. *Clin Exp Allergy*, 38, 1548-1558. (\*equal contribution)
- Motazacker, M.M., **Rost, B.R.**, Hucho, T., Garshasbi, M., Kahrizi, K., Ullmann, R., Abedini, S.S., Nieh, S.E., Amini, S.H., Goswami, C., Tzschach, A., Jensen, L.R., Schmitz, D., Ropers, H.H., Najmabadi, H. & Kuss, A.W. (2007) A defect in the ionotropic glutamate receptor 6 gene (GRIK2) is associated with autosomal recessive mental retardation. *Am J Hum Genet*, 81, 792-798.
- Heilborn, U., **Rost, B. R.**, Arborelius, L. and Brodin, E. (2007) Arthritis-induced increase in cholecystinin release in the rat anterior cingulate cortex is reversed by diclofenac. *Brain Res*, 1136, 51-8.
- Dietrich, A., Chubanov, V., Kalwa, H., **Rost, B.R.** & Gudermann, T. (2006) Cation channels of the transient receptor potential superfamily: their role in physiological and pathophysiological processes of smooth muscle cells. *Pharmacol Ther*, 112, 744-760.
- Dietrich, A., Kalwa, H., **Rost, B.R.** & Gudermann, T. (2005) The diacylglycerol-sensitive TRPC3/6/7 subfamily of cation channels: functional characterization and physiological relevance. *Pflugers Arch*, 451, 72-80.

## 5.9 Symposia and meetings contributions

- Benjamin R. Rost, Patrick Nicholson, Christian Rosenmund, Joerg Breustedt, Dietmar Schmitz: GABA<sub>B</sub> receptors increases the energy barrier for vesicle fusion. *Poster*. European Synapse Meeting, Amsterdam 2010
- Benjamin R. Rost, Anke Schönherr, Ralf Nehring, Christian Rosenmund, Christoph Harms, Dietmar Schmitz: Silencing neuronal activity with a designer receptor activated by a designer drug. *Poster*. Berlin Neuroscience Forum 2010
- Benjamin R. Rost: *Talk* Berlin Brain Days 2009
- Benjamin R. Rost, J. Breustedt, P. Nicholson, C. Rosenmund, Dietmar Schmitz: Mechanisms of presynaptic GABA<sub>B</sub> receptors. *Poster*. American Society of Neuroscience meeting, Chicago 2009
- Benjamin R. Rost: *Talk* Graduate school 1123, Berlin symposium 2009
- Benjamin R. Rost, Gudrun Ahnert-Hilger, Gisela Grosse, Dietmar Schmitz, Jörg Breustedt: mGluR group II-mediated presynaptic inhibition at the mossy fiber synapse. *Poster*. Berlin Brain Days 2008
- Benjamin R. Rost, Gudrun Ahnert-Hilger, Gisela Grosse, Dietmar Schmitz, Jörg Breustedt: mGluR group II-mediated presynaptic inhibition at the mossy fiber synapse. *Poster*. European Society of Neuroscience meeting, Geneva 2008

---

### **5.10 Erklärung an Eides statt**

Hiermit erkläre ich, Benjamin Rainer Rost, geboren am 24. März 1980 in Darmstadt, dass ich die vorliegende Dissertation selbständig verfasst und keine anderen als die angegebenen Hilfsmittel verwendet habe.

Berlin, den 12. Oktober 2010

Benjamin Rost